

MASTER

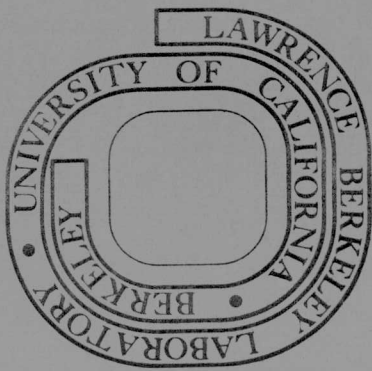
CHANGES IN THE PORE STRUCTURE OF COAL  
WITH PROGRESSIVE EXTRACTION

David J. Medeiros\* and Eugene E. Petersen

December 1975

Prepared for the U. S. Energy Research and  
Development Administration under Contract W-7405-ENG-48

\* Filed as a M. S. thesis



LBL-4439

DISTRIBUTION OF THIS DOCUMENT IS UNLIMITED

## **DISCLAIMER**

**This report was prepared as an account of work sponsored by an agency of the United States Government. Neither the United States Government nor any agency thereof, nor any of their employees, makes any warranty, express or implied, or assumes any legal liability or responsibility for the accuracy, completeness, or usefulness of any information, apparatus, product, or process disclosed, or represents that its use would not infringe privately owned rights. Reference herein to any specific commercial product, process, or service by trade name, trademark, manufacturer, or otherwise does not necessarily constitute or imply its endorsement, recommendation, or favoring by the United States Government or any agency thereof. The views and opinions of authors expressed herein do not necessarily state or reflect those of the United States Government or any agency thereof.**

---

## **DISCLAIMER**

**Portions of this document may be illegible in electronic image products. Images are produced from the best available original document.**

**NOTICE**  
This report was prepared as an account of work sponsored by the United States Government. Neither the United States nor the United States Energy Research and Development Administration, nor any of their employees, nor any of their contractors, subcontractors, or their employees, makes any warranty, express or implied, or assumes any legal liability or responsibility for the accuracy, completeness or usefulness of any information, apparatus, product or process disclosed, or represents that its use would not infringe privately owned rights.

-iii-

## Changes in the Pore Structure of Coal with Progressive Extraction

### Contents

<b>Abstract</b> . . . . .	1
I.    Introduction . . . . .	3
A. Pore Structure of Coal. . . . .	3
B. Internal Surface Area of Coal . . . . .	7
C. BET Method . . . . .	12
D. Dubinin-Polanyi Adsorption Equations . . . . .	17
E. Objectives . . . . .	19
References . . . . .	21
II.    Equipment and Procedures . . . . .	23
A. Adsorption Equipment . . . . .	23
B. Calibration of Equipment . . . . .	30
C. General Degassing and Adsorption Procedures . . . . .	33
D. Equations for Surface Area Determinations . . . . .	37
E. Vapor-Pressure Data . . . . .	41
References . . . . .	43
III.    Adsorption on Porous Solids . . . . .	44
A. Types and Properties of the Porous Solids Used. . . . .	44
B. Molecular Cross-Sectional Area Determinations . . . . .	45
C. BET versus Dubinin-Polanyi Equations . . . . .	48
D. High Temperature Adsorptions. . . . .	50
References . . . . .	53
IV.    Adsorption on Raw Coals . . . . .	54
A. Analysis of the Raw Coals Used . . . . .	54

B. Low Temperature Gas Adsorption . . . . .	58
C. High Temperature Adsorption . . . . .	60
References . . . . .	64
<b>V. Surface Area Variations of Extracted Coal . . . . .</b>	<b>65</b>
A. Extracted Coal Samples . . . . .	65
B. Surface Areas of the Extracted Coal . . . . .	65
References . . . . .	71
<b>VI. Discussions of Results . . . . .</b>	<b>72</b>
A. Adsorption on Catalysts and Molecular Sieves . . . . .	72
B. Adsorption on Raw Coals . . . . .	78
C. Surface Area Variations of Extracted Coal . . . . .	83
D. Suggestions for Future Work. . . . .	86
References . . . . .	88
<b>Appendix A . . . . .</b>	<b>89</b>
<b>Appendix B . . . . .</b>	<b>92</b>

## Changes in the Pore Structure of Coal with Progressive Extraction

David J. Medeiros\* and Eugene E. Petersen

Lawrence Berkeley Laboratory  
University of California  
Berkeley, California 94520

December 1975

### ABSTRACT

Adsorption of four gases ( $\text{CO}_2$ ,  $\text{CF}_4$ ,  $\text{N}_2$ , and  $\text{Ar}$ ) on Wyodak mine, Roland seam, coal, Illinois No. 6 high-sulfur coal, and 4A and 5A Linde molecular sieves has been studied. The results strongly suggest that coals possess a molecular sieve structure. The Roland seam coal is found to resemble the 4A sieve in its microporous structure (in which a majority of the pores are  $4\text{\AA}$  in diameter), whereas the Illinois No. 6 coal closely resembles the 5A sieve (with a majority of the pores just under  $5\text{\AA}$ ). To interpret these measurements the molecular cross-sectional areas of argon at  $77^\circ\text{K}$  and of carbon dioxide and carbon tetrafluoride at  $196^\circ\text{K}$  were determined by comparison to nitrogen adsorptions at  $77^\circ\text{K}$  on two Harshaw catalysts. Values of  $17.0$ ,  $23.4$ ,  $17.3 \text{\AA}^2$  were obtained for the argon, carbon dioxide, and carbon tetrafluoride molecules, respectively.

Comparisons between surface areas determined by both the Brunauer-Emmett-Teller and Dubinin-Polanyi equations for the low-temperature adsorptions of  $\text{N}_2$ ,  $\text{Ar}$ , and  $\text{CO}_2$  on the catalysts, molecular sieves, and raw coals indicate that either equation gives similar surface areas.

On the raw coals the adsorption of  $\text{CO}_2$  at 196 °K yields values representative of total surface areas,  $106 \text{ m}^2/\text{g}$  for Roland seam and  $227 \text{ m}^2/\text{g}$  for Illinois No. 6, whereas the adsorption of argon and nitrogen at 77 °K and  $\text{CF}_4$  at 196 °K gives much lower values.

The effect of progressive extraction of the Roland seam coal on its surface area (determined by  $\text{CO}_2$  adsorptions at 196 °K) has also been investigated in this study. Surface areas of the extracted coal varied with extraction time, yield, and solvent used. A maximum surface area of  $265 \text{ m}^2/\text{g}$  was obtained using tetralin at 350 °C for 4 hours as the solvent, for which the extraction yield was 31.7%. At low extraction temperatures of 250 °C and below, solvent effects were the dominate effects on the variations in surface areas. However, at temperatures near or above the pyrolysis temperature (320 °C) of the raw Roland seam coal, thermal effects overshadowed solvent effects, and yielded areas above  $200 \text{ m}^2/\text{g}$ .

## I. Introduction

In order to process coal the processing fluid (solvent, reactant, etc.) must be in contact with as much of the solid coal as possible.

To achieve this, coal would have to be ground to molecular dimensions or the processing fluid would have to be capable of penetrating the internal structure of this solid. Grinding coal to molecular dimensions is both impractical and economically infeasible, therefore the fluids must be capable of penetrating the porous solid.

The high internal structure of coal should be preserved during processing to enable high rates of reactions or extractions. Accordingly, internal structure and area should be measured with progressive processing to determine if the high surface area is being utilized. If not, the processing variables should be modified to do this whenever possible. Therefore, reliable methods must be developed to determine initial areas on the original coal and the areas subsequent to processing. Coal, having very fine pores similar to molecular sieves, is a difficult material with respect to surface area determinations.

### A. Pore Structure of Coal

The internal structure of coal is a very important characteristic. In order for chemical reactions, gas adsorptions, and extractions to take place, reagents or vapors have to pass into the fine micropore structure of the coal. Rates of mass transfer are greatly restricted by the very small size of the openings in the coal structure.

Van Krevelen and Zwietering<sup>1</sup> first applied Ritter and Drake's method of mercury penetration to the study of coal. This work suggested

<sup>\*</sup>References are listed at the end of this chapter

that coal contains two pore systems: 1. a macropore system and 2. a micropore system. Mercury is able to penetrate the macropore system, but even at high pressures is unable to penetrate the micropore system of coal. However, both pore systems are accessible to helium at room temperature. Generally pores in the size range below  $12 \text{ \AA}^+$  are described as micropores, those above about  $200 \text{ \AA}$  as macropores, and those in between as transitional or intermediate pores. Depending on the rank of coal, the pore size distribution can differ greatly.

Gan, Nandi, and Walker<sup>2</sup> measured the gross pore size distributions for a number of coals, by nitrogen adsorption isotherms at  $-196^\circ\text{C}$ . They determined the cumulative pore volume, in the pore range  $29600 \text{ \AA}$  to about  $12 \text{ \AA}$ . For an Illinois No. 6, high-volatile C bituminous coal, 30.2% of the pore volume is smaller than about  $12 \text{ \AA}$ , 52.6% between about  $12 \text{ \AA}$  and  $300 \text{ \AA}$ , and 17.2% above  $300 \text{ \AA}$ . For a low-volatile bituminous Pennsylvania coal, 73% of the pore volume is under  $12 \text{ \AA}$ , 0% between  $12$  and  $300 \text{ \AA}$ , and 27% above  $300 \text{ \AA}$ .

It is clear from the work of both Van Krevelen and Walker that coal, in general, contains a very fine micropore system with the average pore size less than  $12 \text{ \AA}$  in diameter.

### 1. Average Pore Diameter

Insight into the approximate average pore diameter of coal can be obtained from the work of Bond and Spencer<sup>3</sup> and Lamond and Marsh.<sup>4</sup> The former team observed that the heat of wetting (see Section B, following) for any rank of coal decreases as the molecular volume of the wetting

---

<sup>†</sup>  $1 \text{ \AA}$  (angstrom) =  $10^{-10}$  meters

liquid increases. They obtained a relationship for the differential internal surface area as a function of the size of the ultrafine pores of coal. Their results show that the critical dimensions of the ultrafine pores are 5 Å and 8 Å in approximate diameters, corresponding to molecular diameters of wetting liquids whose molecular volumes are around 50 and 150 cc/mole.

Lamond and Marsh<sup>4</sup> using 4A and 5A molecular sieves came to a similar conclusion. For nitrogen at -196 °C they found a very small surface area of less than 1 m<sup>2</sup>/g for the 4A, whereas they obtained a surface area of 730 m<sup>2</sup>/g for the 5A. By contrast, carbon dioxide molecules at both -78 of 0 °C were capable of penetrating both the 4A and 5A sieves giving surface areas of 610 and 700 m<sup>2</sup>/g, respectively.

Comparing the results of Lamond and Marsh to the adsorption of nitrogen in coals (nitrogen adsorption in coals is discussed in Section B, following), it appears that the ultrafine pore structure of coals and molecular sieves are similar leading to the conclusion that the average pore diameter of coals is roughly 4 Å or approximately the same as in 4A sieves.

One can get a reasonably good breakdown of the surface area versus pore diameter distribution of coals from the data reported by Walker, et al.<sup>2</sup> on the Illinois No. 6 and Pennsylvania coals (discussed above). Assuming densities and porosities of coals to be 1.5 g/cc and 20%, respectively, the total pore volume per gram of coal is found to be 0.13 cc/g.

The pore volume distribution, cc/g, for the two coals then becomes:

pore size distribution	Illinois No. 6	Penn. Coal
< 12 Å	0.039 (30%)	0.095 (73%)
12 Å - 300 Å	0.065 (50%)	0 (0%)
>300 Å	0.026 (20%)	0.035 (27%)

The percentages listed above in parenthesis are the pore volume percentages of the various pore ranges reported by Walker.

Assuming the pores of coals to be made up of uniform cylindrical nonintersecting capillaries, the relationship between surface area, pore volume, and pore diameter is given by

$$S = \frac{4v \times 10^4}{d} \quad (1)$$

where S is the surface area,  $\text{m}^2/\text{g}$ ; v the pore volume,  $\text{cc/g}$ ; and d the average pore diameter, Å.

Using average pore diameters of 10,100, and 1000 Å for the pore size distributions of < 12, 12-300, and > 300 Å, respectively, the surface area distribution,  $\text{m}^2/\text{g}$ , for the two coals using Equation 1 becomes:

pore size distribution	Illinois No. 6	Penn. Coal
< 12 Å	156	380
12 Å - 300 Å	26	0
>300 Å	1	1.4

The above surface area breakdowns show that the majority of the internal surface area of coals is contained in the very fine micropores, diameters less than 12 Å.

## B. Internal Surface Area of Coal

Porous solids containing fine micropores generally have a high internal surface area, and it follows that coal should contain a relatively high surface area per unit weight.

### 1. Gas Adsorption

Griffith and Hirst<sup>5</sup> and Maggs<sup>6</sup> initially determined the total internal surface area of coal by the heat of wetting method. This is perhaps the oldest surface area method and is based upon a measurement of the amount of heat liberated when the internal surface is completely wetted, methanol or water being usually used. The method is criticized as only approximate because it is necessary to know *a priori* a conversion factor (the heat of wetting per unit surface area for the liquid-solid pair) to convert energy units into surface area units, and because some of the heat being liberated is actually due to swelling and not adsorption.

Using a conversion factor of 400 ergs/cm<sup>2</sup>, Bond and Maggs<sup>7</sup> found surface areas of coal between 20 and 200 m<sup>2</sup>/g depending on the rank of coal studied.

The work based upon the heat of wetting method were severely criticized when surface areas as measured by the adsorption of nitrogen and argon at low temperatures (77-90 °K) gave much lower surface areas than the corresponding heat of wetting areas. P.L.R. Malherbe<sup>8</sup> measured the internal surface areas of South African coals with argon at -184 °C and with methanol as the wetting liquid. His methanol results were 16 to 68 times as large as his argon results. Because of the swelling of the coal when using methanol as the liquid, the heat liberated is considered to be mostly from swelling and only a small part due to the

actual wetting of the internal surface of the coal.

Maggs<sup>9-11</sup> showed that the adsorption isotherm for nitrogen on coal reaches a maximum at 195 °K; below this temperature the rate of adsorption is very low. This work confirmed the result that the low temperature surface area values on coal are very small. Maggs concluded that either some temperature dependent physical change in the coal was occurring such as thermal contraction of the coal to make the area inacessible but accessible at temperatures greater than 100 °K or the diffusion of nitrogen into the very fine pores of coal is an activated process whereupon the rate of diffusion into the micropores would become sufficiently rapid above about 100 °K.

Bangham and Franklin<sup>12</sup> determined the coefficient of linear expansion of coal at room temperature to be  $3.3 \times 10^{-5}$  degrees<sup>-1</sup>. Anderson, Hall, and Stein<sup>13</sup> have also determined the linear expansion of coal by direct optical measurements of a polished surface of coal at room temperature and also at liquid nitrogen temperatures of -196°C. The maximum linear coefficient of expansion was found to be  $4.8 \times 10^{-5}$  degrees<sup>-1</sup>. Van Krevelen and Schuyer<sup>14</sup> measured the linear coefficient of a series of vitrinites, the principal coal maceral and primary constituent of bright coals, from 20 to 45°C and observed values decreasing from  $4 \times 10^{-5}$  to  $1 \times 10^{-5}$  degrees<sup>-1</sup> for coals increasing in carbon content from 85 to 96%. Anderson et al.<sup>13</sup> concluded that in going from 0 to -195°C (liquid nitrogen temperature) the volume of coal decreases by about 3% or less. Zwietering and Van Krevelen<sup>1</sup> measured the density of a coal sample in helium over a temperature range from 100°C to -196°C and observed no contraction of the internal volume of the coal. Thus it appears

that the low surface areas calculated from argon and nitrogen adsorptions at low temperatures are a result of the inability of the molecules to diffuse into the ultrafine pore structure of coal and not due to the thermal contraction of coal as previously considered.

The adsorption of rare gases on coal has also been measured. Lahiri et al.<sup>15</sup> studied the adsorption of argon at -183°C, and Kini<sup>16</sup> studied the adsorption of xenon at 0°C on several coals and cokes. Lahiri obtained surface areas ranging from 13 to 51 m<sup>2</sup>/g using the BET equation for the briquetted coal and a surface area of approximately 7 m<sup>2</sup>/g for adsorption on a British anthracite coal. Using a molecular area of 25 Å<sup>2</sup> for xenon and a pressurized system, Kini observed surface areas from 140 to 200 m<sup>2</sup>/g depending on the sample of coal studied.

The use of carbon dioxide as an adsorbate on coal has in recent years been used extensively to measure the internal surface area of coal. Anderson et al.<sup>17</sup> have obtained surface areas for a low-volatile bituminous Pittsburgh coal of 114 and 140 m<sup>2</sup>/g from carbon dioxide isotherms at -78°C. Walker and Geller<sup>18</sup> also using carbon dioxide as the adsorbate obtained 175 m<sup>2</sup>/g on an anthracite coal. A comparison of the surface areas as calculated by the heat of wetting method using methanol and by adsorption of carbon dioxide at -78°C on several coals was determined by Czerski, Korla, and Lason.<sup>19</sup> The carbon dioxide areas were lower than the heat-of-wetting values on all samples tested. Surface areas of 59 and 208 m<sup>2</sup>/g were obtained for low-rank coals whereas areas of 18 and 43 m<sup>2</sup>/g were obtained for a high-rank coal using carbon dioxide isotherms and the heat of wetting method, respectively.

Lamond, Marsh, and Wynne-Jones<sup>4,20,21</sup> studied the adsorption of

carbon dioxide on many carbonaceous materials. From their studies, they concluded that carbon dioxide can be used satisfactory at  $-78^{\circ}\text{C}$  as an adsorbate to determine surface areas of coal. Anderson et al.<sup>13</sup> also arrived at a similar conclusion: that the true value of the total surface area of coal probably lies between the value obtained from carbon dioxide adsorption at  $-78^{\circ}\text{C}$  and heat of wetting values using methanol.

Since then, carbon dioxide has been used extensively to determine the internal areas of coal. Walker and Nadi<sup>2</sup> compared carbon dioxide adsorption at  $-78^{\circ}\text{C}$  and nitrogen adsorption at  $-196^{\circ}\text{C}$  on several types of coal. On all of their samples, the areas obtained using nitrogen are lower than those obtained using carbon dioxide. For some coals the nitrogen surface area values were less than  $1 \text{ m}^2/\text{g}$  while for other coal samples, the nitrogen area varied up to  $90 \text{ m}^2/\text{g}$ . The carbon dioxide areas ranged from 100 to  $430 \text{ m}^2/\text{g}$  also depending on the sample of coal. From their study, it is seen that coal with a nitrogen surface area greater than  $10 \text{ m}^2/\text{g}$  fell in a carbon content range of 75.5 to 81.5%.

## 2. Activated Diffusion

The role of activated diffusion of carbon dioxide and nitrogen into the porous structure of coal was investigated by Nandi and Walker.<sup>22</sup> They measured the unsteady-state diffusion of carbon dioxide and nitrogen from several coals over the temperature range of 25 to  $140^{\circ}\text{C}$ . They charged the samples with nitrogen or carbon dioxide to a pressure of 1204 torr absolute, allowing an equilibration time of 24 hours, then measured the unsteady-state release of gas after sudden pressure reductions outside the samples down to atmospheric pressure. Activation energies obtained from Arrhenius plots show that the activation energy for nitrogen is from 1.62 to 3.37 times the activation energy of carbon dioxide. For example,

for a Pittsburgh coal, the activation energies obtained were 6.3 and 3.9 kcal/mole for nitrogen and carbon dioxide, respectively. Walker and Nandi extrapolated their Arrhenius plots from a temperature range between 25 and 140°C to liquid nitrogen temperature of -196°C and dry ice temperature of -78°C, and concluded that a negligible fraction of the ultrafine pore structure of coal is available to nitrogen at -196°C, whereas a substantial fraction of the ultrafine pores of coal is available to carbon dioxide at -78°C. (Note: on their Arrhenius plots the ordinate,  $1000/T(^{\circ}\text{K})$ , ranged from 2.4 to 3.4. In order to extrapolate to -196°C the ordinate would have to be extended to 12.96- a factor of 10.56 times the original ordinate range.) They also concluded that the internal surface areas of coal, as calculated using carbon dioxide adsorption at -78°C, give roughly the total surface area whereas areas calculated from nitrogen adsorption at -196°C differ considerably.

If one assumes that the activation energy for both carbon dioxide and nitrogen in coals is 4.0 kcal/mole, the ratio of the diffusivities for nitrogen at -196°C and carbon dioxide at -78°C would be  $1.3 \times 10^{-7}$  using the equation

$$D = D_0 e^{-E/RT} \quad (2)$$

for the relationship between diffusivity and activation energy. In Equation 2 D is the diffusivity;  $D_0$  the pre-exponential constant; E the activation energy; R the gas constant; and T the absolute temperature.

This ratio of diffusivities,  $1.3 \times 10^{-7}$ , seems to indicate by itself that nitrogen at -196°C cannot diffuse into the pores of coal except, if at all, at a much slower rate than carbon dioxide at -78°C.

Using the same procedure as described above, Nandi and Walker<sup>23</sup> determined the activation energy of diffusion for methane in various ranks of coal from low-volatile anthracite to high-volatile bituminous. They determined that the diffusion of methane from coal was indeed activated and obtained activation energies varying from 3.5 kcal/mole for the low-volatile anthracite to 7.0 kcal/mole for the bituminous coal. The flow of methane through discs of coal was studied by Karn et al.,<sup>24</sup> activation energies of 13.6 kcal/mole were found for the methane flow measured along and across the bedding plane.

### C. BET Method

#### 1. BET Model and Equations

In 1938, Brunauer, Emmett, and Teller<sup>25</sup> extended the Langmuir<sup>26</sup> adsorption model that regarded the solid surface as an array of adsorption sites, each being capable of adsorbing one molecule. According to Langmuir's model, when a molecule from the vapor phase collides with an empty adsorption site, the molecule condenses and remains on the site for a mean period then evaporates. His model was based on adsorption restricted to a monolayer, even though he noted the possibility that the condensation and evaporation mechanism might apply to higher molecular layers.

The Braunauer, Emmett, and Teller approach extended Langmuir's mechanism to second and higher molecular layers in agreement with experimental results that adsorption was in fact occurring in multilayers.

Braunauer, Emmett, and Teller assumed that when equilibrium is reached at any pressure, varying numbers of molecules are being condensed at any site, and the heat of adsorption in all layers above the first is equal

to the latent heat of condensation.

In mathematical form, the results of Braunauer, Emmett, and Teller (the BET equation) can be expressed as<sup>27,28</sup>

$$\frac{P_2}{x_m(P_0 - P_2)} = \frac{1}{x_m C} + \frac{(C-1)}{x_m C} \frac{P_2}{P_0} \quad (3)$$

where  $P_2$  and  $P_0$  are the pressure in the vapor phase and the vapor pressure of the adsorbate at the adsorption temperature, respectively;  $x_m$  is the monolayer amount of adsorbate per weight of solid sample in cc/g at STP; and  $C$  is a constant given by:

$$C = \frac{a_1 b_2}{a_2 b_1} e^{(E_1 - E_L)/RT} \quad (4)$$

where  $E_1$  is the heat of adsorption in the first layer;  $E_L$  is the heat of liquefaction of the adsorbate;  $R$  is the gas constant; and  $T$  is the adsorbate temperature. The pre-exponential coefficient is generally considered unity.<sup>27</sup>

According to Equation 3 a plot of

$P_2/[x_m(P_0 - P_2)]$  versus  $P_2/P_0$  is linear, with the slope equal to  $(C-1)/x_m C$  and an intercept at  $P_2/P_0 = 0$  of  $1/x_m C$ . Solving for  $C$  and  $x_m$ , it is readily seen that:

$$x_m = (\text{slope} + \text{intercept})^{-1} \quad (5)$$

$$C = \text{slope}/\text{intercept} + 1. \quad (6)$$

Representative plots of this type as published in the original paper of Braunauer, Emmett, and Teller<sup>25</sup> using nitrogen at -196°C as

the adsorbate on various catalysts, are linear between a relative pressure ( $P_2/P_0$ ) of about 0.05 and 0.350. In most adsorbate-adsorbent systems, a linear BET plot does occur in that pressure range (0.05 to 0.350) although some workers (see reference 28) have found linear plots well outside that relative pressure range.

Once  $x_m$  has been determined by use of a BET plot and Equation 5, the calculation of the internal surface area is relatively straightforward. The specific surface  $S(m^2/g)$  is related to the monolayer capacity by means of the equation:

$$S = \frac{x_m N A_m}{M} \times 10^{-20} \quad (7)$$

where  $x_m$  is expressed as grams of adsorbate per gram of solid;  $M$  is the molecular weight of the adsorbate;  $N$  is Avogadro's constant ( $6.02 \times 10^{23}$  molecules/mole); and  $A_m$  in  $\text{\AA}^2$  is the molecular cross-sectional area of the adsorbate (the area one adsorbed molecule occupies on the surface of the solid in a complete monolayer). If  $x_m$  is expressed as cc. at STP per gram of solid, the molecular weight,  $M$ , is replaced with  $V_c$ , the volume in cc. at STP that one mole of an ideal gas occupies (22414 cc. per mole).

To use Equation 7 it is necessary to determine the value of the cross-sectional area of the adsorbate,  $A_m$ . Emmett and Braunauer<sup>29</sup> suggested that one could calculate this cross-sectional area by use of the density of the liquified or solidified adsorbate by use of the following equation:

$$A_m(\text{\AA}^2) = (4)(0.866) \left[ \frac{M}{4 \sqrt{2} N d} \right]^{2/3} \times 10^{16} \quad (8)$$

where  $M$  is the molecular weight of the adsorbate;  $N$  is Avogadro's number; and  $d$  is the density of the solidified or liquified adsorbate, g/cc. Equation 8 is based on the molecules being held in a two-dimensional close packing on the solid surface. For nitrogen as the adsorbate at -196°C, using a density of liquified nitrogen of 0.808 cc/g, Equation 8 yields  $A_m = 16.2 \text{ } \text{\AA}^2$ .

The BET model has had a number of criticisms because the model assumes that the surface is energetically uniform (that all adsorption sites are equal) and there is evidence that most solid surfaces are heterogeneous in adsorption energies. The model also considers molecules in all layers after the first as identical, implying that the adsorption potential is constant in all layers. Braunauer, Emmett, and Teller stated that the failure of the BET equation to fit data in relative pressure ( $P_2/P_0$ ) below 0.05 was due to the surfaces of the solid being heterogeneous, but they were unable to allow for this in their model.

## 2. Nitrogen Adsorption

The validity of internal surface areas as calculated by nitrogen adsorption isotherms (BET method) has been checked by electron microscopy. With the use of electron microscopy to determine the specific surface area of finely divided solid, comparisons between the two areas reveal that the BET surface areas, when using nitrogen at -196°C as the adsorbate ( $A_m = 16.2 \text{ } \text{\AA}^2$ ), generally give the correct value of the surface area of non-porous solids to within a few percent.

The use of the BET method and Equation 5, as stated previously, is a relatively straightforward procedure once the value of  $A_m$  for use in

Equation 7 is known. The value of  $16.2 \text{ \AA}^2$  for nitrogen at  $-195^\circ\text{C}$  as calculated from Equation 8 has been questioned by several workers.

Values for  $A_m$  for nitrogen at  $-195^\circ\text{C}$  have been reported in a range from  $13.0 \text{ \AA}^2$  to  $20 \text{ \AA}^2$ .<sup>\*</sup> Pierce and Ewing<sup>30</sup> have found that adsorption of nitrogen at  $-196^\circ\text{C}$  is localized on graphite, and have suggested that each molecule of nitrogen occupies a site covering four hexagons of the surface, with  $20.0 \text{ \AA}^2$  as the effective or apparent cross-sectional area of  $\text{N}_2$ .

### 3. Adsorption of Other Gases

Numerous other gases (adsorbates) have been used to determine internal surface areas by applying the BET method and Equation 8 to determine the cross-sectional areas of the liquified or solidified adsorbate molecules,  $A_m$ . When these values of  $A_m$  are used in Equation 7, significantly different values are obtained for the surface area of a solid compared with the areas obtained by use of nitrogen adsorptions at  $-196^\circ\text{C}$  with  $16.2 \text{ \AA}^2$  as the value of  $A_m$  for the nitrogen molecule.

Gregg and Sing<sup>28</sup> summarize results of many workers using different adsorbates including krypton, argon, n-butane, Freon-21, benzene, water, n-hexane, and many others. From experimental data by these workers, Gregg and Sing conclude that the differences in surface areas as calculated for nitrogen at  $-196^\circ\text{C}$  and for other vapors using Equations 7 and 8 are greater when the value of C in Equation 3 is small. Since C is a rough measure of the heat of adsorption and since the heat of adsorption depends on the degree of interaction between the solid and

---

<sup>\*</sup>Gregg and Sing (reference 28) summarize the results of several workers and list ranges of  $A_m$  that have been used.

vapor being used, a vapor may give different values of  $C$  and therefore  $A_m$  will be different on different adsorbents. Therefore it is necessary, whenever possible, to determine  $A_m$  for each adsorbate on each adsorbent by just determining the internal surface area of each adsorbent with nitrogen at  $-196^\circ\text{C}$  ( $A_m = 16.2 \text{ \AA}^2$ ), then by the adsorption of the other adsorbates and determine  $A_m$  from Equation 7 using  $S$  as the nitrogen based surface area in  $\text{m}^2/\text{g}$ .

Gregg and Sing<sup>28</sup> summarize values of the apparent cross-sectional area,  $A_m$ , commonly used for surface area determinations (calculated as stated above). Some of the vapors listed are argon at  $-195^\circ\text{C}$  with a range for  $A_m$  used of  $13-17 \text{ \AA}^2$ , krypton at  $-195^\circ\text{C}$  with a range for  $A_m$  of  $17-22 \text{ \AA}^2$ , and xenon at  $-195^\circ\text{C}$  with a range for  $A_m$  of  $18-27 \text{ \AA}^2$ . Values obtained for  $A_m$  from Equation 8 are 14.4, 20.0, and 25.0 for argon, krypton, and xenon (all at  $-195^\circ\text{C}$ ) respectively.

The value of  $A_m$  for the carbon dioxide molecule, as determined by Equation 8, at  $-80^\circ\text{C}$  and using a density of 1.56 for the solidified  $\text{CO}_2$  molecule, is  $14.1 \text{ \AA}^2$ . Walker and Kini<sup>31</sup> determined the cross-sectional areas of carbon dioxide at both  $-78^\circ\text{C}$  and  $25^\circ\text{C}$  and found that the average  $A_m$  is 20.7 and  $25.3 \text{ \AA}^2$ , respectively, on Graphon, Wear-Dust, and Vulcon 3 when compared to areas calculated from nitrogen at  $-195^\circ\text{C}$ . Aylmore<sup>32</sup> using carbon dioxide adsorption on various clay materials found the cross-sectional area of carbon dioxide molecules at  $-77^\circ\text{C}$  to vary from about 15.4 to  $42.2 \text{ \AA}^2$  when compared to nitrogen at  $-195^\circ\text{C}$  determined areas.

#### D. Dubinin - Polanyi Adsorption Equations

Dubini<sup>33,34</sup> extended the Polanyi Potential Theory<sup>35</sup> to predict

the variation in extent of micropore filling by adsorbates with variations in adsorption potential.

For adsorption of gases and vapors below their critical temperatures on carbonaceous adsorbents with extremely small micropores, where the interaction of opposite walls of the pores is the predominant effect to increase the adsorption potential, the adsorption equation takes the following form:<sup>4</sup>

$$\log_{10} V = \log_{10} V_0 - \frac{BT^2}{\beta^2} \log_{10}^2 \left( \frac{P_0}{P_2} \right) \quad (9)$$

where  $V$  = volume of gas adsorbed at STP per gram of solid at equilibrium pressure,  $P_2$ , expressed as cc/g.

$V_0$  = micropore capacity, cc/g

$P_0$  = vapor pressure of the adsorbate at the adsorption temperature,  $T(^{\circ}K)$

$\beta$  = affinity coefficient of adsorbate relative to nitrogen

$B$  = constant

A plot of  $\log_{10} V$  against  $\log_{10}^2 \left( \frac{P_0}{P_2} \right)$  is linear, with an intercept [at  $\log_{10}^2 \left( \frac{P_0}{P_2} \right) = 0$ ] equal to  $\log_{10} V_0$  and a slope equal to  $BT^2/\beta^2$ .

For gas adsorption at temperatures above the critical temperature of the adsorbate, the following equation was derived to describe the variation of the extent of pore filling with adsorption potential:<sup>36</sup>

$$\log_{10} V = \log_{10} V_0 - \frac{BT^2}{\beta^2} \log_{10}^2 \left( \frac{\tau^2 P_c}{P_2} \right) \quad (10)$$

where  $\tau$  = reduced temperature,  $T/T_c$ ;  $T_c$  being the critical temperature of the adsorbate,  $^{\circ}K$

$P_c$  = critical pressure of the adsorbate

$P_2$ ,  $V$ ,  $V_0$ ,  $B$ ,  $T$ , and  $\beta$  have the same meaning as for Equation 9.

If the adsorptions of the gases or vapors are restricted to a monolayer, then the micropore capacity  $V_0$  is equal to the monolayer volume of adsorbed gas  $x_m$  (refer to Equation 3). Emmett<sup>37</sup> suggested that the monolayer volume of gas,  $V_m$ , should be determined at final equilibration pressures corresponding to  $0.1 P_0$ . Emmett reasoned that  $x_m$  generally occurs at roughly a relative pressure ( $P_2/P_0$ ) of 0.1 on most adsorbates.

On a plot of Equation 9, according to Emmett's suggestion,  $\log_{10} x_m$  would equal  $\log_{10} V$  at  $\log_{10}^2 P_0/P_2$  equal to 1.0. On a plot of Equation 10,  $\log x_m$  would equal  $\log V$  when  $P_2$  was replaced with  $0.1 P_0$  in the abscissa,  $\log_{10}^2 (\tau^2 P_c/P_2)$ .

Once the value of  $x_m$  is known, the surface area of the adsorbent can be determined with the use of Equation 7.

#### E. Objectives

The objective of this research is to characterize the internal structure of raw coal and to follow the changes in the surface areas of coal with progressive extraction.

Before this can be reliably accomplished values for the molecular cross-sectional areas of the adsorbed molecules,  $A_m$ , must be determined. Using two Harshaw catalyst as adsorbates, the values of  $A_m$  for argon at  $-196^\circ\text{C}$ , carbon dioxide and carbon tetrafluoride at  $-77^\circ\text{C}$  have been determined using nitrogen at  $-196^\circ\text{C}$  as a standard.

Further studies were deemed necessary to characterize the adsorption of gases on 4A and 5A Linde molecular sieves. The molecular sieves

were chosen because their structures have been well studied and their structures are similar to coals. By comparing the results obtained by adsorption on sieves with those obtained on coal, many insights into the actual internal structure of coals are possible without extensive studies.

Surface area values determined by low-temperature (-196°C) adsorptions of either nitrogen or argon on coals are much lower than areas determined by the adsorption of carbon dioxide at -78°C, leaving in doubt what the true area is. Therefore, alternate methods to determine the internal surface areas of coal need to be investigated to ensure consistency of interpretation. Accordingly, the Dubinin-Polanyi equations have been applied to both low and high-temperature adsorption studies.

Lastly, carbon tetrafluoride, as an adsorbate on coals, appeared to be useful because the molecule is relatively inert with respect to the chemical structure of coal. The adsorption of carbon tetrafluoride at -77°C on both coals and sieves have been studied.

References

1. Zwietering, P. and Van Krevelen, D. W., Fuel, 33,331 (1954).
2. Gan, H., Nandi, S. P. and Walker, P. L., Fuel, 51,272 (1972).
3. Bond, R. L. and Spencer, D., Ind. Carbon and Graphite, 231 (1958).
4. Lamond, T. G. and Marsh, H., Carbon, 1,281 (1964).
5. Griffith, M. and Hirst, W., Proceedings of the Conference of the Ultrafine Structure of Coal and Coke, BCRUA, p.80 (1943).
6. Maggs, F.P.A., Proceedings of the Conference of the Ultrafine Structure of Coal and Coke, BCRUA, p.95 (1943).
7. Bond, R. L. and Maggs, F.P.A., Fuel, 28,172 (1949).
8. Malherbe, P. LE R., Fuel, 30,97 (1951).
9. Maggs, F.P.A., Nature,169,793 (1952).
10. Maggs, F.P.A. and Dryden, I., Nature,169,269 (1952).
11. Maggs, F.P.A., Research, Vol VI, No. 2, D1 (1952).
12. Bangham, D.H. and Franklin, R.E., Trans. Faraday Soc.,42B, 289 (1946).
13. Anderson, R.B., Hall, W.K., Lecky, J., and Stein,K., J. P. Chem., 60, 1548 (1956).
14. Schuyer,J. and Van Krevelen, D.W., Fuel,34,345 (1955).
15. Kini, K.A., Nandi,S.P., Sharma, J.N., Iyengar, M.S. and Lahiri, A., Fuel,35,71 (1956).
16. Kini, K.A., Fuel,43,173 (1964).
17. Anderson, R.B., Hofer, L.J.E. and Bayer, J., Fuel,41,559 (1962).
18. Walker, P. L. and Geller, I., Nature, 178,1001 (1956).
19. Czerski, L., Korta, A. and Lasoń, M., Roczn. Chem., 31,227 (1957).
20. Marsh, H. and Wynne-Jones, W.F.K., Carbon,1,269 (1964).

21. Lamond, T.G. and Marsh, H., Carbon, 1, 293 (1964).
22. Nandi, S.P. and Walker, P.L., Fuel, 43, 385 (1964).
23. Nandi, S.P. and Walker, P.L., Fuel, 49, 309 (1970).
24. Karn, F.S., Friedel, R.A., Thomas, B.M. and Sharkey, A.G., Fuel, 49, 249 (1970).
25. Braunauer, S., Emmett, P.H. and Teller, E., J.Am.Chem.Soc., 60, 309 (1938).
26. Langmuir, J.Am.Chem.Soc., 38, 2221 (1916).
27. Emmett, P.H., "Catalysis", Vol 1, chapter 2, New York (1954).
28. Gregg, S.J. and Sing, K.S.W., "Adsorption, Surface Area, and Porosity", chapter 2, Academic Press, New York (1967).
29. Braunauer, S. and Emmett, P.H., J.Am.Chem.Soc., 59, 310 (1937).
30. Pierce, C. and Ewing, B., J.Phys.Chem., 68, 2562 (1964).
31. Walker, P.L. and Kini, K.A., Fuel, 44, 453 (1965).
32. Aylmore, L.A.G., Clays and Clay Minerals, 22, 175 (1974).
33. Dubinin, M.M., Ind. Carbon and Graphite, 272 (1958).
34. Dubinin, M.M., Chem. Rev., 60, 235 (1960).
35. Young, D.M. and Crowell, A.D., "Physical Adsorption of Gases", p.13, Butterworths, London (1962).
36. Nikolaev, K.M. and Dubinin, M.M., Izvest.Akad.Nauk S.S.S.R., Otdel. Khim. Nauk, 1165 (1958).
37. Emmett, P.H., Private Communication, Aug. 15, 1975, U.C. Berkeley, Department of Chem. Eng.

## II. Equipment and Procedures

### A. Adsorption Equipment

#### 1. Manifold

Two volumetric apparatus were used to measure the internal surface areas of porous materials, one for pressures below atmospheric and one for normal and high pressures (to 1200 psig.). These were designed by the writers, and constructed in the University of California, College of Chemistry, machine shop. A mobile system was selected so that the entire adsorption apparatus could easily be moved, if necessary, from one laboratory to another laboratory with a minimum of disassembling and reassembling. The system also had to be capable of handling up to four different samples in any one day, either for degassing or for surface area determinations. Therefore four sample holders were required. This was convenient because four adsorption points on the BET plot could be taken in a two-hour period when allowing 30 minutes for equilibration. Thus in a 24-hour period, eight hours were required to determine the surface areas of all four samples, and the remaining 16 hours was available to degas the samples completely before starting the gas adsorptions.

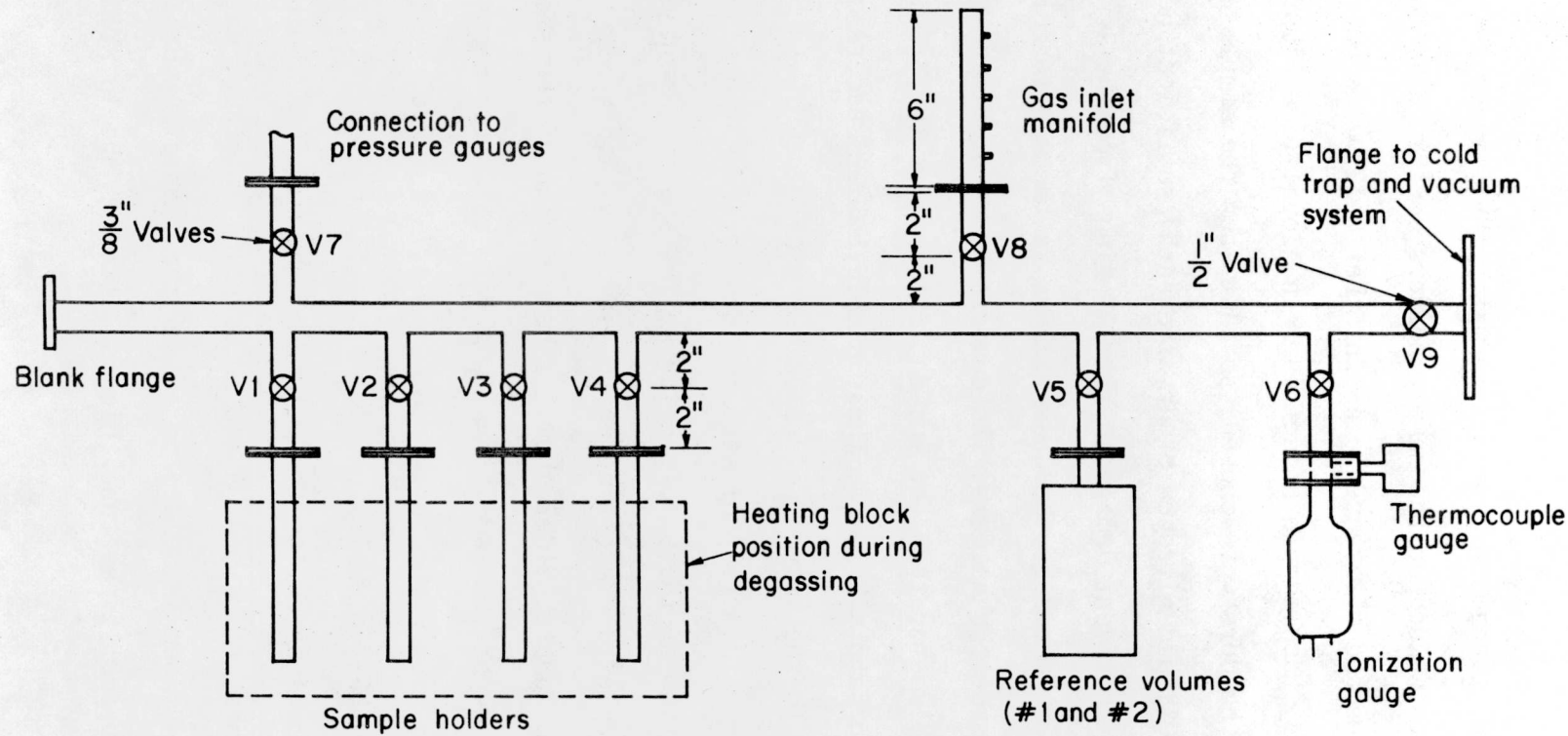
In order to prevent breakage during moving and/or experimentation, glassware was ruled out early in the design for the low-pressure apparatus and was not considered for the high pressure system. The material of construction selected for both systems was 304 stainless steel. Although the wall thicknesses of the tubes used are different for the low- and high-pressure systems, the linear dimensions of the two systems are identical so that each is interchangeable when mounting on the moveable frame.

Figure A-1 is the general drawing of the adsorption manifolds for both the low- and high-pressure apparatus. A  $\frac{1}{2}$  in. outside diameter (o.d.) 304 stainless steel tube is used as the manifold, with  $\frac{3}{8}$  in. o.d. stainless steel tubes welded to it to provide inlets for four sample holders, gas inlets, pressure gauges, ionization gauge, thermocouple gauge, and an outlet to the vacuum system. A total of nine valves were needed for each manifold; eight  $\frac{3}{8}$  in. valves and one  $\frac{1}{2}$  in. valve. Each valve is welded in place as shown in Figure 2-1. (Note: Figure A-1 shows the location of the holes drilled in the manifold where the  $\frac{3}{8}$  in. tubes and valves are welded.)

Tube extensions with  $\frac{3}{8}$  in. o.d. are welded onto each  $\frac{3}{8}$  in. valve and also onto connecting flanges at the other end, as shown in Figure 2-1. The flanges, 1.75 in. in diameter, were cut and drilled from 304 stainless steel bar stock. The flanges are 0.25 in. thick and contain an "O" ring groove cut into them to fit  $5/8" \times 3/32" \times 1/2"$  "O" rings. All connections to the manifolds are made by means of these flanges, using four 10-32,  $1/2"$  Allen-head bolts. The threaded holes for these bolts are symmetrically located on each of the flanges welded to the manifold. A total of 10 pairs of flanges were needed for all  $\frac{3}{8}$  in. tubing and one flange pair for the  $\frac{1}{2}$  in. manifold to close off one end with a blank half flange. (Refer to Figure 2-1).

Figure A-1c shows the two flanges that are attached to the rear of the manifold. These flanges are extra but are needed for calibration of the manifold volumes or other volumes.

The sample holders consist of  $\frac{3}{8}$  in. o.d. 304 stainless steel tubing, with caps welded at one end to seal the sample holder at that end. On the



-25-

XBL7510-7732

Figure 2-1. Assembled Adsorption Manifold

opposite end, flanges are welded to match the flanges on the manifold. These flanges welded on the sample holders contain drilled holes for the 3/8 in. tubes and clearance holes for the 10-32 bolts but contain no "O" ring grooves. Each sample holder is 7 in. long. (See Figure A-2). Seven inch sample holders were chosen, so that when the sample holders are immersed in a liquid nitrogen or dry-ice bath, sufficient heat transfer can take place to prevent damage to the "O" rings from the low temperatures.

In order to reduce the dead volumes in the sample holders, spacers are used inside the holders. The spacers are approximately 0.012 in. smaller in diameter than the inside diameters of the 3/8 in. o.d. tubes used for the sample holders. These sample holder spacers also extend through the flanges to the valves welded on the manifold.

The porous samples for surface-area determinations are placed into the bottom of the sample holders. The spacers are then inserted into the sample tubes resting on the samples. Figure A-2 shows a cross-section of a sample holder showing the position of the spacer and sample.

In the event that additional manifold volume is required, two reference volumes were constructed from 2.75 in. o.d. stainless steel tubes with 0.035 in. walls and are 6 and 12 in. long, to add approximately 550 or 1100 cc. to the volume of the manifold. Both ends of the 2.75 in. tubes are capped. A 3/8 in. tube, 1 in. long, with flange of the type described is welded to one of the caps after drilling a hole into the cap to fit the tube. Figure 2-1 shows the location of the reference volume(s).

The assembled manifold is shown in Figure 2-1. Valves V1 to V4

are the sample-holder valves, and V7 is the valve connected to the pressure gauges.

## 2. Auxiliary Equipment

Three interchangeable pressure gauges were purchased from Heise Bourdon Tube Co., all with 12 in. dials. The gauges are:

Heise Gauge No. 66027  
0-800 mm Hg. absolute incremented by 1 mm  
maximum hysteresis 0.8 mm

Heise Gauge No. 67578  
dual scale - 0-30 in. Hg.; 0-80 psig. incremented by 0.1 psig.  
maximum hysteresis 0.08 psig.

Heise Gauge No. 67577  
dual scale- 0-30 in. Hg.; 0-800 psig. incremented by 1 psig.  
maximum hysteresis 0.8 psig.

The pressure gauges are flush-mounted to the front of the moveable frame and connected to the flange on valve V7 by means of 3/8 in. tubing with 0.035 in. walls.

The gas inlet system to the manifold is attached to the flange on valve V8. The inlet gas manifold consists of a 6 in. 3/8 in. o.d. tube with 0.035 in. walls. (See Figure 2-1). Five 1/4 in. Gyrolok connectors are welded one inch apart on the gas inlet manifold. Quarter inch tubing connects the inlet gas manifold to the various gas cylinders. The 1/4 in. tubing connects the gas cylinders, first to Hoke #3232 M4B valves mounted on the front of the moveable frame, then to the Gyrolok fittings. The Hoke valves are used to control more closely the amount of gas expanded from the gas cylinders into the adsorption manifold.

Connected to the flange on valve V6 are the ionization and thermo-couple gauges. A Phillips ionization gauge is used with a glass-to-metal

seal attached to it. The metal portion of the seal is a 3/8 in. o.d. tube with a flange (identical to the flanges welded to the adsorption manifold) welded to it. The thermocouple gauge is an Ion Equipment Corp. Model TGC-102 and is connected to a flange spacer by means of a 1/8 in. threaded hole. The ionization and thermocouple gauges were connected in this manner so that both gauges would be connected to the same valve. The control units for these gauges are mounted on the right front side of the moveable frame in a 19 in. panel.

Valve V9 is the 1/2 in. valve. Welded to the tube extension leading from this valve is a 4 in. o.d. (3/8 in. thick) flange. This flange enables the adsorption manifold to be connected to a liquid nitrogen cold trap by means of 6-1/4×3/8 in. steel bolts. The cold trap is capable of holding approximately 2 liters of liquid nitrogen for approximately 8 hours. Connected to the other end of the cold trap is an oil diffusion pump, Consolidated Vacuum Corp. Model PMCS-2C with Dow Corning DC 704 diffusion pump oil. A Kinney KC-2 vacuum pump (capacity 2 ft<sup>3</sup>/min) is used as the forepump. The vacuum pump is connected to the diffusion pump by a 2-ft section of 3/4 id. flexible copper tubing.

### 3. Manifold Specifications

The following specifications were adopted:

#### a. Low-Pressure Manifold

Wall thicknesses of all tubes (3/8 and 1/2 in. tubes), 0.035 in.

Length of sample volume space (X in Figure A-2), 1.2 in.

Sample-holder spacer design, hollow tube w/welded caps on each end.

Length of spacer (Z in Figure A-2), 9.8 in.

Valves: Vacuum Accessories Corp. of America, stainless steel--

8 - 3/8 in. model #TE-SSV-038-IL

1 - 1/2 in. model #TE-SSV-050

b. High Pressure Manifold

Wall thicknesses of all tubes, 0.049 in.

Length of sample volume space (X in Figure A-2), 2.0 in.

Sample-holder spacer design-solid 0.250 bar stock with a slightly reduced o.d.

Length of spacer (Z in Figure A-2), 7.0 in.

Valves: Hoke Manufacturing Co., stainless steel--

8 - 3/8 in. model #4213Q6Y

1 - 1/2 in. model #4313R8Y

System: pressure-tested to 2000 psig. hydraulically.

4. Heating Block

The heating block was constructed from a solid aluminum block and is used to heat the samples during degassing. Four 1/2 in. o.d. holes were drilled into the top of the block for the four sample holders, while a 1/4 in. hole was drilled at an angle for thermometers.

A Briskeat flexible heating tape (1" x 6 feet, 432 watts, 115 volts) is wrapped around the sides of the heating block and is covered with one inch asbestos insulation. Asbestos insulation with four 1/2 in. and one 1/4 in. holes cut into it was also placed on the top of the heating block.

A temperature controller (Hallikinen Instrument Model #1109A) is used to control the temperature of the heating block by means of a Hallikinen #1196 Resistance thermometer with a fiberglass block sensor

attached to the top of the aluminum heating block by two sheet metal screws. The resistance thermometer temperature range is -100° F to 500° F so that the maximum temperature of degassing is 260° C. The temperature controller controls the temperature of the heating block  $\pm 1^{\circ}\text{C}$ .

Aluminum sheet metal was placed around the side insulation. The heating block assembly was mounted to a laboratory jack stand so that it could easily be lowered and raised into position to heat the samples. In Figure 2-1, the dashed lines indicate the position of the heating block during the heating (degassing) of the samples.

#### B. Calibration of Equipment

##### 1. Procedure

A calibrated volume of  $515 \pm 1\text{cc}$ . was used to calibrate the volumes of the manifolds, sample holders, and reference volumes. The calibrated volume was connected to flange F1 (see Figure A-1) by means of another flange half which had a Hoke 1/8" needle valve #4171M2B attached to it.

The calibrations were all constant-temperature expansions from one volume into another volume, since pressure equilibration time is very rapid. The temperature of the manifold was recorded during the expansions by use of a 0-50° C thermometer having 0.1° C increments. It was attached to the 1/2 in. manifold tube with fiberglass insulation wrapped around the bulb of the thermometer.

Valve V7 was open during all the calibrations, since this valve connects the manifold to the pressure gauges. First, the manifold with the Hoke valve attached to flange F1 was calibrated. The smaller reference volume (#1) was then calibrated using this manifold plus valve volume. After removing the calibrated volume from flange F1 and

replacing the flange half with the blank flange, the manifold was then calibrated using the reference volume (#1). Finally, the sample holders and larger reference volume (#2) were calibrated by use of the manifold.

The following equations and procedures were used for the constant temperature calibrations using nitrogen.

a. Manifold with Hoke valve attached to flange F1

With the Hoke valve open, the manifold and calibrated volume (515cc) were evacuated to a pressure less than 100 microns (1 micron =  $10^{-3}$  torr). The Hoke valve was then closed, and nitrogen expanded into the manifold. The initial pressure  $P_1$  was recorded along with the temperature of the manifold. The gas was then expanded into the calibrated volume by opening the Hoke valve. The final pressure  $P_2$  was then recorded.

Volume of manifold plus Hoke valve,  $V_{MH} = 515/[ (P_1/P_2) - 1 ]$  cc.

b. Reference Volume (#1)

With the Hoke valve closed, valve V5 was opened. The manifold and reference volume were evacuated to a pressure less than 100 microns. Valve V5 was then closed, and nitrogen expanded into the manifold. Both the initial pressure  $P_1$  and temperature of the manifold were recorded. The final pressure  $P_2$  was recorded after expanding the gas into the reference volume by opening valve V5.

Volume of reference volume (#1),  $V_{R1} = V_{MH}(P_1/P_2 - 1)$  cc.

c. Manifold

With the calibrated volume and the Hoke valve removed, both the

manifold and reference volume (#1) were evacuated to a pressure less than 100 microns. Valve V5 was then closed and nitrogen expanded into the manifold. The initial pressure  $P_1$  and temperature of the manifold were recorded. Valve V5 was then opened and the final pressure,  $P_2$ , recorded.

Volume of the manifold,  $V_M = V_{R1}/[(P_1/P_2) - 1]$  cc.

d. Sample holders and reference volume (#2)

The calibration procedure for each sample holder and reference volume (#2) were identical. The manifold and the volume to be calibrated were evacuated to below 100 microns. The valve to the volume to be calibrated was then closed and nitrogen expanded into the manifold. The initial pressure  $P_1$  and temperature of the manifold were then recorded. After expanding the gas into the volume, the final pressure  $P_2$  of the system was recorded.

Volume to be calibrated =  $V_M(P_1/P_2 - 1)$  cc.

Each volume was calibrated ten times so that the  $\pm$  limits of the uncertainty could be determined from the standard deviation  $\sigma$ . For ten calibrations, at a 90% confidence level, the limits of the uncertainty is 0.611 times the standard deviation.<sup>1\*</sup>

2. Calibration Results

a. Low-Pressure Manifold with 800 mm Hg. gauge

$$V_{MH} = 523 \pm 1 \text{ cc.}$$

$$V_{R1} = 563 \pm 1 \text{ cc.}$$

\* References are listed at the end of this chapter.

$V_M = 470 \pm 1 \text{ cc.}$

Sample Holder #1 =  $20.92 \pm 0.09 \text{ cc.}$

Sample Holder #2 =  $20.99 \pm 0.09 \text{ cc.}$

Sample Holder #3 =  $20.84 \pm 0.07 \text{ cc.}$

Sample Holder #4 =  $21.19 \pm 0.08 \text{ cc.}$

Reference Volume (#2) =  $1102 \pm 1 \text{ cc.}$

b. High Pressure Manifold with 80 psig. gauge <sup>\*\*</sup>

$V_{MH} = 170.9 \pm 0.1 \text{ cc.}$

$V_{R1} = 550.4 \pm 0.4 \text{ cc.}$

$V_M = 149.5 \pm 0.1 \text{ cc.}$

Sample Holder #1 =  $6.09 \pm 0.03 \text{ cc.}$

Sample Holder #2 =  $5.94 \pm 0.04 \text{ cc.}$

Sample Holder #3 =  $6.00 \pm 0.04 \text{ cc.}$

Sample Holder #4 =  $5.97 \pm 0.04 \text{ cc.}$

### C. General Degassing and Adsorption Procedures

#### 1. Preparation of Samples Before Degassing

The samples (raw coal, extracted coal, and porous solids) were placed in a vacuum oven at  $130^\circ\text{C}$  overnight for approximately 16 hours with a vacuum pump running continuously to maintain a pressure of about 10 torr.

The samples were then cooled to room temperature and weighed with a microbalance to  $\pm 0.0001$  grams. This weight represented the dry weight of the raw coal only, since at the temperatures and pressures of degassing, both the extracted coals and the porous solids

\*\*

The 800 psig. gauge was not used in these studies.

lose volatiles that could not be removed at the oven conditions.

The samples were then placed into the sample holders, and the sample-holder spacers inserted so that they rested on the samples. The sample-holder assembly was then attached to the manifold by means of the flanges.

The weight of the samples used in the sample holders varied from 0.7 to 1.1 grams depending upon the specific volume of the sample. The weight of the raw or extracted coal samples was approximately one gram whereas the weight of the catalysts and molecular-sieve samples varied from 0.7 to 1.1 grams.

## 2. Degassing Procedure

After the sample holders were attached to the manifold, valves V1 to V4, V6, and V9 were opened while all other valves remained closed. The vacuum pump was then turned on to evacuate the system. The temperature controller was set at the desired temperature for the degassing of the samples; 130°C for both the raw and extracted coals and 240°C for the molecular sieves and catalysts. The heating block was raised to its heating position as indicated in Figures 2-1.

When the pressure in the system was below 0.1 torr as indicated on the thermocouple gauge, the cooling water to the diffusion pump was adjusted to a flow rate of approximately one-third gallon per minute. At the pressure of 0.1 torr or below, the diffusion pump was turned on and liquid nitrogen poured into the cold trap to condense any oil vapors and prevent them from entering the system.

The temperature of degassing was controlled within  $\pm 1.0^{\circ}\text{C}$  as measured by either a 0-150°C or 0-260°C thermometer inserted into the heating block.

The samples were degassed for approximately 16 hours at the appropriate temperature. Two hours before the end of the degassing period, liquid nitrogen was again poured into the cold trap. After 16 hours both the temperature and pressure of degassing were recorded. A pressure of  $10^{-5}$  torr as indicated by the Phillips ionization gauge was generally obtained in the system at the end of the degassing time.

The valves to the sample holders and valve V9 were then closed to seal the samples from the manifold and vacuum system. The temperature controller and diffusion pump were shut off. The heating block was then lowered to its lowest position, and then pulled out from under the sample holders. The vacuum pump and cooling water were left on for another half hour to cool the diffusion pump oil to room temperature before exposing the oil to atmospheric pressure, so as to minimize atmospheric oxidation of the oil.

### 3. Adsorption Procedure

When using the Heise 800 mm Hg absolute pressure gauge, the gauge was zeroed when the manifold was at a pressure less than 100 microns as indicated on the thermocouple gauge control. However, when the 80 psig. Heise gauge was used, the gauge was zeroed when exposed to atmospheric pressure. The system and gauge were both vented to atmospheric pressure then this gauge was zeroed. The barometric pressure in the laboratory was recorded from a Princo mercurial barometer.

After valve V6 was closed in order to isolate both the ionization and thermocouple gauges from the system, a 0.25 liter Dewar flask with either liquid nitrogen, dry ice/methanol, or distilled water was used to maintain the adsorption temperatures. The Dewar was placed on a

laboratory jack stand and raised so that approximately three inches of the sample holder was immersed into the bath.

The adsorbate gas was then expanded into the manifold with all valves closed except V7. The initial pressure and temperature of the manifold were recorded. The valve to the sample holder that contained the sample having its area determined was then opened, allowing the adsorbate gas to expand into that sample holder and be adsorbed on the sample. An equilibration time of 30 minutes was allowed for each adsorption. After this time, the final temperature and pressure of the system was recorded. The temperature of the liquid bath was also recorded. When either a dry ice/methanol or distilled water bath was used in the Dewar, the temperature was measured by a -100°C to 50°C toluene thermometer or by a 0-50°C thermometer, respectively.

The temperature of the liquid nitrogen bath was determined by inserting the barometric pressure of the laboratory into the vapor pressure equation for liquid nitrogen, [Equation 20, below] , and solving for the temperature. This temperature was then used as the temperature of the liquid nitrogen bath.

Successive adsorption points were determined for each sample over a relative pressure range of 0.05 to 0.30 for all low-temperature adsorptions, and up to pressures of 800 mm Hg. for the high-temperature adsorptions. The amount of gas adsorbed was obtained by first closing the valve to the sample holder, expanding additional adsorbate gas into the manifold, recording the pressure and temperature of the manifold, and subsequently expanding the gas into the sample holder by opening the valve. The final pressure and temperature of the system

and the bath temperature were again recorded after allowing the 30-minute equilibration time.

The procedure for each sample holder was identical to that described above. Before starting gas adsorptions on another sample, the valve to the previous sample was closed and the manifold evacuated to a pressure below 100 microns. The Dewar was also moved to the new sample holder. The above procedure for gas adsorptions were then repeated.

After the gas adsorptions, the samples were allowed to reach room temperature, then the samples were reweighed to determine the amount of volatiles released during degassing. The initial weights minus the amount of volatiles released were used as the true weights.

#### D. Equations for Surface Area Determinations

The following nomenclature and equations were used to determine the amount of adsorbate gas adsorbed on the porous samples at standard temperature and pressure.

##### 1. Nomenclature

$n$  adsorption point indicator;  $n = 1, 2, 3, 4$

$n_a$  amount of adsorbate adsorbed on the sample, moles

$m$  weight of the porous solid less volatiles, grams

$P_{1,n}$  initial pressure in manifold before expanding the adsorbate into the sample holder for the  $n$ th adsorption point. When  $n-1 = 0$ ,  $P_{n-1}$  is equal to 0

$P_{2,n}$  final pressure in manifold after expanding the adsorbate gas into the sample holder for the  $n$ th adsorption point

$P_0$  vapor pressure of adsorbate at the adsorption temperature

$P_s$  standard pressure, 1 atm.

$R$  the gas constant

$T_{1,n}$  initial temperature of manifold for the nth point, °K

$T_{2,n}$  final temperature of manifold for the nth point, °K

$T_0$  adsorption temperature, °K

$T_s$  standard temperature, 273 °K

$V_M$  manifold volume, cc.

$V_{sh}$  sample holder volume, cc.

$V_{sh2}$  volume of sample holder immersed in the liquid bath, cc.  
This volume was considered to be at temperature,  $T_0$ .

$V_{sh1}$  volume of sample holder not immersed in the liquid bath, cc.  
This volume was considered to be at the same temperature as the manifold

$V_s$  volume of porous solid, cc.

$V$  volume of gas adsorbed at STP per gram of sample, cc/g

Note:  $V_{sh} = V_{sh1} + V_{sh2}$  (11)

## 2. Volume of Gas Adsorbed

initial moles of gas in manifold and sample holder for the nth adsorption point equals

$$\frac{P_{1,n} V_M}{R T_{1,n}} + \frac{P_{2,n-1} V_{sh1}}{R T_{2,n-1}} + \frac{P_{2,n-1} (V_{sh2} - V_s)}{R T_0} \quad (12)$$

final moles of gas in manifold and sample holder after the nth adsorption equals

$$\frac{P_{2,n} V_M}{R T_{2,n}} + \frac{P_{2,n} V_{sh1}}{R T_{2,n}} + \frac{P_{2,n} (V_{sh2} - V_s)}{R T_0} \quad (13)$$

moles of gas adsorbed = initial moles - final moles =  $n_a$

$$n_a = \frac{1}{R} \left[ V_M \left( \frac{P_{1,n}}{T_{1,n}} - \frac{P_{2,n}}{T_{2,n}} \right) + V_{sh1} \left( \frac{P_{2,n-1}}{T_{2,n-1}} - \frac{P_{2,n}}{T_{2,n}} \right) + (V_{sh2} - V_s) \frac{(P_{2,n-1} - P_{2,n})}{T_0} \right] \quad (14)$$

Note: the n-1 terms represent the amount of gas in the sample holder when it was closed after the last adsorption point.

$$\text{Volume of gas adsorbed at STP} = \frac{n_a R T_s}{P_s} \quad (15)$$

$$V = \frac{n_a T_s R}{P_s} \quad (16)$$

Substituting Equation 14 into Equation 16 and rearranging:

$$V = \frac{T_s V_M}{P_s} \left[ \frac{P_{1,n}}{T_{1,n}} - \frac{P_{2,n}}{T_{2,n}} + \frac{V_{sh1}}{V_M} \left( \frac{P_{2,n-1}}{T_{2,n-1}} - \frac{P_{2,n}}{T_{2,n}} \right) + \frac{(V_{sh2} - V_s)}{V_M T_0} \frac{(P_{2,n-1} - P_{2,n})}{T_0} \right] \quad (17)$$

The value of V obtained from Equation 17 was then used in Equations 3, 9, or 10 to construct either BET or Dubinin-Polanyi plots.  $P_2$  in these equations above also correspond to  $P_2$  in both the BET and D-P equations.

### 3. Low-Pressure Manifold

The internal volumes of the sample holder valves used on this manifold are approximately 16.5 cc. The sample holder spacers extend up to these valves leaving only a annulus volume between the spacers and the inside walls of the sample holders of approximately 0.54 cc. The value of  $V_{sh1}$  was taken equal to the sum of these two volumes, 17.0 cc. The

values of  $V_{sh2}$  differed for each sample holder and were determined by use of equation 11.

The values of  $V_{sh1}$  and  $V_{sh2}$  (cc.) used were:

	$V_{sh1}$	$V_{sh2}$
sample holder #1	17.0	3.92
sample holder #2	17.0	3.99
sample holder #3	17.0	3.84
sample holder #4	17.0	4.19

#### 4. High-Pressure Manifold

The internal volumes of the Hoke valves used are 0.2 cc. The values used for  $V_{sh2}$  were determined as follows: the volume of the 1.2 in. sample space was calculated, then the volume of an annulus of length 1.8 in. was determined and added to the former volume. Thus the values of  $V_{sh2}$ , the volumes of the sample holders immersed to a depth of 3 in. into the adsorption bath were determined to be 1.80 cc.

$V_{sh1}$  and  $V_{sh2}$  values (cc.) used were:

	$V_{sh1}$	$V_{sh2}$
sample holder #1	4.29	1.80
sample holder #2	4.14	1.80
sample holder #3	4.20	1.80
sample holder #4	4.17	1.80

The volume of the solid samples,  $V_s$ , used in Equation 17 depended on the sample used. For the catalysts and molecular sieves,  $V_s$  was determined from the density data reported by the manufacturers. For all the coal samples (raw and extracted), the value used for  $V_s$  was

determined by using 1.50 as the true density of all coals. If the value for  $V_s$  is in error by 100%, the maximum error in the amount of gas adsorbed per gram,  $V$ , would be roughly 2% in a typical gas adsorption calculation using Equation 17. Because the volume ratios of sample holders to manifolds are relatively small, the last two terms on the right side of Equation 17 are considerably smaller than the first two terms, thus allowing the use of approximate values for  $V_s$  when the exact values are not available.

#### E. Vapor-Pressure Data

The compressed gases used in the adsorption studies were obtained from Lawrence Berkeley Laboratory, except for the carbon tetrafluoride (Freon-14) which was obtained from the Matheson Company Inc., Newark, California.

The vapor pressure equations for the gases used are as follows  
( $T$  is in degrees K):

##### 1. Carbon Dioxide<sup>2</sup>

Boiling point - 56.6 °C; sublimation point -78.5° C.

a. Below atmospheric pressure

$$\log_{10} P_{\text{mm Hg.}} = - \frac{1.367 \times 10^3}{T} + 9.9082 \quad (18)$$

b. Above atmospheric pressure

$$\log_{10} P_{\text{atm.}} = 1.863 - \frac{(T_c - T)}{T} \left[ 3.0067 - 9.03 \times 10^{-3} (T_c - T) + 2.37 \times 10^{-4} (T_c - T)^2 + \dots \right] \quad (19)$$

where  $T_c$  is the critical temperature ( = 304.2 °K)

2. Nitrogen<sup>2</sup>

Boiling point, 77°K.

a. Below atmospheric pressure

$$\log_{10} P_{\text{mm Hg.}} = - \frac{334.6}{T} + 7.578 - 0.00476 T \quad (20)$$

b. Above atmospheric pressure

$$\log_{10} P_{\text{atm.}} = 5.764 - \frac{853.5}{T} + \frac{54372}{T^2} - \frac{17883500}{T^3} \quad (21)$$

3. Argon<sup>2</sup>

Boiling point, 87.5 °K.

a. Below atmospheric pressure

$$\log_{10} P_{\text{mm Hg.}} = - \frac{356.5}{T} + 6.9605 \quad (22)$$

b. Above atmospheric pressure

$$\log_{10} P_{\text{atm.}} = 4.85 - \frac{634.4}{T} + \frac{30769}{T^2} - \frac{1076464}{T^3} \quad (23)$$

4. Carbon Tetrafluoride,  $\text{CF}_4$ <sup>3</sup>

Boiling point, 145 °K.

$$\log_{10} P_{\text{mm Hg.}} = 5.044 - \frac{701.7}{T} + 1.75 \log_{10} T - 0.00767T \quad (24)$$

References

1. ASTM Manual on Quality Control of Materials, Publication 15-C, p.43, Philadelphia, Pa. (1951)
2. Washburn, E.W. (Ed.) "International Critical Tables", Vol III, p.203, 204, and 235
3. Stacey, M., Tatlow, J.C. and Sharpe, A.G. (editors), "Advances in Fluorine Chemistry", Vol 4, p.158, Butterworths, London (1965)

### III. Adsorption On Porous Solids

#### A. Types and Properties of the Porous Solids Used

##### 1. Harshaw Catalyst

Two Harshaw Chemical Company catalysts were used as adsorbents in these studies, silicated high activity alumina catalyst, Al-1602 T1/8, and a iron catalyst, Fe-301 T1/8. They have the following bulk properties, as reported by the manufacturer:

	<u>Al-1602 T1/8</u>	<u>Fe-301 T1/8</u>
Apparent Bulk Density, lb/ft <sup>3</sup>	52	62
Pore Volume, cc/g	0.48	0.31
Surface Area, m <sup>2</sup> /g	210-240	41
Composition	91% Al <sub>2</sub> O <sub>3</sub> , 6% SiO <sub>2</sub>	20% Fe <sub>2</sub> O <sub>3</sub> on alumina

The catalyst were used in their pelleted form, except where indicated, for the surface area determinations. The true specific volumes of the solid catalysts, calculated from the manufacturer's data, were found to be 0.696 and 0.72 cc/g for the iron and alumina catalysts respectively. These values for the true specific volumes were used in Equation 17 to determine the volume of gas adsorbed at STP.

The average pore diameters of the two catalysts were also determined by a rearranged Equation 1

$$d = 4v/S \times 10^4 \quad (1a)$$

and found to be 302 and 91-94 Å for the iron and alumina catalyst, respectively.

##### 2. Linde Molecular Sieves

Adsorption studies were also performed on two molecular sieves obtained from Union Carbide Corporation, Linde Division. Both 4A and

5A molecular sieves were used as adsorbents; they have the following bulk properties, as reported by Linde:

	<u>4A</u>	<u>5A</u>
Nominal Pore Diameter, Å	4	5
Hydrated Particle Density, g/cc	2.03	2.03
Activated Particle Density, g/cc	1.57	1.57
Bulk Density, lb/ft <sup>3</sup>	41	45

The true specific volumes of the solid sieves were taken to be equal to 0.50 cc/g and used for  $V_s$  in Equation 17.

#### B. Molecular Cross-Sectional Area Determinations

The catalysts and molecular sieves were both degassed for 16 hours at a temperature of 240 °C to a pressure of  $10^{-5}$  torr. An equilibration time of 30 minutes was allowed for all adsorptions. The catalysts were used to determine the molecular cross-sectional areas of the adsorbed gases at low temperatures. Four gases were used: nitrogen and argon adsorbed at 77 °K, and carbon dioxide and carbon tetrafluoride at 196 °K. A liquid nitrogen bath was used for the 77 °K bath and a dry ice/methanol bath for the 196 °K bath.

The high-pressure adsorption apparatus was used for the carbon tetrafluoride adsorptions at 196 °K, since the vapor pressure at that temperature is 181 psi.<sup>1</sup> \* All other adsorptions were done with the low-pressure apparatus except where noted differently. All low-temperature adsorptions were conducted in a relative pressure range of 0.05 to 0.30.

\* References are listed at the end of this chapter

Gas adsorptions on each catalyst using  $N_2$ , Ar, and  $CO_2$  were repeated three times, while  $CF_4$  adsorptions were repeated four times. All the adsorption data are presented in Table 3-1. Surface areas are listed in the first four columns of Table 3-1. These areas were determined using  $A_m$  values calculated by use of Equation 8 or with  $A_m$  values most commonly used. A density of 1.96 g/cc was used in Equation 8 to determine the  $A_m$  value for  $CF_4$  at 196°K. All  $A_m$  values used to determine the surface areas are listed in Table 3-1.

The last three columns in Table 3-1 indicate the values of  $A_m$  required to give surface areas identical to those obtained from nitrogen adsorption at 77 °K. The surface areas as determined by nitrogen adsorptions at 77 °K ( $A_m = 16.2 \text{ } \text{\AA}^2$ ) were thus used as the standard. The surface areas as determined by the adsorption of  $CO_2$ , Ar, and  $CF_4$  were then compared to average surface areas of 50.4 and  $170.5 \text{ m}^2/\text{g}$  for the iron and alumina catalyst, respectively, to obtain the values needed for  $A_m$ .

For example, the adsorption of  $CO_2$  at 196 °K gave a surface area of  $117 \text{ m}^2/\text{g}$  using  $A_m = 17.0 \text{ } \text{\AA}^2$  on the alumina catalyst. The value of  $A_m$  needed for the  $CO_2$  molecule at 196 °K on the alumina catalyst would have to be  $170.5/117$  times 17.0, or  $24.8 \text{ } \text{\AA}^2$ . Similar calculations were made to obtain other cross-sectional areas.

The BET plots for the adsorption data presented in Table 3-1 are included in Appendix B, as Figures B-1 to B-10. Figures B-1 and B-6 show representative adsorption data of all four gases on a particular catalyst. The data used in these two figures were taken from the other figures presented in Appendix B.

Table 3-1. BET Surface Areas

Catalyst	Surface Areas Based on Assumed Molecular Areas (m <sup>2</sup> /g)				Best Molecular Areas Based on N <sub>2</sub> Surface Area (Å)		
	N <sub>2</sub> 77 °K A <sub>m</sub> =16.2	Ar 77 °K A <sub>m</sub> =14.4	CO <sub>2</sub> 196 °K A <sub>m</sub> =17.0	CF <sub>4</sub> 196 °K A <sub>m</sub> =19.3	Ar 77 °K	CO <sub>2</sub> 196 °K	CF <sub>4</sub> 196 °K
Fe-301 T1/8	52.3	41.6	39.5	71.5	17.4	21.7	13.6
	50.0	41.2	38.3	67.1	17.6	22.4	14.5
	48.8	43.5	38.6	63.2	16.7	22.2	15.4
				61.6			15.8
average	50.4						
Al-1602 T1/8	172	148	118	166	16.6	24.6	19.8
	170	147	116	193	16.7	25.0	17.1
	170*	145	117	164	16.9	24.8	20.1
	170			147			22.4
average	170.5						
					17.0 <sup>†</sup>	23.4 <sup>†</sup>	17.3 <sup>†</sup>

<sup>\*</sup> High Pressure Manifold<sup>†</sup> Average A<sub>m</sub>

### C. BET Versus Dubinin-Polanyi Equation

Comparison between surface areas as determined by the use of the BET equation and by the Dubinin-Polanyi equation for adsorptions below the critical temperatures of the adsorbates are listed in Table 3-2.

All surface area data listed in Table 3-2 were determined by using the average  $A_m$  values listed in Table 3-1 for carbon dioxide, argon, and carbon tetrafluoride. The standard value of  $16.2 \text{ \AA}^2$  was used to determine the nitrogen surface areas.

The experimental adsorption data were used in both the BET and Dubinin-Polanyi equations. The BET surface area data listed in the first four columns of Table 3-2 for the two catalysts were determined by ratios from the average  $A_m$  value to the  $A_m$  value initially used to determine areas listed in Table 3-1. This ratio was then multiplied by the areas in the latter table to obtain the surface areas corresponding to the average  $A_m$  values. For example, on the alumina catalyst,  $\text{CO}_2$  adsorption at  $196^\circ \text{ K}$  ( $A_m = 17.0 \text{ \AA}^2$ ) gave a surface area of  $118 \text{ m}^2/\text{g}$ . Using the average  $A_m$  listed in Table 3-1 of  $23.4 \text{ \AA}^2$ , the adjusted surface area becomes:

$$\left(\frac{23.4}{17.0}\right) (118 \text{ m}^2/\text{g}) = 162 \text{ m}^2/\text{g}$$

and is presented in Table 3-2. Similar calculations were done for all adsorptions on these two catalysts.

Adsorption studies on both the 4A and 5A molecular sieves and on the alumina catalyst ground to a fine powder are also presented in Table 3-2. BET plots for these three adsorbents are included in the Appendix, as Figures B-11, B-12, and B-13 for the 4A, 5A, and powdered alumina catalyst respectively.

Table 3-2. Surface Area Data ( $\text{m}^2/\text{g}$ )  
Based on Best Molecular Areas

Gas and Temperature Adsorbent	BET Equation				D-P Equation		
	$\text{N}_2$ 77 °K $A_m = 16.2$	Ar 77 °K $A_m = 17.0$	$\text{CO}_2$ 196 °K $A_m = 23.4$	$\text{CF}_4$ 196 °K $A_m = 17.3$	$\text{N}_2$ 77 °K $A_m = 16.2$	Ar 77 °K $A_m = 17.0$	$\text{CO}_2$ 196 °K $A_m = 23.4$
Fe-301 T1/8	52.3	49.1	54.4	64.1	56.6	51.6	53.3
	50.0	48.6	52.7	60.1	55.0	56.7	53.3
	48.8	51.4	53.1	56.7 55.2	55.2	51.6	55.9
Al-1602 T1/8	172	175	162	149 173	192	169	148
	170	174	160	147	187	172	151
	170	171	161	132	187	174	142
4A Sieve	11	10	480	< 1	12	11	540
5A Sieve	480	540	570	250	580	620	690
Al-1602 T1/8 Powder	169						

Dubinin-Polanyi plots for the adsorption of nitrogen, argon, and carbon dioxide are also included in the Appendix, labeled Figures B-14 to B-16. The Dubinin-Polanyi surface areas were determined by using a value of  $x_m$  taken when the final equilibration pressure,  $P_2$ , in Equation 9 was equal to one-tenth the vapor pressure of the adsorbate at the adsorption temperature. This occurs when the abscissa,  $\log_{10}^2 P_0/P_2$ , is equal to 1.0.

Dubinin-Polanyi surface areas were not determined for carbon tetrafluoride adsorptions or for nitrogen adsorptions on the powdered alumina catalyst.

#### D. High-Temperature Adsorptions

Adsorption of nitrogen and argon at 196 °K and of carbon dioxide at 292 °K was also studied with the use of the Dubinin-Polanyi equations. A methanol/dry ice bath and a distilled water bath were used to obtain temperatures of 196 and 292°K, respectively.

The adsorption of nitrogen and argon were done above their respective critical temperatures\* of 126 and 151°K therefore Equation 10 was used for these two gases. Carbon dioxide adsorptions were done below its critical temperature of 304°K enabling the use of Equation 9.

All high temperature adsorptions were done in the low pressure adsorption apparatus using the 800 mm Hg. Heise gauge over the gauge's full pressure range.

The results of the high temperature adsorptions are presented in Table 3-3. Listed in this table are values obtained for  $x_m$  after extrapolating the absorption data on Dubinin-Polanyi plots to where the final

\*Vapor pressures for N<sub>2</sub> and Ar at 196 °K were obtained by extending the vapor pressure Equations 21 and 23 beyond the critical temperatures.

equilibration pressure,  $P_2$ , was equal to one-tenth the vapor pressure of the adsorbate at the adsorption temperature.

For carbon dioxide adsorptions at 292°K, the value of  $x_m$  was taken where the abscissa,  $\log_{10} P_0/P_2$ , on the Dubinin-Polanyi plot was equal to 1.0. Whereas, the abscissa on the nitrogen and argon plots,  $\log_{10} \tau^2 P_c/P_2$ , was 0.10 and 0.40, respectively.

Also listed in Table 3-3 are  $A_m$  values needed to give correct surface areas for the adsorbents used in the high-temperature adsorptions. The surface areas of these adsorbents were taken from the previous section and are 50.4, 171, and  $480 \text{ m}^2/\text{g}$  for the iron catalyst, alumina catalyst, and 4 Å sieve, respectively.

The Dubinin-Polanyi plots for these adsorptions are included in Appendix B and are labeled Figures B-17 to B-20.

Table 3-3. High-Temperature Adsorption Data

Adsorbent		$x_m$ at 0.1 $P_0$ (cc/g)	$A_m^2$ ( $\text{\AA}^2$ )
Fe-301 T1/8 $S = 50.4 \text{ m}^2/\text{g}$	$\text{CO}_2$ at 292 °K	42.3	4.4
		51.0	3.7
Al-1602 T1/8	$\text{N}_2$ at 196 °K	188	3.4
		240	2.7
		222	2.9
$S = 171 \text{ m}^2/\text{g}$	$\text{Ar}$ at 196 °K	235	2.7
		255	2.5
4A Sieve $S = 480 \text{ m}^2/\text{g}$	$\text{CO}_2$ at 292 °K	48.0	13.3
		45.8	13.9
		50.9	12.7
4A Sieve	$\text{N}_2$ at 196 °K	329	5.4
$S = 480 \text{ m}^2/\text{g}$	$\text{Ar}$ at 196 °K	500	3.6
	$\text{CO}_2$ at 292 °K	103	17.3

References

1. Stacey, M., Tatlow, J.C., and Sharpe, A.G. (editors), "Advances in Fluorine Chemistry", Vol 4, p. 158, Butterworths, London (1965).

#### IV. Adsorption on Raw Coals

##### A. Analysis of the Raw Coals Used

###### 1. Roland Seam Coal

One of the coals studied was a Wyoming subbituminous coal from the Roland top seam of the Wyodak Mine at Gillette, Wyoming. This raw coal is the same coal that was used in the extraction studies done by Draemel and Grens.<sup>1</sup>\*

The raw coal was obtained from the Wyodak Corp. and reduced to minus -1/32" following ASTM Method D-346. This minus-1/32" coal was separated by alternate shovels into 15-pound portions and sealed in plastic bags which were stored in a 55-gallon drum. Representative samples from these bags were taken as needed<sup>\*\*</sup> with the use of a riffler, further reduced in a ball mill to minus-28 Tyler mesh (30 U.S. mesh)<sup>†</sup> and placed in a desiccator under either vacuum or 100-300 mm helium pressure. This coal, minus-28 mesh, was used in these gas adsorptions and also by Draemel and Grens.<sup>††</sup>

---

\* References are listed at the end of this chapter

\*\* Not all of the minus-1/32" bagged coal was reduced to minus-28 mesh initially: only when additional minus-28 mesh coal was needed. The minus-1/32" coal was exposed to an air atmosphere while stored in the plastic bags.

† Tyler mesh sizes are used for all coal particle sizes.

†† Draemel and Grens describe in detail the handling procedure for the Roland seam coal.

From the minus-28 mesh coal, 28 to 150 and minus-150 mesh samples were obtained by sieving and riffling. Separate ASTM ultimate analysis were done by Commerical Testing and Engineering Co., Denver Laboratory (CT&E) on both the minus-28 and 28 to 150 mesh samples. The results of these tests\* indicate the same composition for both samples. The ranges of the coal analysis are presented in Table 4-1.

The weight percents of the two sieved samples obtained from the minus-28 mesh coal used in these studies were 80 and 20% for the 28 to 150 and minus-150 mesh samples, respectively.

## 2. Illinois No. 6 Coal

The other coal studied was an Illinois No. 6 bituminous coal. This coal was obtained through the Illinois State Geological Survey, Urbana, Illinois and shipped from the mine in two 55 gallon drums. The coal as received had a particle size of 1.5 in. Two separate proximate and ultimate analysis were done on the as received coal by CT&E. The analysis ranges are presented in Table 4-2.

A representative sample of the as received coal was then reduced to minus-28 mesh according to ASTM Method D-346. From this minus-28 mesh coal, both a 28 to 150 and a minus-150 mesh samples were obtained by sieving and riffling.

All three samples (minus-28, 28 to 150, and minus-150) were stored in friction-lid paint cans under an atmosphere of nitrogen until needed.

---

\* A total of four separate analysis were performed by CT&E on both the minus-28 and 28 to 150 samples.

Table 4-1  
Analysis of Roland Seam Coal

Proximate Analysis		
	as received	dry basis
% Moisture	23.43-23.83	-----
% Ash	10.40-11.49	13.64-15.08
% Volatile	29.04-35.52	37.93-47.23
% Fixed Carbon	30.16-36.17	39.60-47.23
BTU	8226-8372	10800-10954
% Sulfur	0.70-0.94	0.92-1.23

Ultimate Analysis		
	as received	dry basis
% Moisture	23.43-23.83	-----
% Carbon	47.02-47.37	61.67-62.19
% Hydrogen	3.79-4.04	4.97-5.30
% Nitrogen	0.73-0.87	0.96-1.13
% Chlorine	0	0
% Sulfur	0.70-0.94	0.92-1.23
% Ash	10.40-11.49	13.64-15.08
% Oxygen (difference)	11.72-13.35	15.40-17.51

Table 4-2  
Analysis of Illinois No. 6 Coal

Proximate Analysis		
	as received	dry basis
% Moisture	12.62-12.67	-----
% Ash	14.53-14.61	16.63-16.73
% Volatile	32.54-33.39	37.24-38.23
% Fixed Carbon	39.33-40.31	45.04-46.13
BTU	9988-10001	11431-11452
% Sulfur	3.64-3.95	4.17-4.52

Ultimate Analysis		
	as received	dry basis
% Moisture	12.62-12.67	-----
% Carbon	56.03-56.31	64.16-64.44
% Hydrogen	3.89- 3.92	4.45- 4.49
% Nitrogen	1.15- 1.17	1.32- 1.34
% Chlorine	0	0
% Sulfur	3.64- 3.95	4.17- 4.52
% Ash	14.53-14.61	16.63-16.73
% Oxygen (difference)	7.42- 7.85	8.49- 8.98

The weight percents of the two sieved fractions obtained from the minus-28 mesh coal were 55 and 45% for the 28 to 150 and minus-150 mesh samples, respectively.

#### B. Low-Temperature Gas Adsorption

All coal samples were first placed in a vacuum oven overnight (approximately 16 hours) at 130 °C with a vacuum connected to the oven. A pressure of about 10 torr was maintained while drying the coal samples.

The raw coal was then cooled to room temperature, weighed, and placed in the adsorption apparatus. The coal was then degassed at 130 °C for 16 hours to a pressure of  $10^{-5}$  torr. An equilibration time of 30 minutes and a relative pressure range to 0.35 was used for all adsorptions. Adsorption temperatures of 77 and 196 °K were maintained with liquid nitrogen and dry ice/methanol baths respectively.

##### 1. Adsorption on Minus-28 Mesh Coals

The adsorption of nitrogen and argon at 77 °K and of carbon dioxide and carbon tetrafluoride at 196 °K were studied on the minus-28 mesh raw coals. All adsorptions were measured in the low-pressure apparatus except for the  $\text{CF}_4$  adsorptions which were made in the high-pressure system. The results are presented in Table 4-3.\* Comparisons of carbon dioxide surface areas determined by both the BET and Dubinin-Polanyi equations are also presented in this table. The Dubinin-Polanyi surface areas were determined from  $x_m$  values taken where the equilibration pressure,  $P_2$ , was equal to one-tenth the vapor pressure of  $\text{CO}_2$  at 196 °K. This corresponds to an abscissa,

\* Ash content (dry basis) used for DAF (dry-ash free) surface areas:  
Roland Seam Coal 15.08%  
Illinois No. 6 16.73 %

Table 4-3. Adsorption on minus-28 mesh raw coals

Adsorbate	Equation	$A_m$ ( $\text{\AA}^2$ )	Roland Seam ( $\text{m}^2/\text{g}$ , DAF basis)	Illinois No. 6 ( $\text{m}^2/\text{g}$ , DAF basis)
$\text{N}_2$ at 77 °K	BET	16.2	< 1	94
Ar at 77 °K	BET	17.0	< 1	68
$\text{CF}_4$ at 196 °K	BET	17.3	<< 1	43
	BET	23.4	106	227
			105	
$\text{CO}_2$ at 196 °K	D-P	23.4	71	208
			75	

$\log_{10}^2 P_0/P_2$ , equal to 1.0 on the D-P plot of Equation 9.

Included in Appendix B are the BET and Dubinin-Polanyi plots for the results presented in Table 4-3. The plots are labeled Figures B-21, 23 and 25. The surface areas noted on these plots are also on a dry basis. For the adsorption of  $CF_4$  at 196 °K on the Roland seam coal, a BET plot was not constructed because  $CF_4$  adsorption did not occur on this coal.

## 2. Surface Area Versus Coal Particle Size

The adsorption of carbon dioxide at 196 °K was studied on the 28 to 150 and minus-150 mesh samples of both the Roland and Illinois No. 6 coals.

Both 28 to 150 coal samples were also reduced by a ball mill to minus-150 mesh size. Carbon dioxide adsorptions were also studied on these samples.

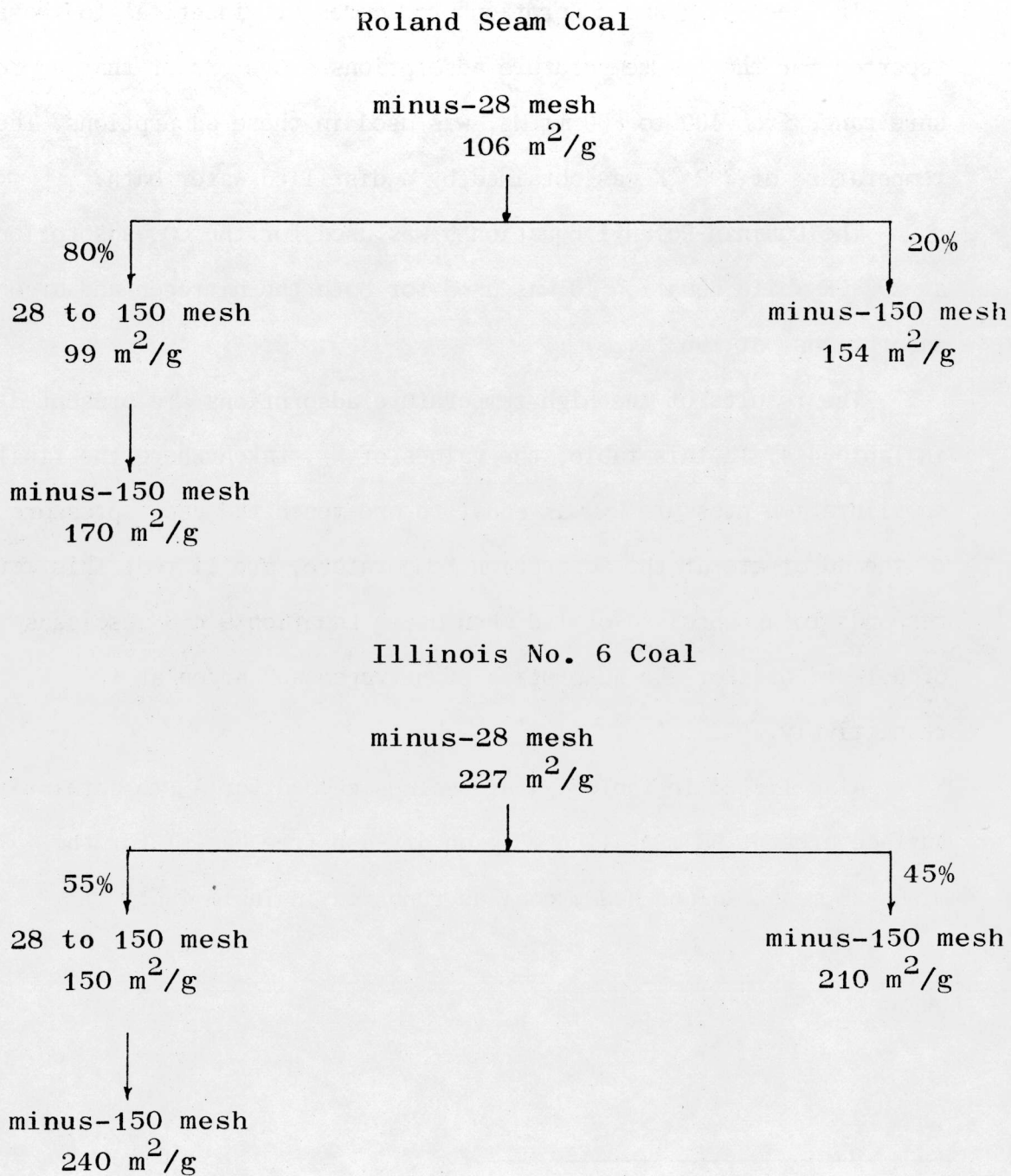
Figure 4-1 shows the results of the  $CO_2$  adsorptions. The BET surface areas listed on that figure are on a dry-ash free basis and were determined by using a value of  $A_m$  equal to  $23.4 \text{ } \text{\AA}^2$ . Also listed on Figure 4-1 are the weight percents of the 28 to 150 and minus-150 mesh samples obtained when the initially minus-28 mesh coal was sieved. The BET surface areas for the minus-28 mesh coals were those reported in Table 4-3 determined from  $CO_2$  adsorptions at 196 °K.

The BET plots for the results presented in Figure 4-1 are included in Appendix B and are labeled Figures B-22 and 24.

## C. High-Temperature Adsorption

The adsorption of nitrogen and argon at 196 °K (above their critical temperatures) and carbon dioxide at 292 °K was also studied

Figure 4-1. Surface Area vs. Particle Size  
(  $\text{m}^2/\text{g}$ , DAF basis )



on the minus-28 mesh Roland seam coal using the Dubinin-Polanyi equations.

The degassing and adsorption procedures are identical to those reported for the low-temperature adsorptions above except that a pressure range from 100 to 800 mm Hg. was used in these adsorptions. The temperature of 292 °K was obtained by a distilled water bath.

The Dubinin-Polanyi Equation 9 was used for the  $\text{CO}_2$  adsorptions at 292 °K while Equation 10 was used for both the nitrogen and argon adsorptions\* at 196 °K.

The results of the high-temperature adsorptions are presented in Table 4-4. In this table, the values of  $x_m$ , taken where the final equilibration pressure  $P_2$  was equal to one-tenth the vapor pressure of the adsorbate at the adsorption temperature, are listed. This corresponds to an abscissa of 1.0 when using Equation 9 and abscissas of 0.1 and 0.4 for the adsorption of nitrogen and argon at 196 °K, respectively.

Also listed in Table 4-4 are values needed for  $A_m$  to obtain a surface area of  $90 \text{ m}^2/\text{g}$  ( $106 \text{ m}^2/\text{g}$  on dry-ash free basis) for the minus-28 mesh, Roland seam, coal as reported in Table 4-3.

---

\* Vapor pressures for  $\text{N}_2$  and Ar were obtained by extending the vapor pressure Equations 21 and 23 beyond the critical temperatures.

Table 4-4. High-Temperature Adsorptions  
minus-28 mesh Roland seam coal  
 $S = 90 \text{ m}^2/\text{g}$  (dry basis)

Adsorbate	$x_m$ (cc/g, STP)	$A_m$ ( $\text{\AA}^2$ )
CO <sub>2</sub> at 292 °K	34.6	9.7
N <sub>2</sub> at 196 °K	340	0.98
Ar at 196 °K	182	1.8

References

1. Draemel, D. and Grens, E., Lawrence Berkeley Laboratory Report: LBL-4434 (1975).

## V. Surface-Area Variations of Extracted Coal

### A. Extracted Coal Samples

The extracted coal samples used in these adsorption studies were obtained from Draemel and Grens.<sup>1\*</sup> The detailed extraction procedures and results are presented by Draemel and Grens in that paper.

They used tetralin, benzene, phenol, decalin, and hexane as solvents in their reflux liquid extractions on the Roland seam coal. Extractions at temperatures below 250°C, were made on minus-28 mesh coal, whereas at temperatures of 250°C and above, 28 to 150 mesh coal was used.

The Roland seam raw coal used for extraction by Draemel and Grens was the coal used for the adsorption studies reported in Chapter IV.

The time and temperatures of the extractions varied, as did the extraction yields obtained. The residues (extracted coal samples) were dried following each extraction at 130 °C and 200 mm Hg. for 24 hours, while N<sub>2</sub> was swept over the samples at 60-80 cc/minute. The dried extracted coals were then stored in a desiccator under vacuum or 100-300 mm Hg. helium pressure until needed.

### B. Surface Areas of the Extracted Coal

The extracted coal samples were taken from the desiccator and redried under the same conditions as reported for the raw coals in Chapter IV. The degassing and adsorption procedures for the extracted

---

\*References are listed at the end of this chapter.

coals were also the same reported for the raw coal samples. However, the final degassing pressure for the extracted coals varied between  $10^{-5}$  and  $10^{-4}$  torr apparently owing to small residues of solvents in some of these samples.

BET surface areas determined by carbon dioxide adsorption at 196 °K were performed on all extracted coal samples using an  $A_m$  value of  $23.4 \text{ \AA}^2$  for the  $\text{CO}_2$  molecule.

The surface areas obtained for the extracted coals are presented in Table 5-1. The yield data listed in this table were taken from Draemel and Grens.<sup>1</sup> Repeat runs (extractions and surface area measurements) were conducted with several solvents at several temperatures and times, as indicated on Table 5-1. The surface area ranges ( $\text{m}^2/\text{g}$ , DAF basis) for the repeated runs are as follows (refer to Table 5-1 for the duration of these extractions):

<u>solvent</u>	<u>temperature (°C)</u>	<u>surface area range</u>
tetralin	200	99-110
tetralin	250	170-177
tetralin	300	215-269
tetralin	350	265-269
phenol	250	189-198

The surface areas of the extracted coal must be compared to the corresponding raw coal surface area. If the coal was extracted below 250°C, the raw coal used (minus-28 mesh) had a initial surface area of  $106 \text{ m}^2/\text{g}$  (DAF basis) whereas, for extractions at 250 °C or above the raw coal (28 to 150) had a surface area of  $99 \text{ m}^2/\text{g}$  (DAF basis).

Table 5-1. Surface Areas of Extracted Roland Seam Coal

Solvent	Temperature (°C)	Time (hr.)	Extraction Yield (DAF,wt.%)	BET	Surface Areas (m <sup>2</sup> /g) <sup>†</sup>
				Dry Basis	A <sub>m</sub> = 23.4 DAF Basis*
Benzene	150	4	5.05	154	181
Benzene	200	4	4.23	158	186
Benzene 1	250	4	7.79	164	193
Benzene	200	72	8.30	167	197
Tetralin	150	4	5.66	95	112
Tetralin 2	200	4	6.58	84	99
Tetralin 1,2	250	4	8.67	144	170
Tetralin 1,2	300	4	15.56	201	237
Tetralin 1,2	350	4	31.72	225	265
Tetralin 1	350	8.5	34.63	221	260
Tetralin	200	67	9.45	131	154
Tetralin	200	200	8.33	118	139
Phenol	200	4	19.01	115	135
Phenol 1,2	250	4	33.99	168	198
Phenol 1	300	4	57.46	197	232
Phenol	200	32	29.57	133	157
Hexane	200	100			
Benzene	200	100			
Tetralin	200	100			
		cumulative	7.13	110	130
Decalin	200	4	5.47	108	127

\* Ash content (dry basis): 15.08%

<sup>†</sup>Minus-28 mesh coal, S = 106 m<sup>2</sup>/g DAF

basis, used as feed except where indicated

1 28 to 150 mesh raw coal used, S = 99 m<sup>2</sup>/g

DAF basis

2 Repeat run(s) conducted

The variation of surface area with extraction yield and with extraction time is shown in Figures 5-1 and 5-2 respectively. The solid lines in these figures connect extractions at the same temperatures (isothermal lines) using the same solvent. The dashed lines in Figure 5-1 are drawn to indicate approximate trends of surface area vs. extraction yield for the three main solvents.\*

Also reported in Figure 5-2 are two 2-hour extractions (tetralin and benzene at 200 °C) not reported by Draemel and Grens but included here to help establish the trends on this figure.

BET plots of the extracted coals are included in Appendix B and are labeled Figures B-28 to 33.

---

\* Verification of the high phenol yields is presently being carried out by Grens.

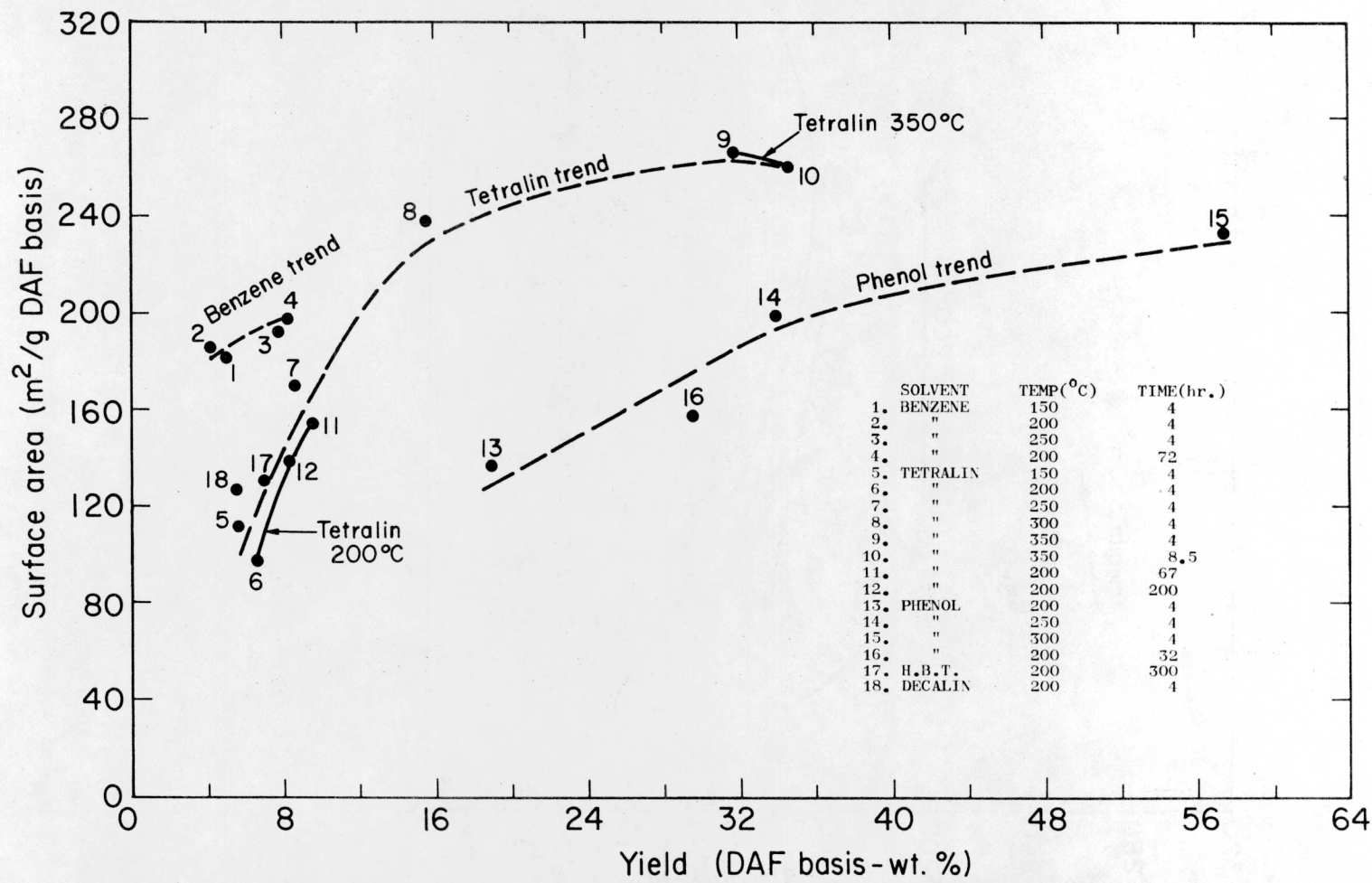


Figure 5-1. Surface Area vs. Extraction Yield

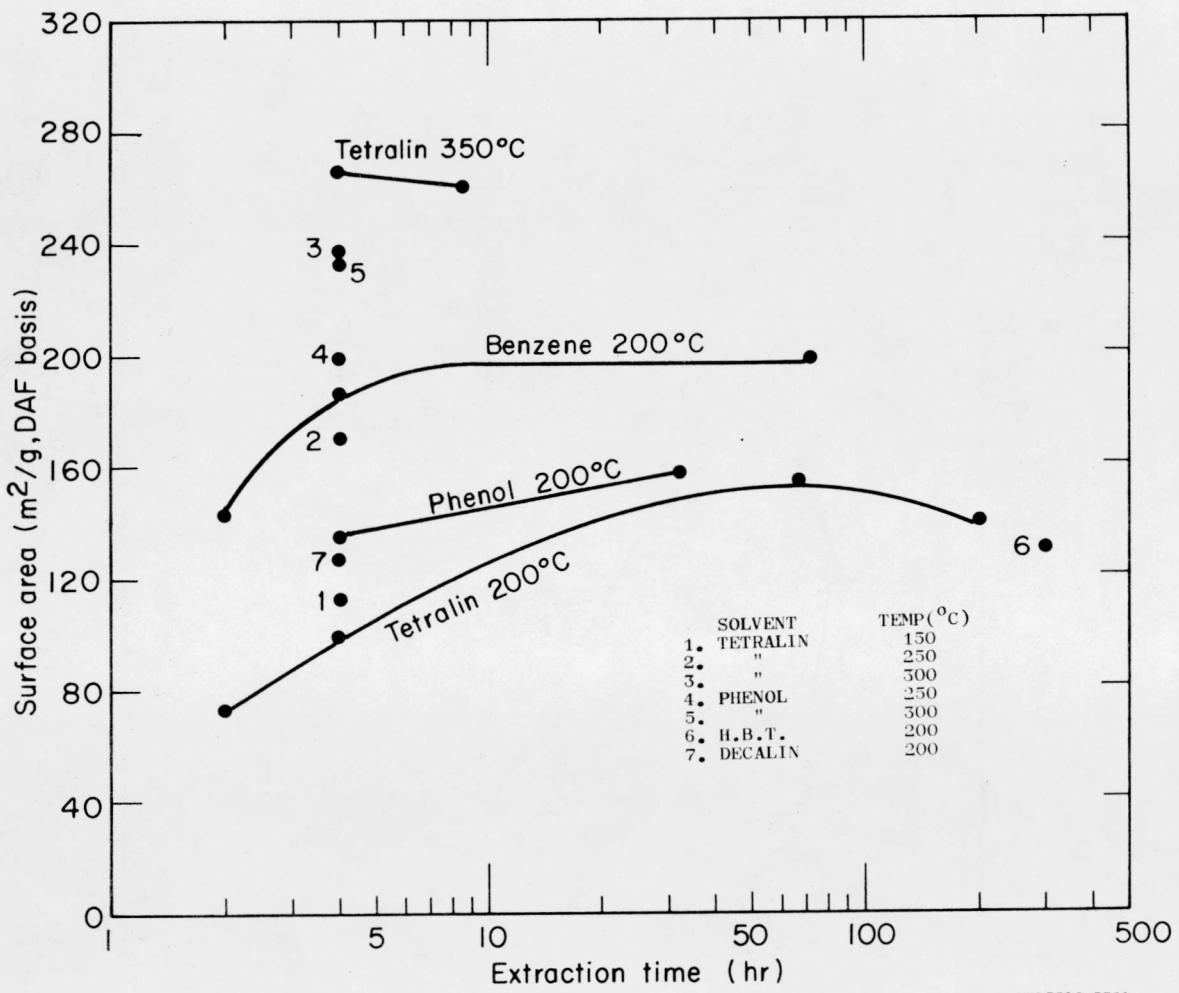


Figure 5-2. Surface Area vs. Extraction Time

References

1. Draemel, D. and Grens, E., Lawrence Berkeley Laboratory Report: LBL-4434 (1975).

## VI. Discussion of Results

In this chapter, comparisons between the results presented in the preceding three chapters are compared to results published in the literature using the same adsorbates and similar adsorbents.

### A. Adsorption on Catalysts and Molecular Sieves

#### 1. Nitrogen Adsorption on Catalysts

Surface areas obtained from the adsorption isotherms of nitrogen at 77 °K on the two Harshaw catalysts, Al-1602 T1/8 and Fe-301 T1/8, compare reasonably well with surface areas reported by the manufacturer. The values reported by Harshaw are bulk properties on representative samples of the particular catalyst and not necessarily absolute values on all catalyst samples. The values reported by Harshaw of 41 and 210-240  $\text{m}^2/\text{g}$  for the Fe-301 T1/8 and Al-1602 T1/8 catalysts, respectively, were obtained after reducing the pelleted catalyst to a powder. Surface areas obtained on the pellet catalysts in this study were 50.4 and 171  $\text{m}^2/\text{g}$  as reported in Table 3-1. The differences should not depend on particle size; they are probably due mostly to variations in the catalysts themselves, and to a lesser extent, to differences in technique in the two different laboratories.

When pellets of the alumina catalyst were ground to a fine powder using a mortar and pestal, the surface area did not change; 171  $\text{m}^2/\text{g}$  for the pelleted and 169  $\text{m}^2/\text{g}$  for the powdered sample.

#### 2. Molecular Cross-Sectional Areas of $\text{CO}_2$ , $\text{Ar}$ , and $\text{CF}_4$

Using nitrogen adsorption at 77 °K as the standard, cross-

sectional areas for the carbon dioxide, argon, and carbon tetrafluoride molecules were determined, using the two Harshaw catalysts as adsorbents. (Refer to Table 3-1.)

The values obtained for the argon molecules at 77°K and for the carbon dioxide molecules at 196 °K can readily be compared to values published in the literature. Gregg and Sing<sup>3</sup> provide a range of values that have been assumed or determined for the argon molecule at 78 °K, 13-17  $\text{\AA}^2$ , depending on the adsorbent used. The average value obtained for argon at 77 °K on the two catalysts in this study was 17.0  $\text{\AA}^2$ .

Carbon dioxide cross-sectional areas were reported by Walker and Kini<sup>4</sup> using several adsorbents. The range of values obtained by these workers was 18.9 to 21.7  $\text{\AA}^2$  at 195°K. Values calculated from the surface areas reported by Alylmore<sup>5</sup> for the  $\text{CO}_2$  molecule at 196 °K range from 15 to 42  $\text{\AA}^2$  on several samples of clay. As reported in Table 3-1, the average value obtained for the  $\text{CO}_2$  molecule at 196 °K was 23.4  $\text{\AA}^2$ .

No adsorption studies of carbon tetrafluoride at 196 °K or at other temperatures are reported in the available literature. An average value of 17.3  $\text{\AA}^2$  was obtained, using the two catalysts used in this study.

Emmett<sup>6</sup> suggested that the reason why  $A_m$  values determined by the use of Equation 8 and by comparisons to the nitrogen isotherms on the same adsorbent are not identical is due to the selectivity of different adsorbates for different adsorption sites. He reasoned

that, when the values from Equation 8 are lower than the calibrated areas, each adsorbed molecule takes up more area than predicted by that equation because most surfaces are not energetically homogeneous. By relating the adsorption isotherms of one adsorbate to nitrogen isotherms at 77 °K on the same adsorbent, an adjusted molecular cross-sectional area is obtained that takes into account the heterogeneity of the adsorbent surfaces.

### 3. Molecular Sieve Areas

Adsorption of nitrogen and argon at 77 °K on Linde 4A molecular sieves (1/8 in. pellets) gave BET surface areas orders of magnitudes smaller than adsorption of carbon dioxide at 196 °K. The areas obtained were 11,10, and  $480 \text{ m}^2/\text{g}$  from the nitrogen, argon, and carbon dioxide adsorptions respectively. (See Table 3-2). These results indicate that at liquid nitrogen temperatures nitrogen and argon molecules are unable to penetrate the ultrafine pores of the 4A sieves which have pore diameters equal to  $4\text{\AA}$  in the 30-minute equilibration time whereas carbon dioxide molecules can, and therefore yield much larger surface areas.

The results obtained in this study using 4A sieves are similar to results published by Lamond and Marsh.<sup>7</sup> They obtained surface areas on powdered Linde 4A sieves less than  $1 \text{ m}^2/\text{g}$  and  $610 \text{ m}^2/\text{g}$  from the adsorption of  $\text{N}_2$  at 77°K and  $\text{CO}_2$  at 195°K, respectively. They did not determine argon adsorptions.

Surface areas obtained in this study on Linde 5A molecular sieves (1/8 in. pellet) were 480, 540, and  $570 \text{ m}^2/\text{g}$  as determined from the adsorption isotherms of  $\text{N}_2$  and Ar at 77 °K and  $\text{CO}_2$  at 196 °K,

respectively. These results show that all three gases are capable of penetrating the 5A porous structure which contains 5Å diameter pores. Lamond and Marsh<sup>7</sup> also obtained similar results for the 5A surface area, 580 and 530 m<sup>2</sup>/g from the adsorption of N<sub>2</sub> at 77 °K and CO<sub>2</sub> at 195 °K respectively.

The ability of carbon dioxide molecules to penetrate the porous structure of the 4A sieve at 196 °K is thought to be due to the higher rate of diffusion that is possible at 196 °K. As reported in Chapter I of this paper, a relative diffusivity ratio of  $1.3 \times 10^{-7}$  is obtained, between nitrogen at 77 °K and carbon dioxide at 196 °K, taking equal activation energies of 4 kcal/mole for both gases. This calculation shows that the time required for the nitrogen molecules to diffuse into the 4A structure at 77 °K would be several orders of magnitude greater than for the carbon dioxide molecules at 196 °K. Therefore, using equilibration times for adsorptions of 30 minutes, the nitrogen molecules do not have time to penetrate the 4A sieve whereas at 196 °K the carbon dioxide molecules penetrate and adsorb on the 4A sieve microstructure. The same reasoning explains the low argon adsorption at 77 °K.

The adsorption of carbon tetrafluoride at 196 °K on both 4A and 5A molecular sieves yielded low surface areas. Values obtained (see Table 3-2) were less than 1 m<sup>2</sup>/g for the 4A sieve, and 250 m<sup>2</sup>/g for the 5A sieve. These results indicate that the carbon tetrafluoride molecules are not capable of penetrating the 4A structure at all and can only penetrate about 50% of the 5A structure in an equilibration time of 30 minutes.

Breck et al.<sup>8</sup> list critical dimensions, i.e. diameters of the circumscribed circle of smallest cross-section of the molecule, for argon and nitrogen at 77 °K and CO<sub>2</sub> at 273 °K. They determined the critical diameters to be 3.84, 3.0, and 2.8 Å for nitrogen, argon, and carbon dioxide, respectively. Huggins<sup>9</sup> determined interatomic distances for the C-F bond in CF<sub>4</sub> and for N-N bonds to be 1.40 and 1.49 Å, respectively. These two sets of atomic distances by Breck and Huggins indicate that the size of the molecules is not the major factor, if any, in the inability of N<sub>2</sub>, Ar, and CF<sub>4</sub> molecules to penetrate 4A (and 5A in the case of CF<sub>4</sub>) sieves: Ar and CO<sub>2</sub> have roughly the same critical dimensions, but one molecule can penetrate the 4A sieve and one cannot.

Owing to differences in the abilities of N<sub>2</sub>, Ar, CF<sub>4</sub>, and CO<sub>2</sub> to penetrate pores of different sizes, it may be possible to estimate pore size distributions. Such a method would use carbon dioxide adsorptions at 196 °K to determine the total surface area of an adsorbent containing ultrafine pores. Then successive determinations of nitrogen adsorptions at 77 °K and CF<sub>4</sub> at 196 °K would permit the estimation of surface areas of pores greater than 4 and 5 Å, respectively.

This suggested method involves less work both experimentally and mathematically than other methods used to determine pore size distributions, described by Gregg and Sing [reference 3, Chapter III].

#### 4. BET Versus Dubinin-Polanyi Surface Areas

Surface areas determined by both the BET and Dubinin-Polanyi equations from low-temperature adsorption data have been compared in this study. (Refer to Table 3-2). The results using nitrogen and argon

at 77 °K and carbon dioxide at 196 °K on both catalysts and sieves indicate that the two equations yield similar surface areas.

Comparisons between BET and D-P surface areas on several adsorbents including 4A powdered and 5A pellet sieves have been reported by Lamond and Marsh,<sup>7</sup> Walker and Patel,<sup>10</sup> and by Marsh and Siemienwska.<sup>2</sup> All three research teams showed that either equation could be used to determine surface areas on these adsorbents satisfactorily.\* Lamond and Marsh obtained surface areas for the 5A sieve of 650 and 580 from  $N_2$  adsorption at 77 °K, and 550 and 530  $m^2/g$  from  $CO_2$  adsorption at 196 °K, using the BET and D-P equations respectively.

##### 5. High-Temperature Adsorptions

The adsorption of nitrogen and argon at 196 °K (above their critical temperatures) and carbon dioxide at 292 °K on one or both catalysts and on the 4A sieve gave high  $x_m$  values for each gas-solid pair studied. (Refer to Table 3-3). When these  $x_m$  values are used in Equation 7 along with surface areas determined from the low-temperature adsorptions, low  $A_m$  values result. The best straight lines through the five adsorption points on the D-P plots (Figures B-17 to B-20) were used to extrapolate these plots to obtain the  $x_m$  values reported in Table 3-3. Although some adsorption points did not lie exactly on straight lines, any straight line through the adsorption data would result in high  $x_m$  values. If the  $x_m$  values had been taken where the abscissas on the D-P plots were equal to zero, higher  $x_m$  values (thus lower  $A_m$  values) would have been obtained.

Final equilibration pressures from 100 to 800 mm Hg. were used

\* All three teams obtained  $x_m$  values where the abscissas on the D-P plots were equal to zero.

in all high-temperature adsorption studies. If the D-P plots did level off or change slope after these pressures, reasonable  $x_m$  and  $A_m$  values would be obtained. Ranges of  $A_m$  values that would be obtained if the slopes did change from the slopes shown in Figures B-17 to B-20 to a zero slope above pressures of 800 mm Hg. are:

Catalyst	Adsorbate	$A_m$ ranges ( $\text{\AA}^2$ )
Al-1602 T1/8	$N_2$ at 196 °K	3* - 40†
	Ar at 196 °K	5* - 60†
	$CO_2$ at 292 °K	13* - 30†
Fe-301 T1/8	$CO_2$ at 292 °K	4* - 15†

The changing of the slopes after pressures of 800 mm Hg. could indicate that the adsorption forces are stronger in the lower pressure ranges than at pressure greater than 800. Extrapolations of these plots from the lower pressures would result in high  $x_m$  values due to the differences in adsorption forces.

Nonlinear Dubinin-Polanyi plots for the adsorption of  $CO_2$  at 293 °K have been reported by Lamond and Marsh.<sup>7</sup> The slope on some of their plots for 4A, 5A, and 13X sieves changes several times. Extrapolating these plots from the low pressure range would result in high  $x_m$  values.

#### B. Adsorption on Raw Coals

##### 1. Molecular Sieve Structure of Coal

The adsorption of Ar and  $N_2$  at 77 °K and  $CF_4$  at 196 °K on both

\* Slope in D-P plots (Appendix B).

† If slope in D-P plots were equal to zero above 800 mm Hg.

raw coals results in low surface areas as compared to  $\text{CO}_2$  adsorptions at 196 °K. (Refer to Table 4-3).

The adsorption studies on the Roland seam coal show that nitrogen and argon at 77 °K and carbon tetraflouride at 196 °K cannot penetrate the fine porous structure of this coal to any extent (the surface area covered is less than  $1 \text{ m}^2/\text{g}$ ); whereas  $\text{CO}_2$  at 196 °K can and yields reasonable surface areas.

Comparisons between adsorption results on the 4A molecular sieve and on the Roland seam coal indicate that the porous structures of both are similar. On both adsorbents argon, nitrogen, and carbon tetraflouride were incapable of penetrating their microporous structures, whereas carbon dioxide did penetrate.

Adsorption results on the 5A sieve differed from that on the Roland seam coal. Adsorption of nitrogen and argon at 77 °K and carbon dioxide at 196 °K gave similar surface areas for this sieve. However,  $\text{CF}_4$  adsorptions at 196 °K showed a surface area roughly 50% that of the nitrogen based surface area. (Refer to Table 3-2). Comparisons between these results and the adsorption results on the Illinois No. 6 coal indicate that the porous structure of this coal resembles more closely the 5A sieve than the 4A. On the Illinois No. 6 coal, nitrogen and argon yielded surface area values roughly 30-40% that from carbon dioxide adsorption at 196 °K. Carbon tetraflouride adsorptions at 196 °K showed a area 46% that of nitrogen at 77 °K. If the Illinois No. 6 coal resembled the 4A sieve, as did the Roland seam coal,  $\text{Ar}$ ,  $\text{N}_2$ , and  $\text{CF}_4$  adsorptions would have yielded much lower surface areas. Because nitrogen

and argon at 77 °K did not yield surface areas comparable to the carbon dioxide based surface areas, the micropore structure of the Illinois No. 6 coal is probably slightly less than 5 Å in diameter but greater than 4 Å.

## 2. Pore Size Distributions

Using the pore size distribution method outlined in Section B-3 of this chapter, the pore size distributions of the two coals were determined from the adsorption results presented in Table 4-3. The pore size distributions are presented in Table 6-1. Percentages for the  $> \sim 5$  and 4 to  $\sim 5$  Å pore ranges are not listed for the Roland seam coal, since absolute surface areas from the nitrogen and carbon tetrafluoride adsorptions were not determined (only  $< 1 \text{ m}^2/\text{g}$ ).

The pore size distributions also indicate that the Illinois No. 6 coal contains slightly larger micropore diameters than the Roland seam coal.

Taking pore volumes reported by Walker<sup>12</sup> of 0.232 and 0.114 cc/g for the Illinois No. 6 and the Roland seam<sup>\*</sup> coals, respectively, insight about the average pore diameters of the macropores<sup>†</sup> of these two coals is possible. First, the volumes of pores less than 4 Å are determined by Equation (1) using surface areas presented in Table 6-1 for this pore size range. These pore volumes were determined to be 0.011 and 0.14 cc/g for the Roland seam and Illinois No. 6 coals, respectively.

<sup>\*</sup>These pore volumes are used for approximate average pore diameters. The 0.114 cc/g pore volume was for a Texas (Darco seam) sub-bituminous coal.

<sup>†</sup>Macropores are considered to be pores greater than 4 Å in this calculation.

Table 6-1. Pore Size Distributions of Raw Coals (minus-28 mesh)

Pore Diameter Range (Å)	Adsorbate	Roland Seam Coal (m <sup>2</sup> /g, DAF basis <sup>*</sup> )	Illinois No. 6 (m <sup>2</sup> /g, DAF basis <sup>*</sup> )
all accessible pores	CO <sub>2</sub> at 196 °K	106	230
> 4	N <sub>2</sub> at 77 °K	< 1 (0%)	94 (41%)
< 4	a	106 (100%)	136 (59%)
> ~ 5	CF <sub>4</sub> at 196 °K	< 1	43 (46%) <sup>c</sup>
4 to ~5	b	~ 0	51 (54%) <sup>c</sup>

18

<sup>a</sup>Surface area determined by subtracting N<sub>2</sub> from CO<sub>2</sub> based areas<sup>b</sup>Surface area determined by subtracting CF<sub>4</sub> from N<sub>2</sub> based areas<sup>c</sup>Surface area percentages of pores >4 Å

<sup>\*</sup>Ash Content (dry basis): Roland Seam Coal 15.08%  
Illinois No. 6 16.73%

The average pore diameters for pores greater than 4 Å are then determined, also by Equation 1. The pore volumes for this size range are 0.103 and 0.218 cc/g (by subtraction). Using these pore volumes and surface areas of 1 and 94  $\text{m}^2/\text{g}$  (from Table 6-1) in Equation 1, the average pore diameters for pores greater than 4 Å becomes 4100 and 93 Å for the Roland seam and Illinois No. 6 coals, respectively.

The above calculation shows that the macropore structure of the Illinois No. 6 coal is smaller than the Roland seam coal. This is the reverse of the micropore structure. This result indicates that it would be easier for solvents, reactants, and gases to penetrate the macropore structure of the Roland seam coal than the Illinois No. 6. The larger macropore structure in the Roland seam coal would seem to be an important physical property of this coal.

### 3. BET versus D-P Surface Areas on Raw Coals

Surface area determinations by both the BET and Dubinin-Polanyi equations using  $\text{CO}_2$  at 196 °K were made on the Roland seam and Illinois No. 6 coals. (Refer to Table 4-3). The agreement between the two surface areas (BET and D-P) is better when the Illinois No. 6 coal is used as the adsorbent. Although the D-P surface areas on the Roland seam coal were lower than the BET areas, the use of either equation gives approximately the total surface area of the coals when using  $\text{CO}_2$  at 196 °K as the adsorbate.

### 4. Surface Area versus Coal Particle Size

The results presented in Figure 4-1 for the effect of coal particle size on surface area show that surface areas of coals are a function

of particle size. These results indicate that additional pores became accessible to carbon dioxide at 196 °K after grinding the 28 to 150 coal to minus-150 mesh. Carbon dioxide adsorptions at 196 °K are considered to yield total surface areas of coals as mentioned in Chapter I of this paper, therefore, increases in surface areas with grinding could be due to pores that were either closed or restricted  $\text{CO}_2$  penetration at 196 °K before grinding being opened and/or accessible to  $\text{CO}_2$  after grinding.

##### 5. High-Temperature Adsorptions

Adsorptions of nitrogen and argon at 196 °K and carbon dioxide at 292 °K on the minus-28 mesh Roland seam coal using the Dubinin-Polanyi equations yielded high  $x_m$  values. When these values were used in Equation 7 along with a surface area of  $90 \text{ m}^2/\text{g}$ , low  $A_m$  values are a result. (Refer to Table 4-4.)

These results are identical to the high-temperature adsorption results on the catalysts and the 4A sieve. The same reasoning and  $A_m$  ranges discussed in section B-4 of this chapter are applicable to these results on the Roland seam coal if the D-P plots either change slope or level off above equilibration pressures of 800 mm Hg.

Many workers<sup>2,10,11</sup> have obtained linear Dubinin-Polanyi plots for various coals. Surface areas obtained by these workers using  $A_m$  values of  $17-25 \text{ \AA}^2$  are reasonable for the coals studied. All these workers used  $x_m$  values determined at a zero value of the abscissa.

##### C. Surface Area Variations of Extracted Coal

The surface areas of the extracted Roland seam coal was found to vary with extraction yield, extraction time, and solvent used. The

maximum surface area obtained on the extracted coal was when tetralin at 350 °C was used as the solvent. For extraction times of 4 and 8.5 hours, surface areas greater than  $260 \text{ m}^2/\text{g}(\text{DAF})$  were obtained. The raw coal had a surface area of  $99 \text{ m}^2/\text{g}(\text{DAF}, 28 \text{ to } 150 \text{ mesh})$ .

Surface areas of the coal extracted with tetralin and phenol at 300 °C were higher than coal extracted at 250 °C or below. Draemel and Grens<sup>13</sup> determined the pyrolysis temperature of the raw Roland seam coal to be approximately 320 °C. It has also been proposed in literature studies that hydrogen transfer in coal/hydrogen donor solvent systems is a thermal process and will only take place when thermal decomposition of the raw coal or extracted coal occurs.<sup>13</sup>

This trend is seen in Figure 5-2; at temperatures of 300 and 350 °C, both surface areas and extraction yields were higher than at lower extraction temperatures.

At the lower extraction temperatures, 250 °C and below, surface area variations seem to be more of a solvent effect than a thermal effect. The extraction at 200 °C using benzene gave higher surface areas than either phenol or tetralin, even though the yields for the benzene extractions were lower. This can be seen on the 200 °C isotherm in Figure 5-2. Also in this temperature range, phenol yielded higher surface areas than tetralin for the same extraction times.

However, at 300 °C, surface areas for the phenol and tetralin extractions were roughly identical at a extraction time of 4 hours. This also indicates that as the extraction temperature nears the pyrolysis temperature of the coal, temperature effects become dominate.

Looking at the tetralin and phenol trends in Figure 5-1, it is readily seen that the surface-area variations reach or approach a maximum. This maximum seems to be reached near a extraction yield of approximately 31% for the tetralin extractions. The phenol trend seems to be slowing, approaching a maximum. Not enough benzene extraction data at higher yields are available to indicate much of a trend.

When the surface areas of extracted coal are plotted against extraction time (Figure 5-2), they again tend to approach or reach maximums. For the tetralin extractions at 200°C, this maximum occurs at an extraction time of approximately 60 hours. Not enough extraction runs using either benzene or phenol at 200°C were available to give quantitative trends.

Higher temperatures are required to increase both extraction yield and surface area even if longer extraction times are used. This is seen with the extraction of hexane, benzene, and tetralin for 100 hours each at 200°C, H.B.T. in Figures 5-1 and 5-2. The surface area obtained for this sample was roughly the same as for other 200°C extractions using tetralin.

It can be concluded from the surface area variations on extracted Roland seam coal that:

1. At extraction temperatures of 250°C or below, solvent effects dominate
2. At higher temperatures, 300 or 350°C, near or above the pyrolysis temperature of this coal, solvent effects become overshadowed by thermal effects.

#### D. Suggestions for Future Work

The research conducted in this report was preliminary work to characterize the porous structure of coal. From this work several areas for future work are suggested.

##### 1. Particle Size Ranges

The size range of coals used in these studies, minus-28, 28 to 150, and minus-150, were too broad and should be reduced in future adsorption studies on coals. By using smaller size ranges, e.g. 28 to 40, particle size effects on surface areas would be minimal.

##### 2. Pore Size Distributions

A method to determine pore size distributions on coals and other porous solids containing ultrafine pores is outlined in this paper. The use of this method should be studied in more detail. Possibly with the use of other adsorbates, pore size distributions could be obtained for additional pore diameter ranges, i.e. 5-10 Å.

##### 3. Extracted Coal Samples

Additional surface area data on extracted coals would be useful to better characterize the structure of coal. In this study the surface area of extracted coals using tetralin at 200°C reached a maximum at an extraction time of about 60 hours. Longer extraction times, up to about 100 hours, using either phenol at 300°C or tetralin at 350°C would give additional data needed to verify the trends indicated in Figures 5-1 and 5-2. These two solvents and temperatures are suggested because surface areas on the 4-hour extraction samples using these solvents and temperatures were high, greater than 230 m<sup>2</sup>/g.

#### 4. Porosity Measurements

Porosity measurements on raw and extracted coals would also give valuable data for the characterizations of the internal structure of coals. True, bulk, and apparent densities are required for the porosity determinations.

#### 4. Diffusion Studies

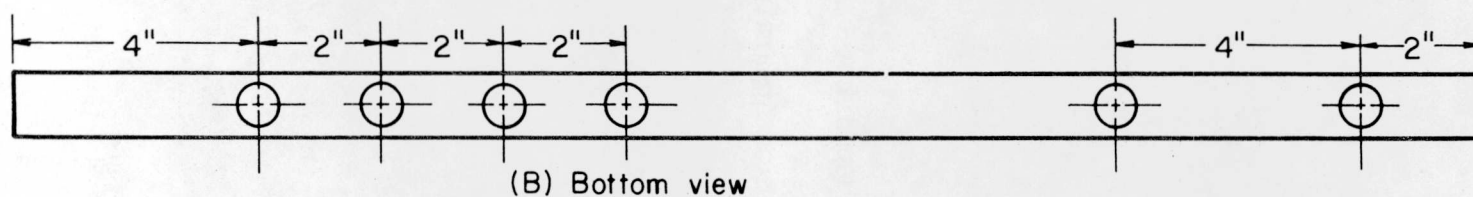
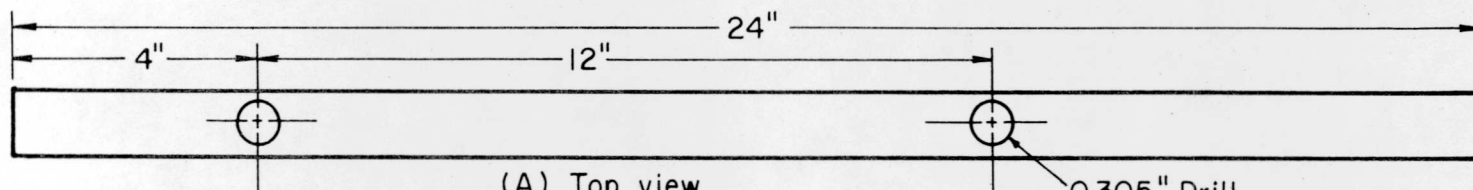
Investigations into the physical reason why nitrogen and argon at 77 °K and carbon tetrafluoride at 196 °C cannot penetrate 4A sieves, whereas CO<sub>2</sub> can, should also be conducted. Diffusion data on 4A and other molecular sieves over a temperature range from -80 to 20 °C using these four gases would be very instructive, since it is believed that these abilities or inabilities of a molecule to penetrate fine micropores is due to differences in activated diffusivities.

References

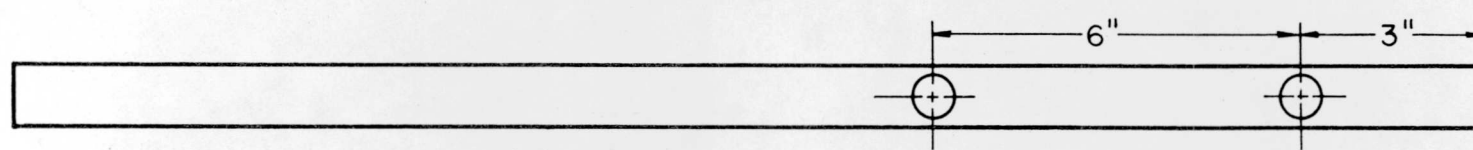
1. Swann, P., Allardice, D. and Evans, D., Fuel, 53, 85 (1974)
2. Marsh, H. and Siemienwska, T., Fuel, 44, 355 (1965)
3. Gregg, S.J. and Sing, K.S.W., "Adsorption, Surface Area, Porosity", Chapter 2 and 3, Academic Press, New York (1967)
4. Walker, P.L. and Kini, K.A., Fuel, 44, 453 (1965)
5. Alymore, L.A.G., Clays and Clay Minerals, 22, 175 (1974)
6. Emmett, P.H., Private Communication, Aug. 15, 1975, U.C. Berkeley, Dept. of Chem. Eng.
7. Lamond, T.G. and Marsh, H., Carbon, 1, 281 (1964)
8. Breck, D.W., Eversole, W.G., Milton, R.M., Reed, T.B. and Thomas, T.L., J. Am. Chem. Soc., 78, 5963 (1956)
9. Huggins, M.L., J. Am. Chem. Soc., 75, 4126 (1953)
10. Walker, P.L. and Patel, R.L., Fuel, 49, 91 (1970)
11. Toda, Y., Hatami, M., Toyoda, S., Yoshida, Y. and Honda, H., Fuel, 50, 187 (1971)
12. Gan, H., Nandi, S.P. and Walker, P.L., Fuel, 51, 272 (1972)
13. Draemel, D. and Grens, E., Lawrence Berkeley Laboratory Report: LBL-4434 (1975)

Appendix A

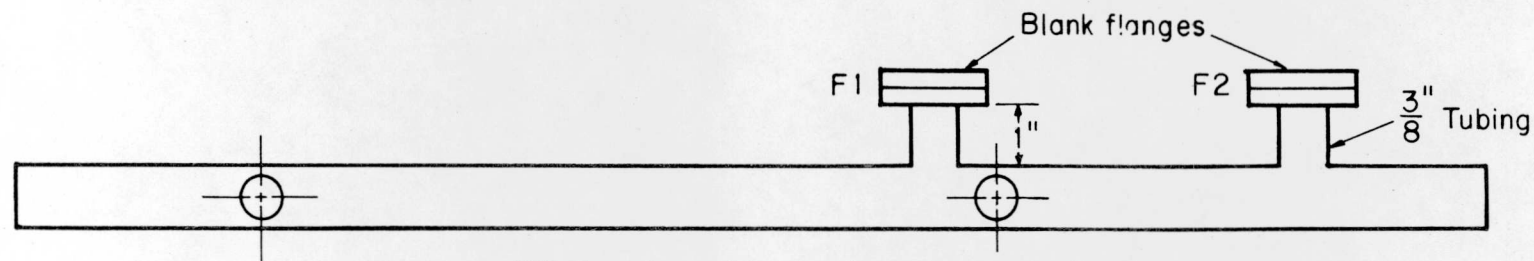
Adsorption Apparatus



(B) Bottom view



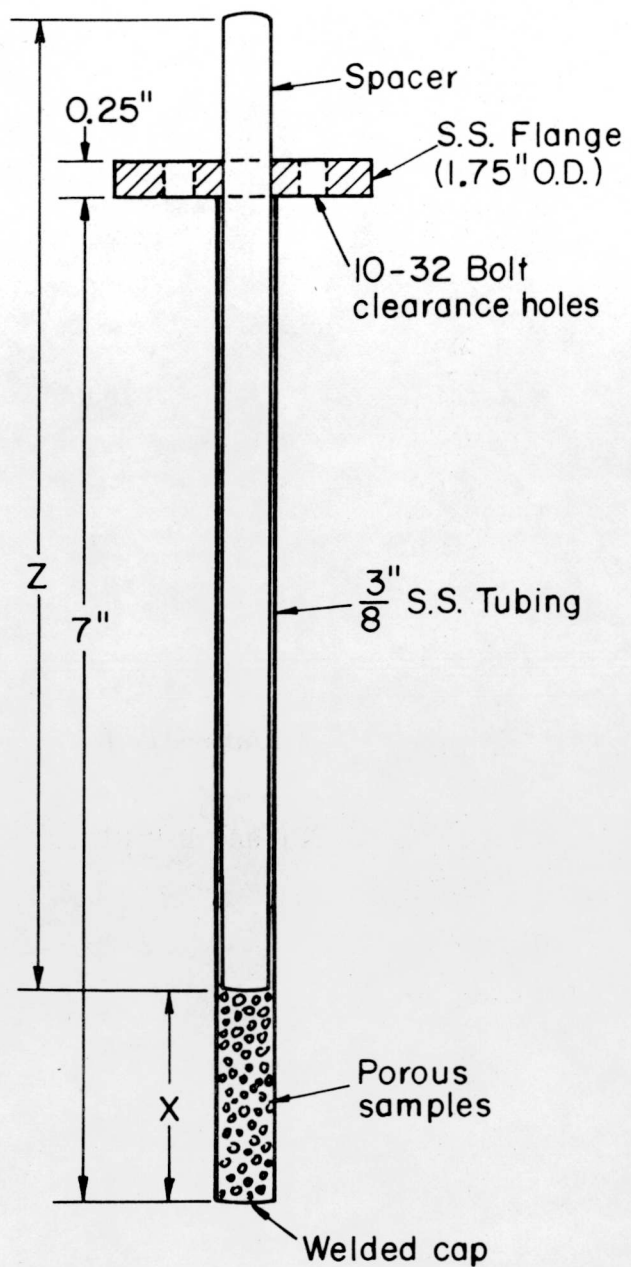
(C) Rear view



(D) Top view with rear flanges attached

XBL7510-7733

Figure A-1 a,b,c,d. Adsorption Manifold



XBL7510-7734

Figure A-2. Sample Holder

Appendix B

BET and D-P Plots

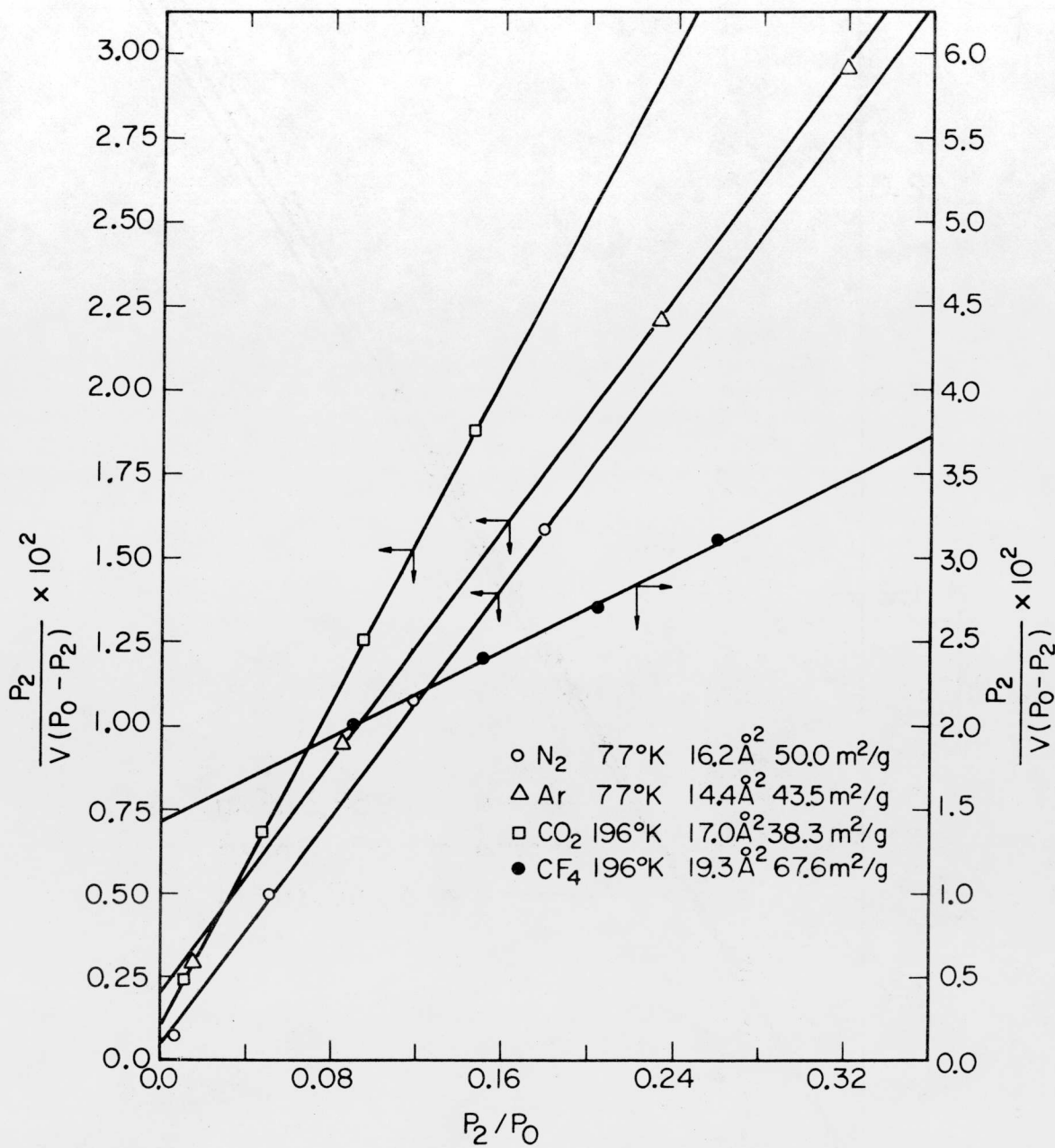


Fig. B-1. Adsorption on Fe-301 T1/8 Catalyst

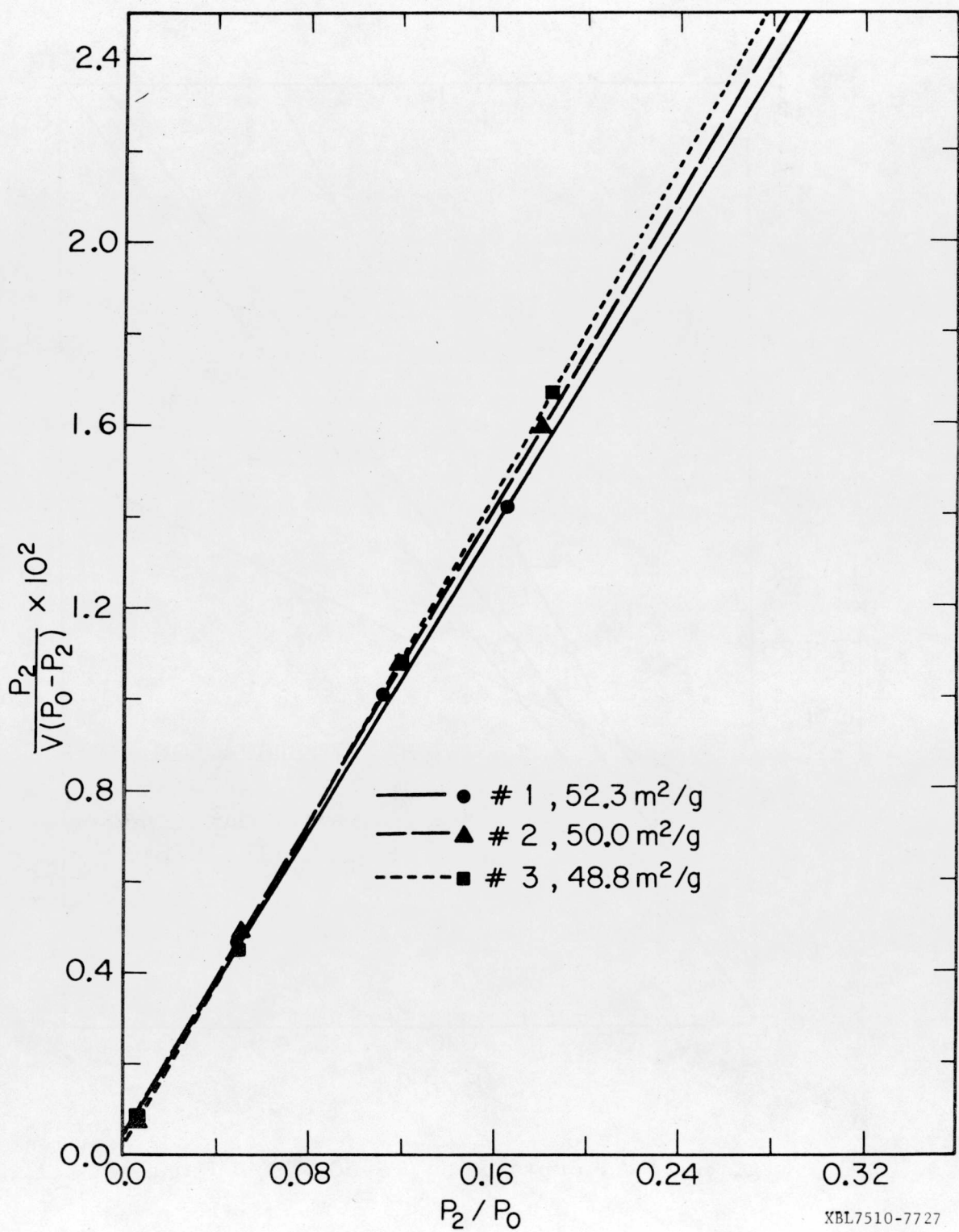


Fig. B-2. Adsorption of  $N_2$  at  $77^0K$  on Fe-301 T1/8,  
 $A_m = 16.2 \text{ \AA}^2$

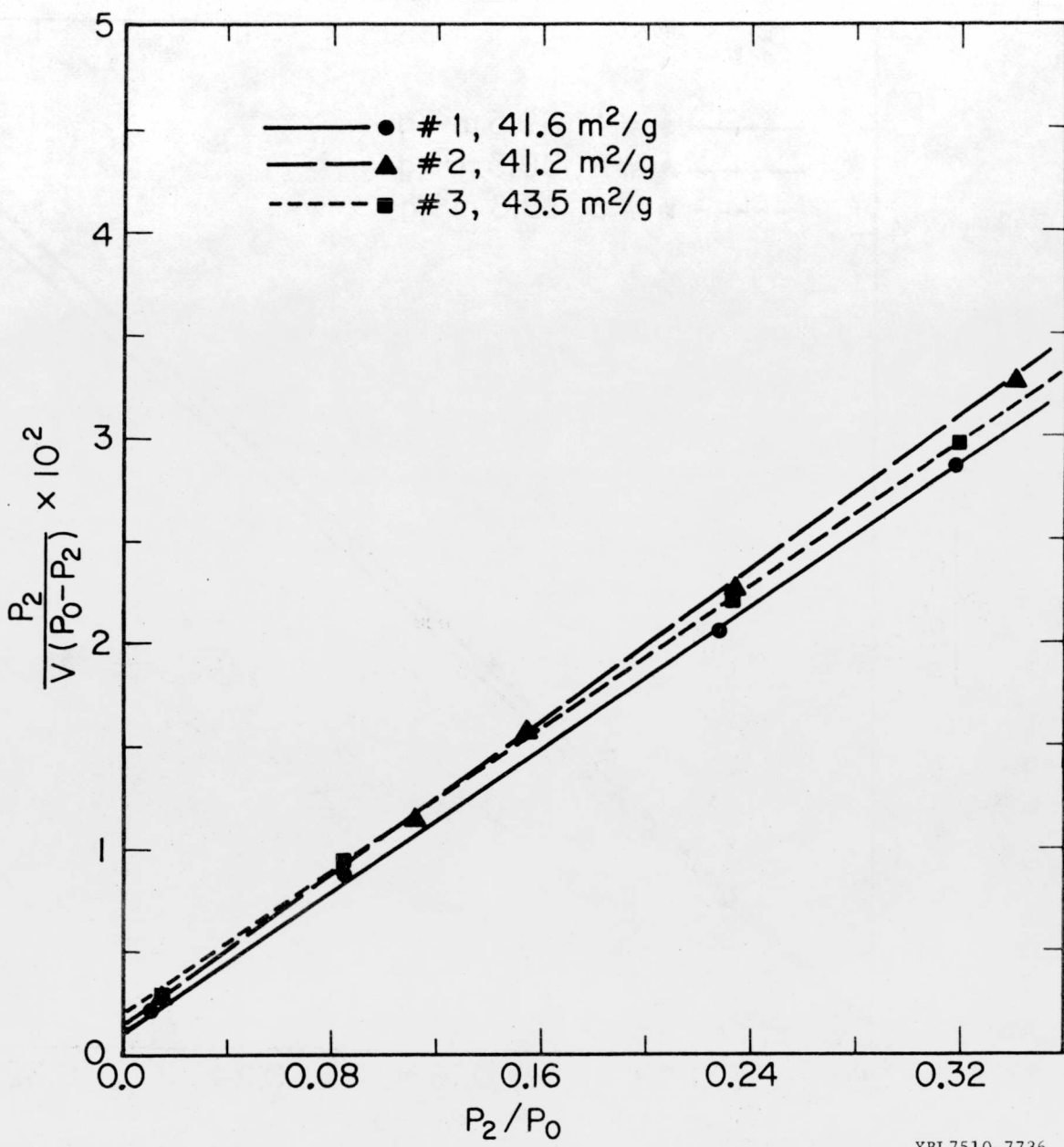


Fig. B-3. Adsorption of Ar at 77°K on Fe-301 T1/8,  
 $A_m = 14.4 \text{ \AA}^2$

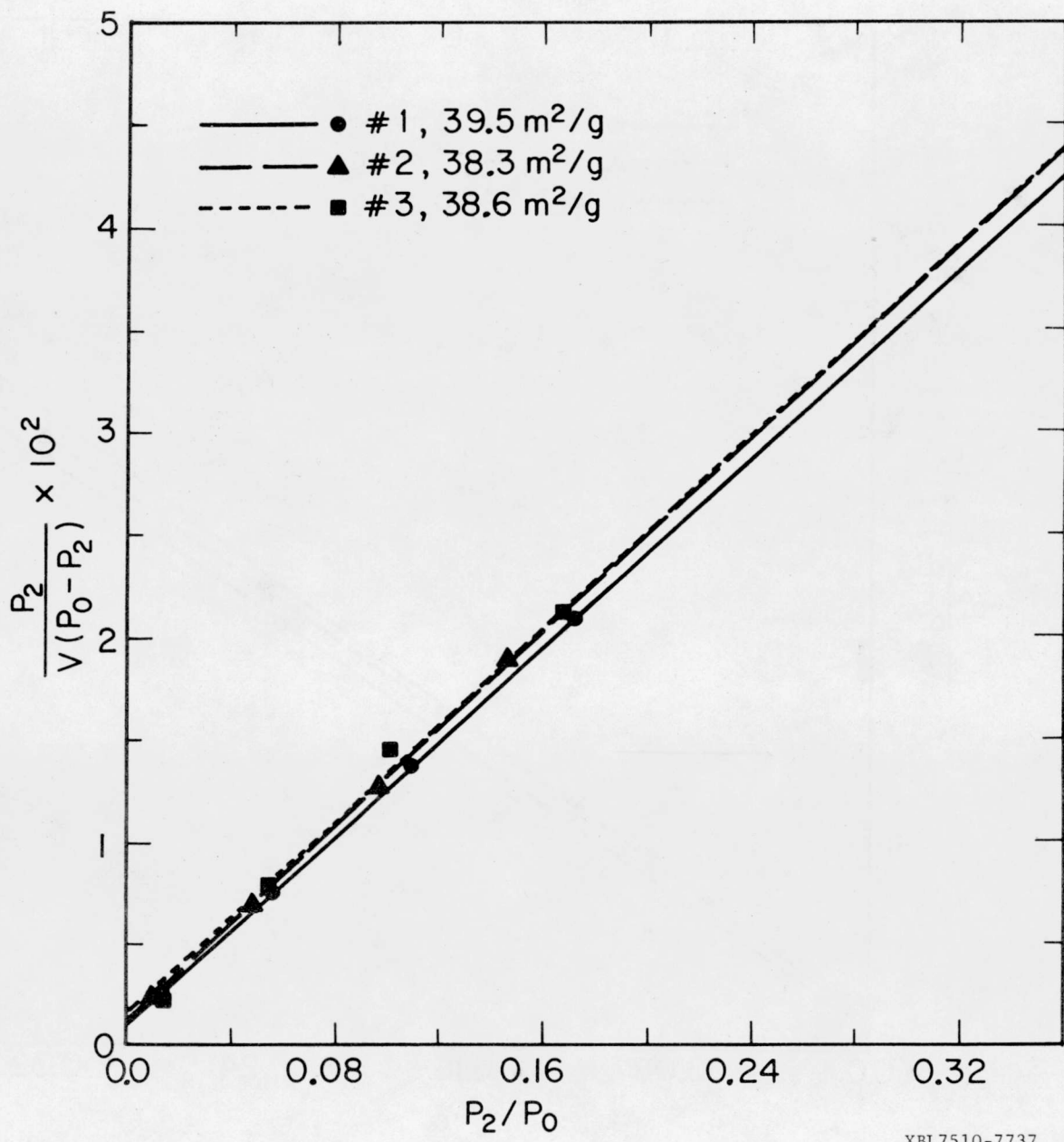
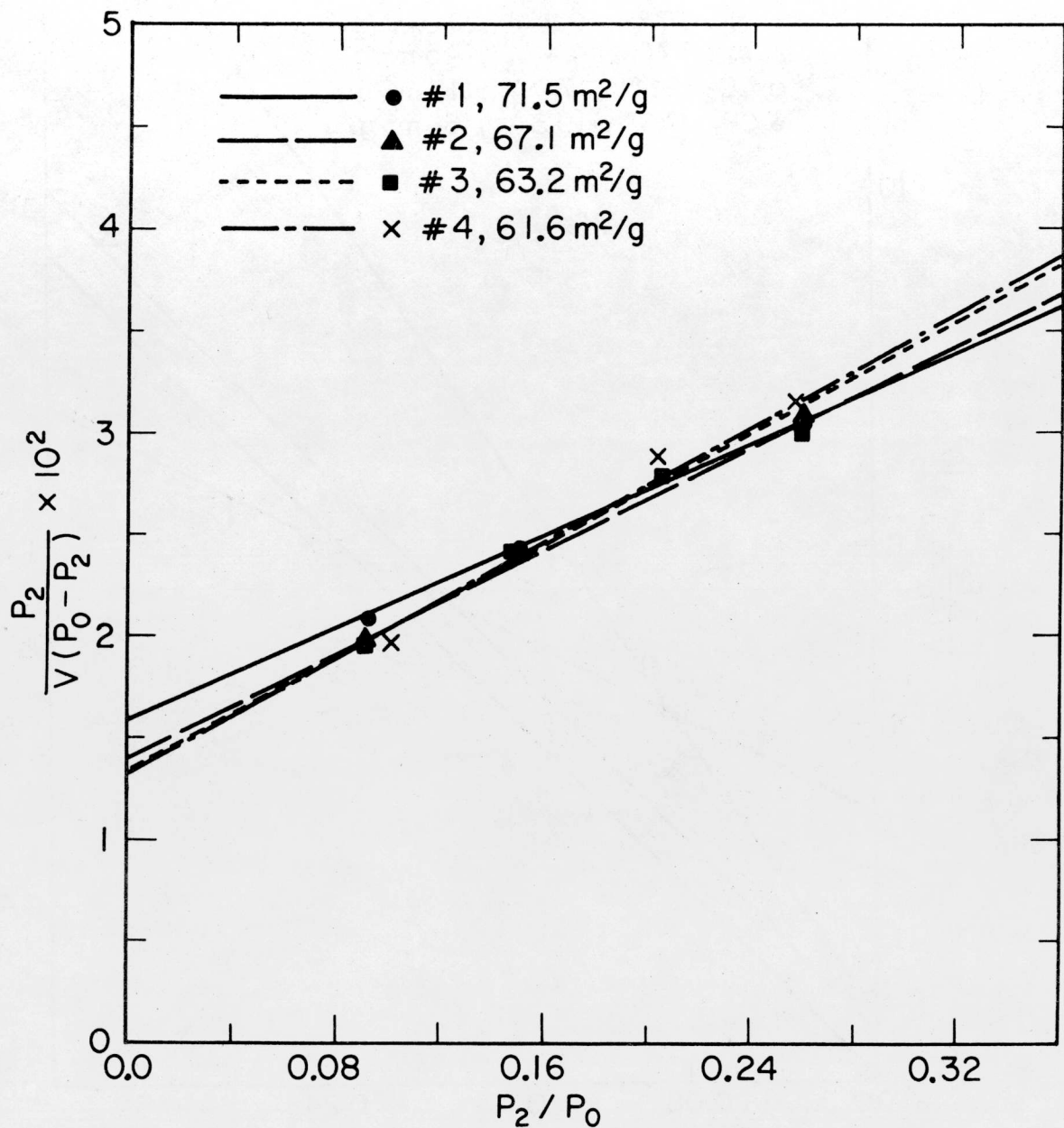
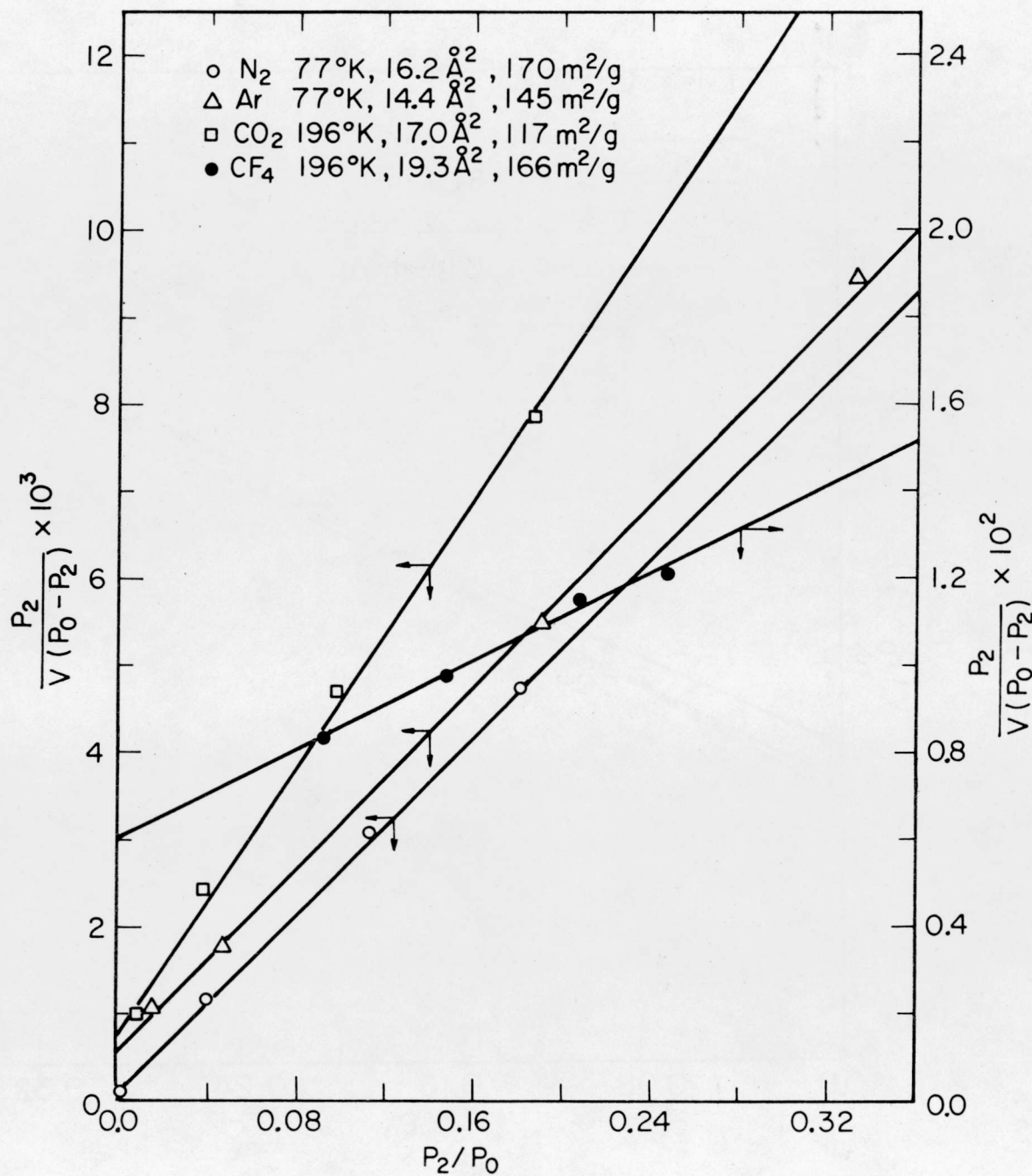


Fig. B-4. Adsorption of  $\text{CO}_2$  at  $196^0\text{K}$  on  $\text{Fe-301 T1/8}$ ,  
 $A_m = 17.0 \text{ \AA}^2$



XBL7510-7728

Fig. B-5. Adsorption of  $\text{CF}_4$  at  $196^\circ\text{K}$  on Fe-301 T1/8,  
 $A_m = 19.3 \text{ \AA}^2$



XBL7510-7738

Fig. B-6. Adsorption on Al-1602 T1/8 Catalyst

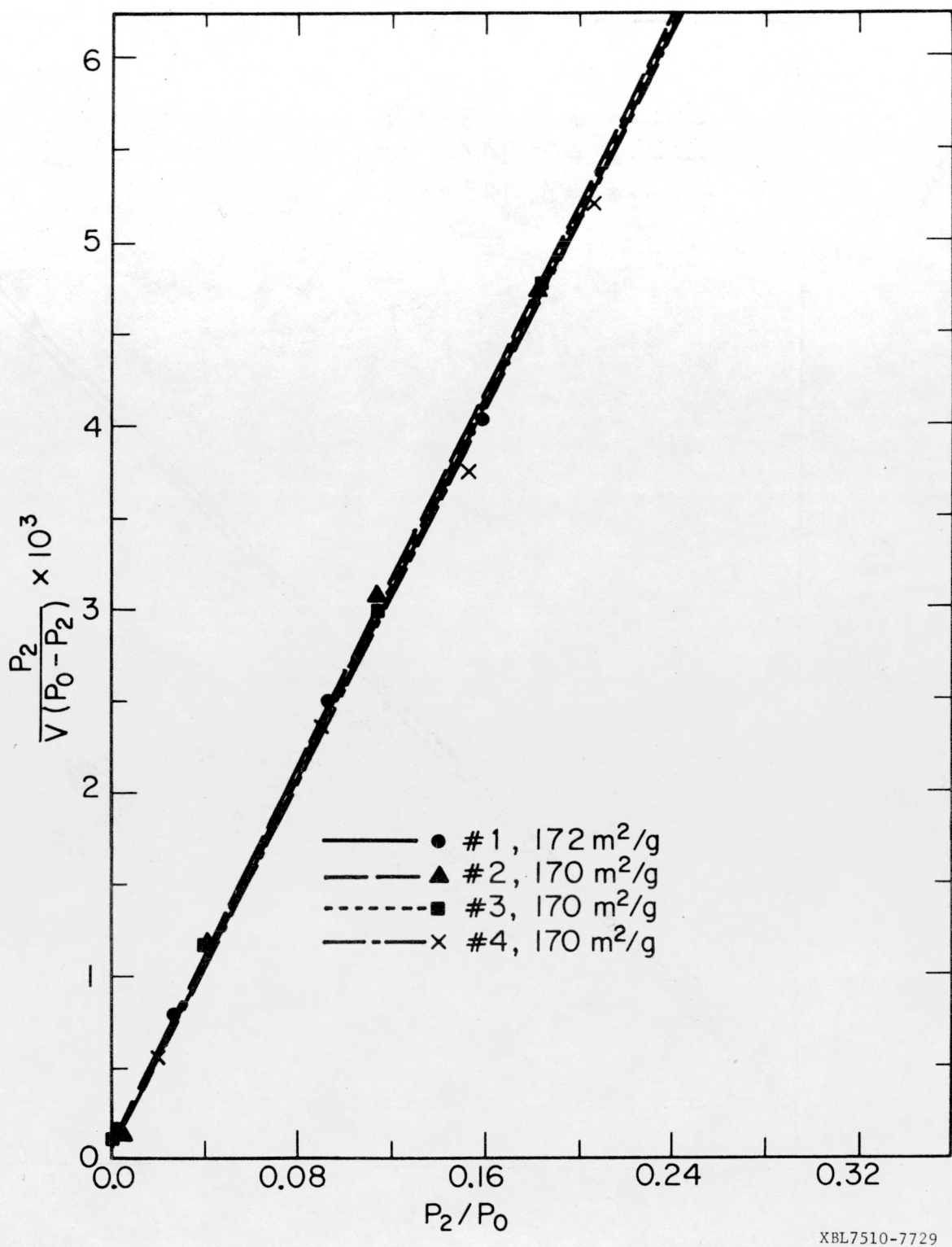
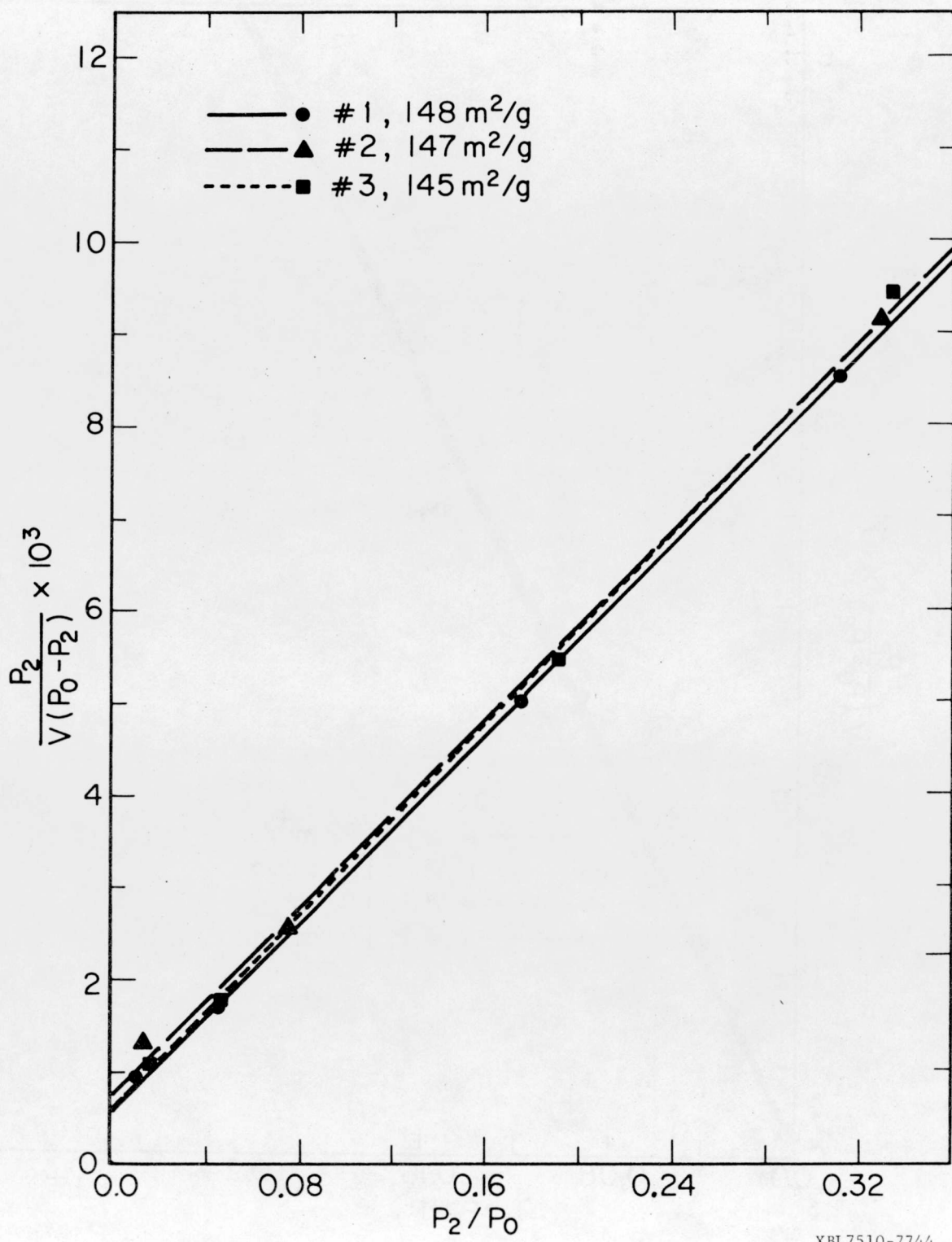


Fig. B-7. Adsorption of  $\text{N}_2$  at  $77^0\text{K}$  on Al-1602 T1/8,  
 $A_m = 16.2 \text{ \AA}^2$



XBL7510-7744

Fig. B-8. Adsorption of Ar at 77°K on Al-1602 T1/8,  
 $A_m = 14.4 \text{ \AA}^2$

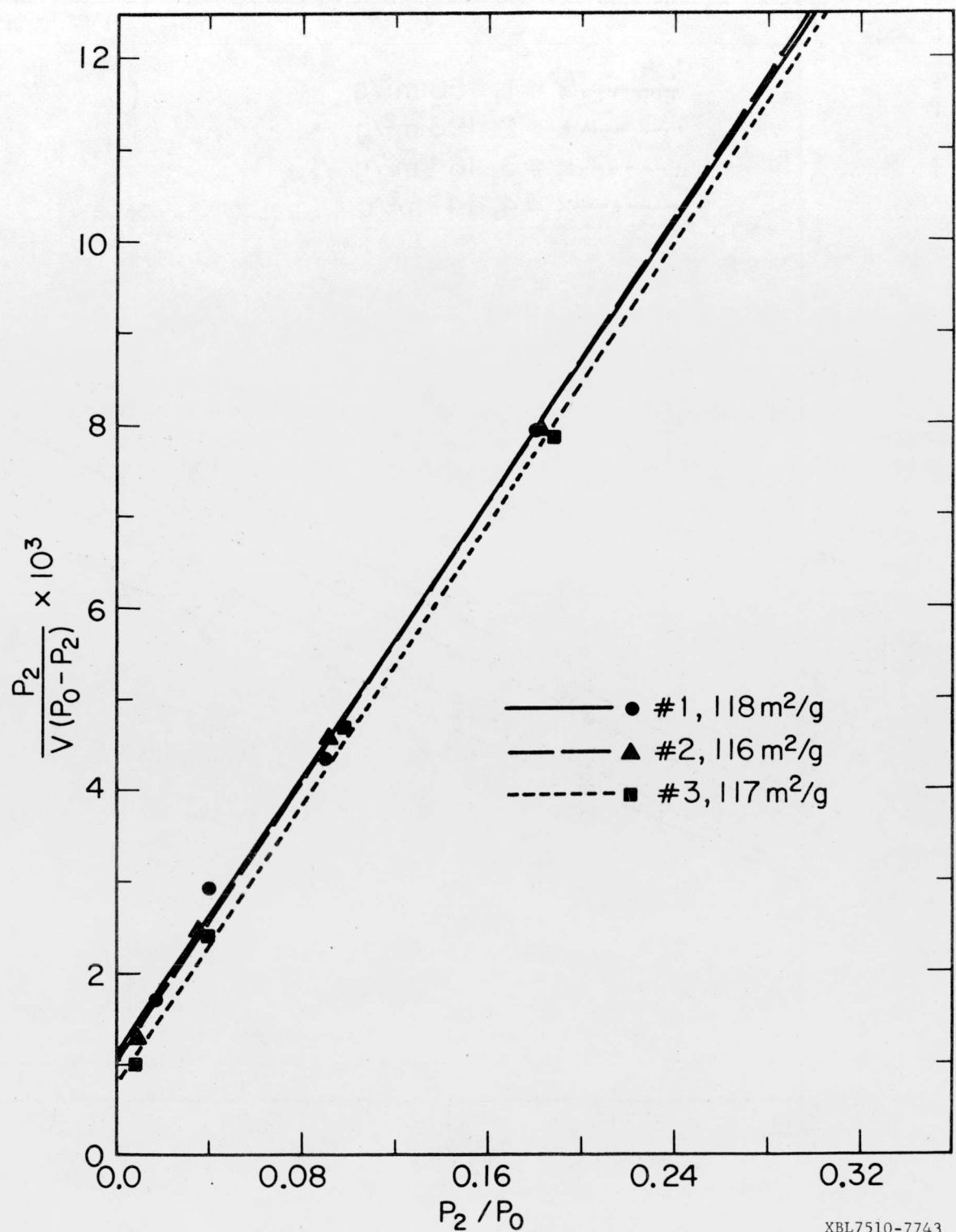


Fig. B-9. Adsorption of CO<sub>2</sub> at 196<sup>0</sup>K on Al-1602 T1/8,  
 $A_m = 17.0 \text{ \AA}^2$

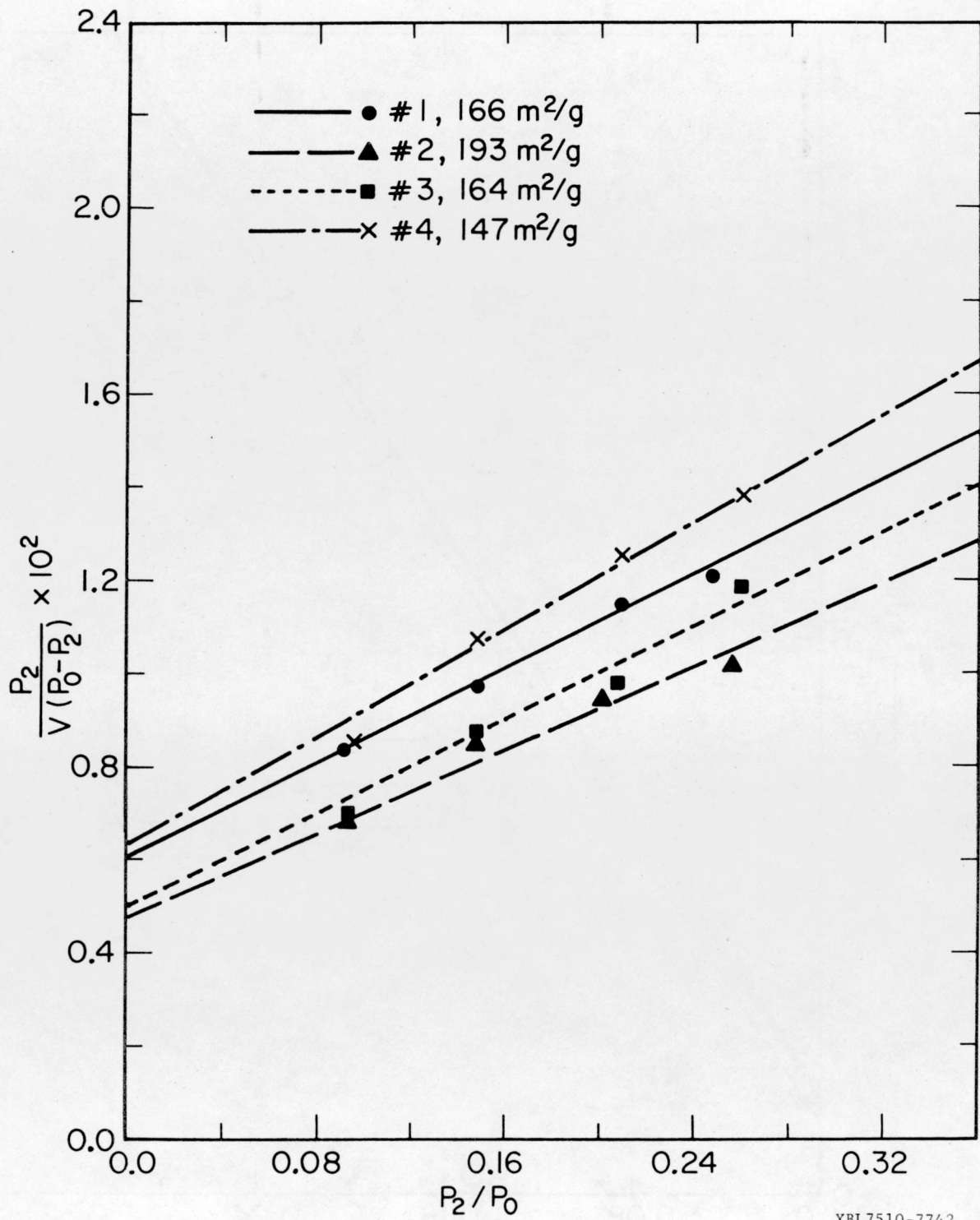


Fig. B-10. Adsorption of  $\text{CF}_4$  at  $196^0\text{K}$  on Al-1602 T1/8,  
 $A_m = 19.3 \text{ \AA}^2$

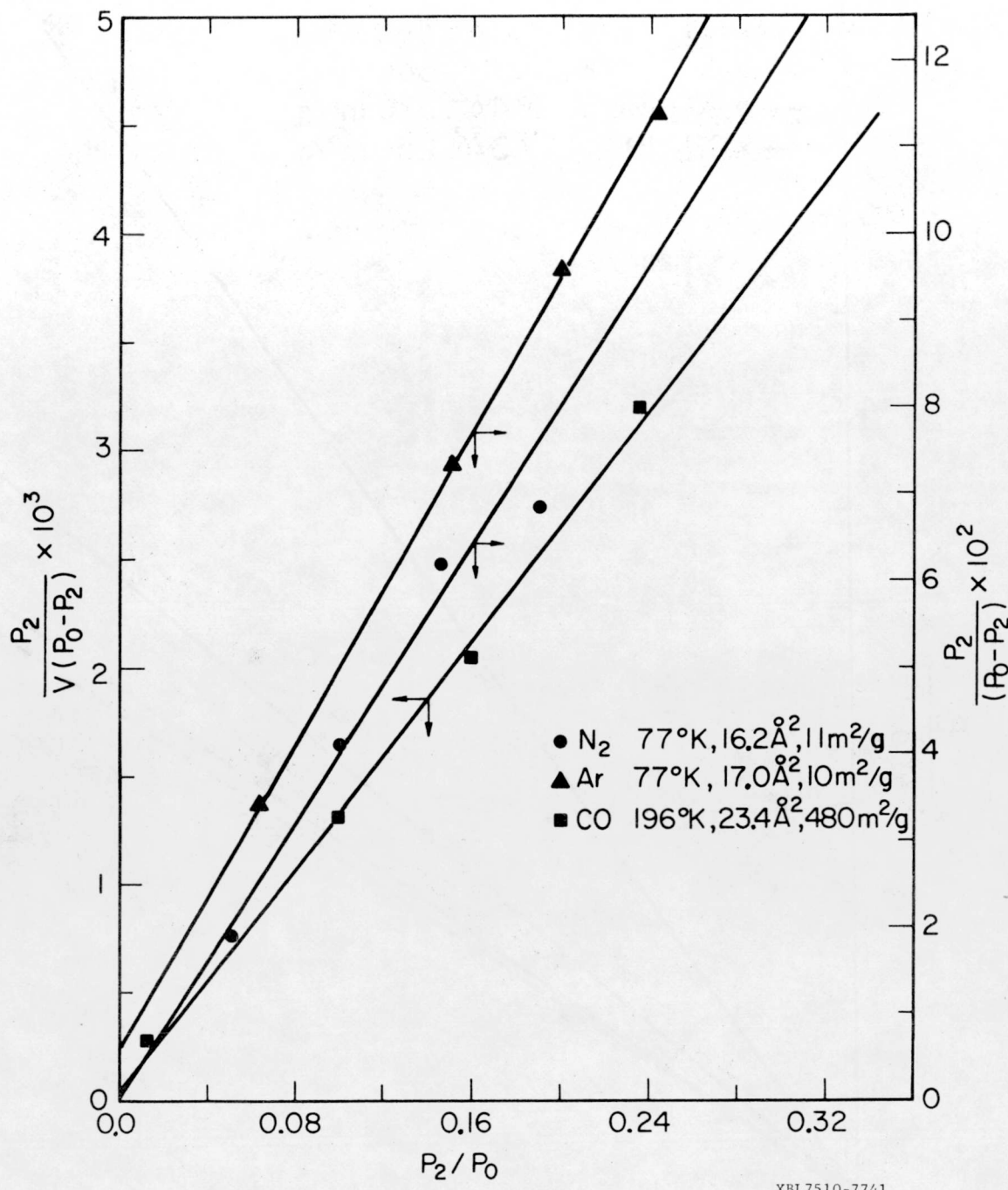


Fig. B-11. Adsorption on Linde 4A Sieve

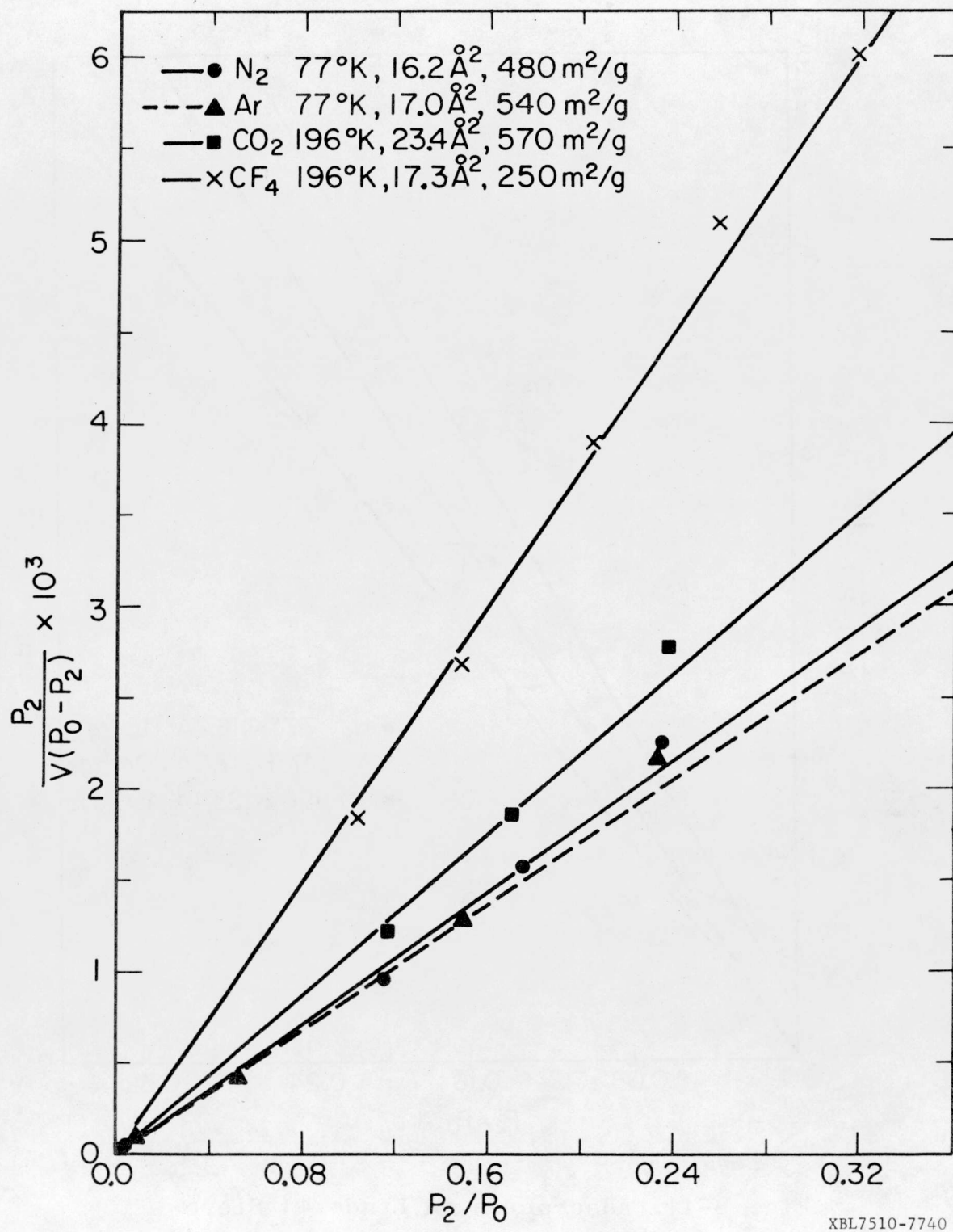


Fig. B-12. Adsorption on Linde 5A Sieve

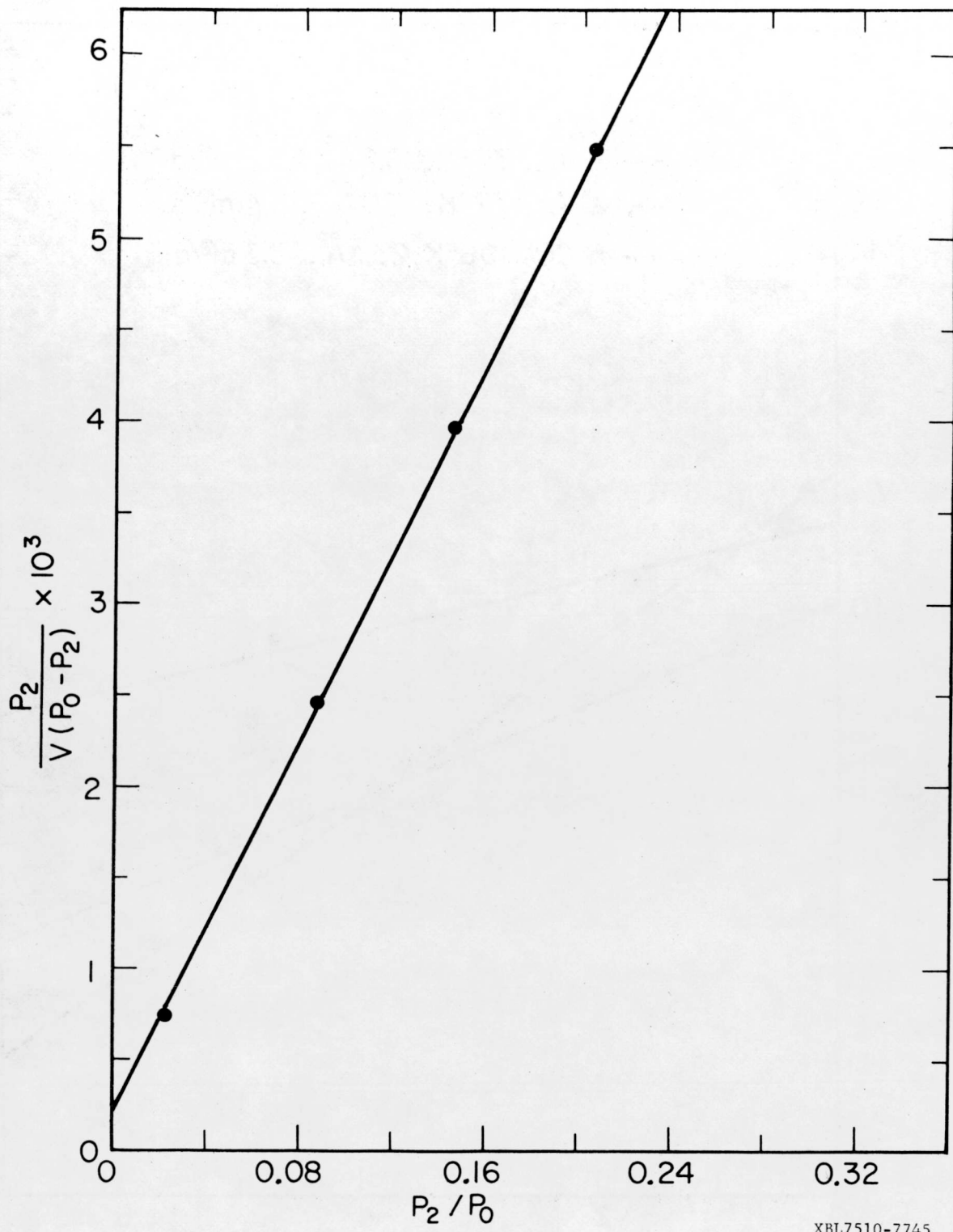


Fig. B-13. Adsorption of  $N_2$  at  $77^0K$  on Al-1602 T1/8 Powder,  $A_m = 16.2 \text{ \AA}^2$ ,  $S = 169 \text{ m}^2/\text{g}$

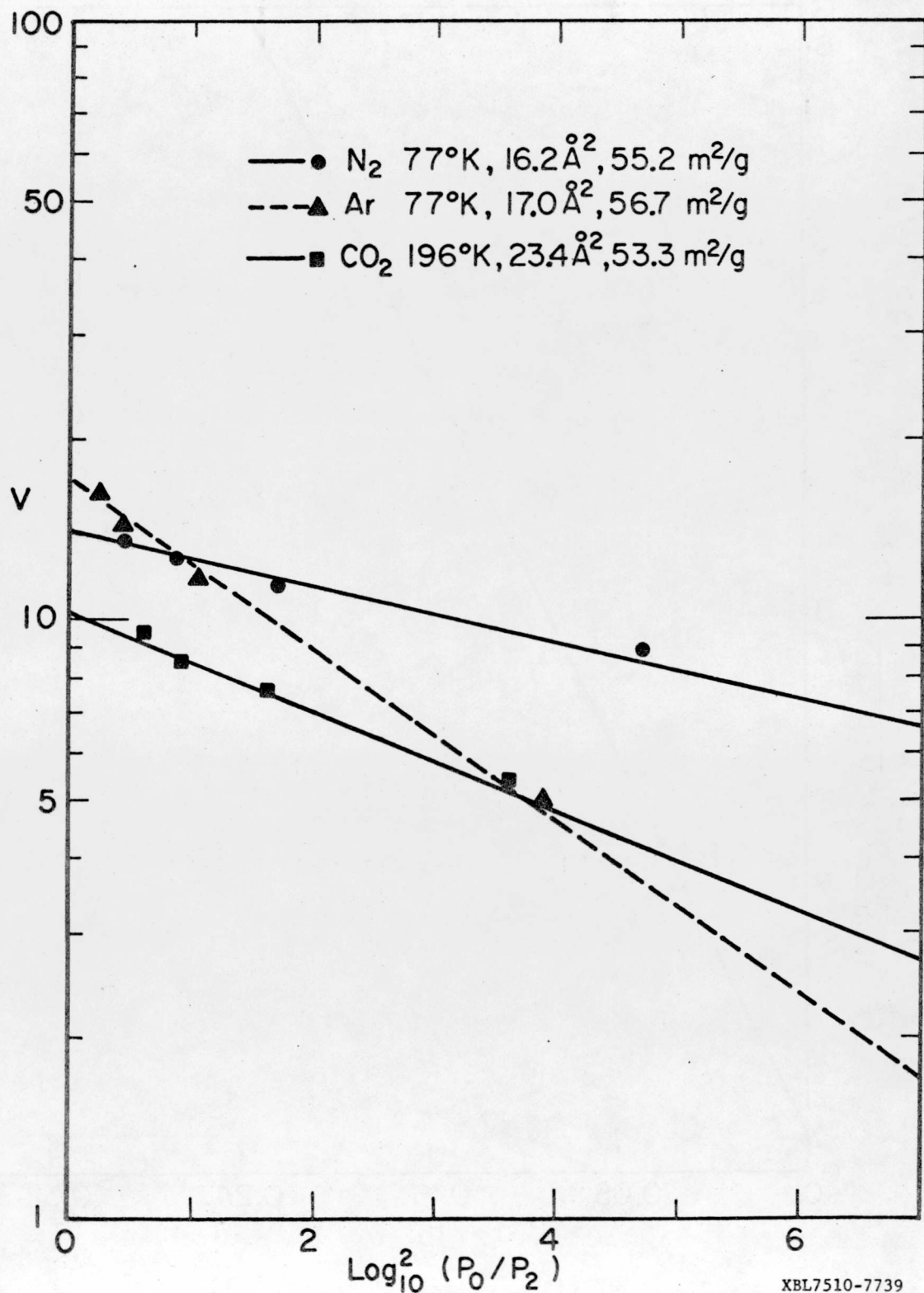


Fig. B-14. D-P Plots for adsorption on Fe-301 T1/8 Catalyst

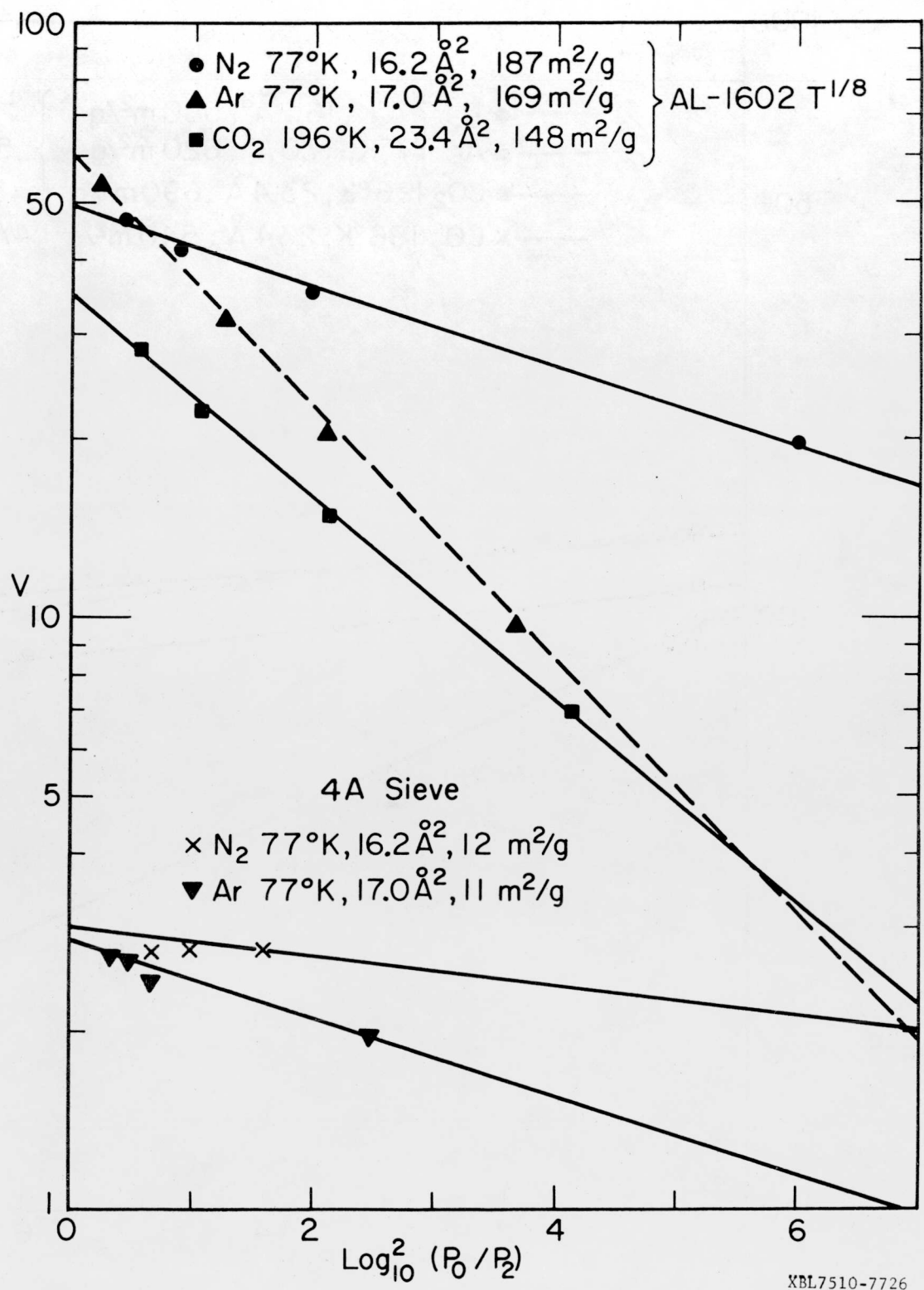


Fig. B-15. Dubinin-Polanyi Plots

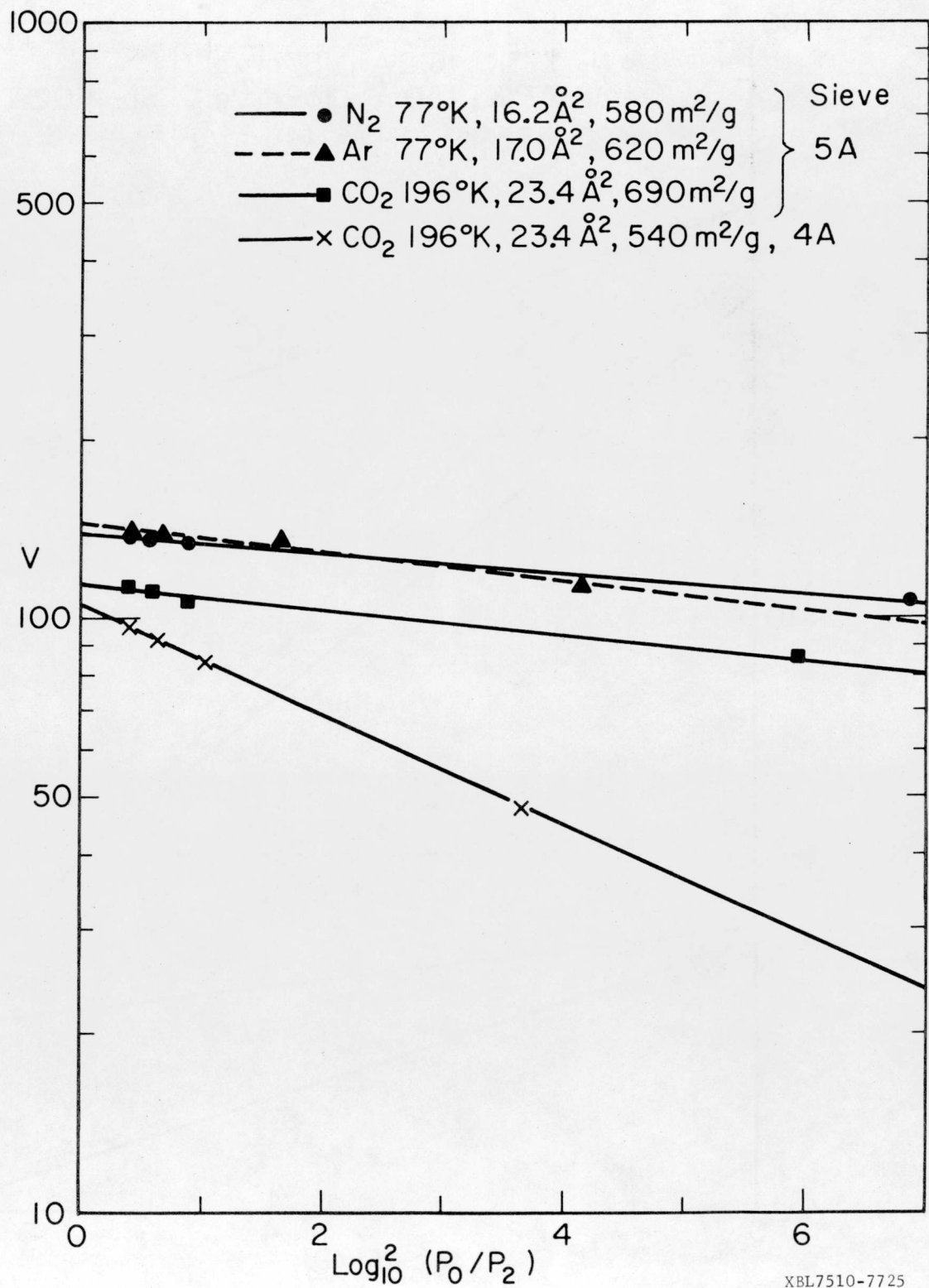


Fig. B-16. Dubinin-Polanyi Plots

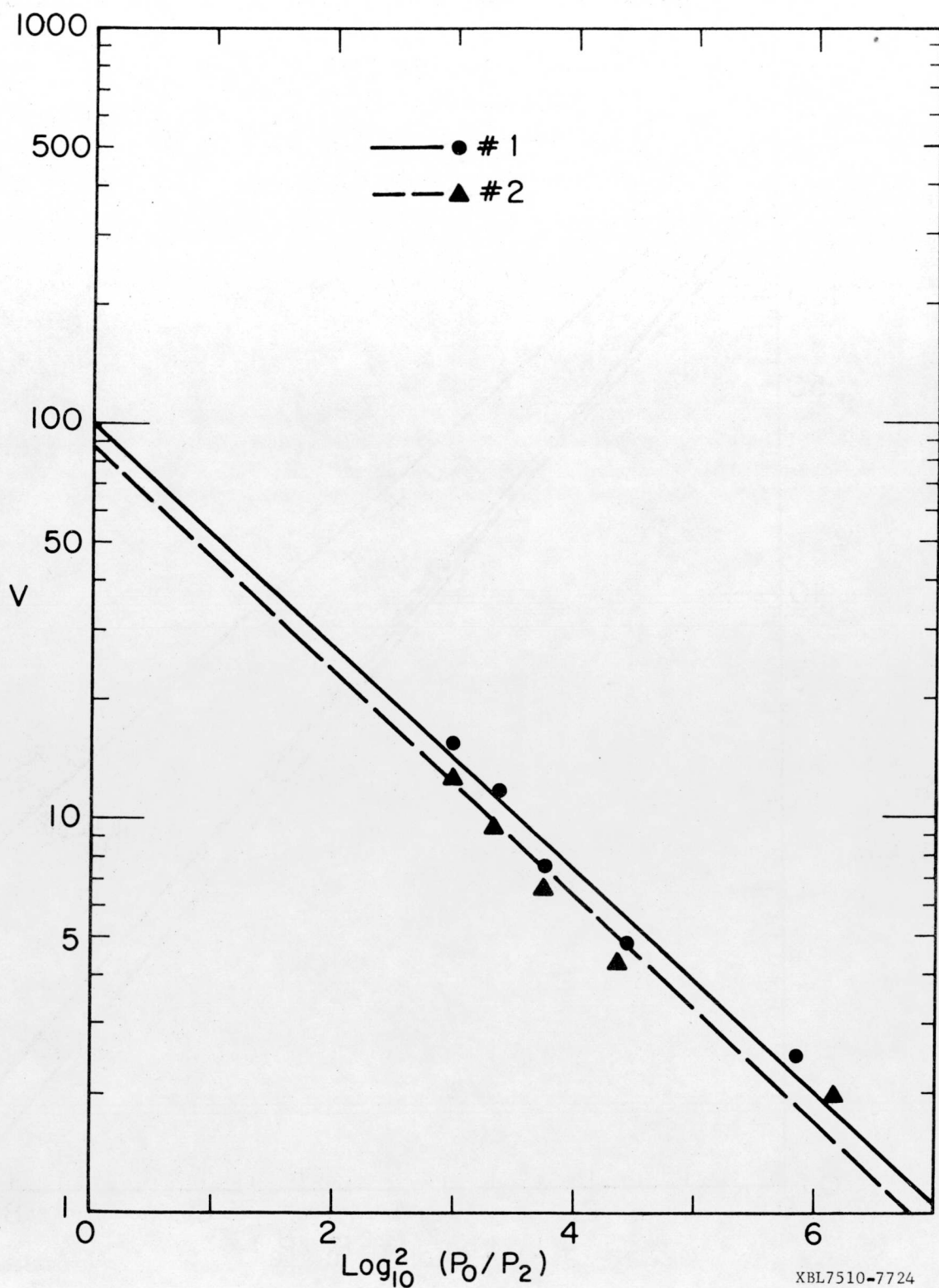


Fig. B-17. D-P Plots for  $\text{CO}_2$  adsorption at  $292^\circ\text{K}$   
on Fe-301 T1/8 Catalyst

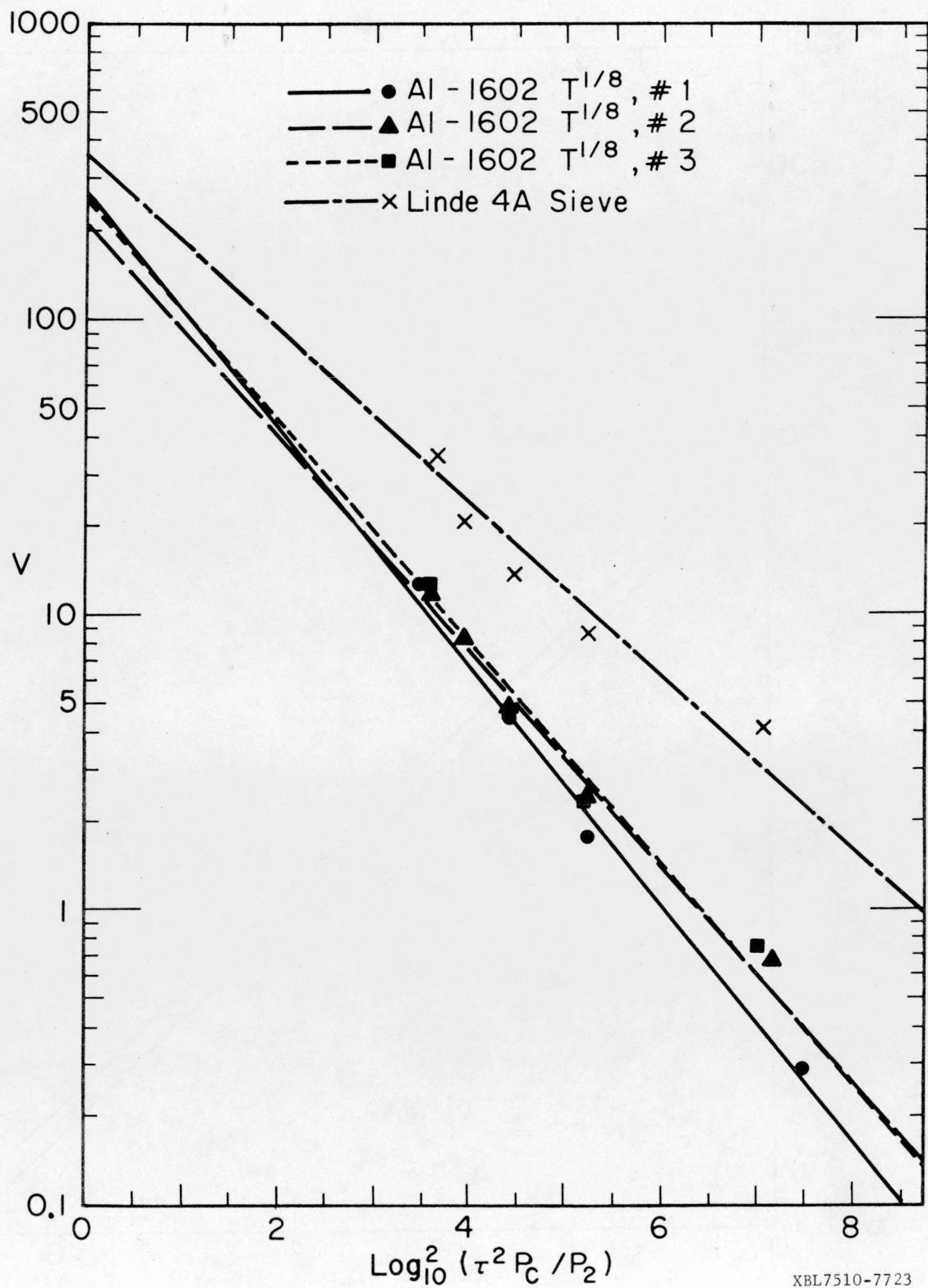


Fig. B-18. D-P Plots for  $\text{N}_2$  adsorption at  $196^{\circ}\text{K}$

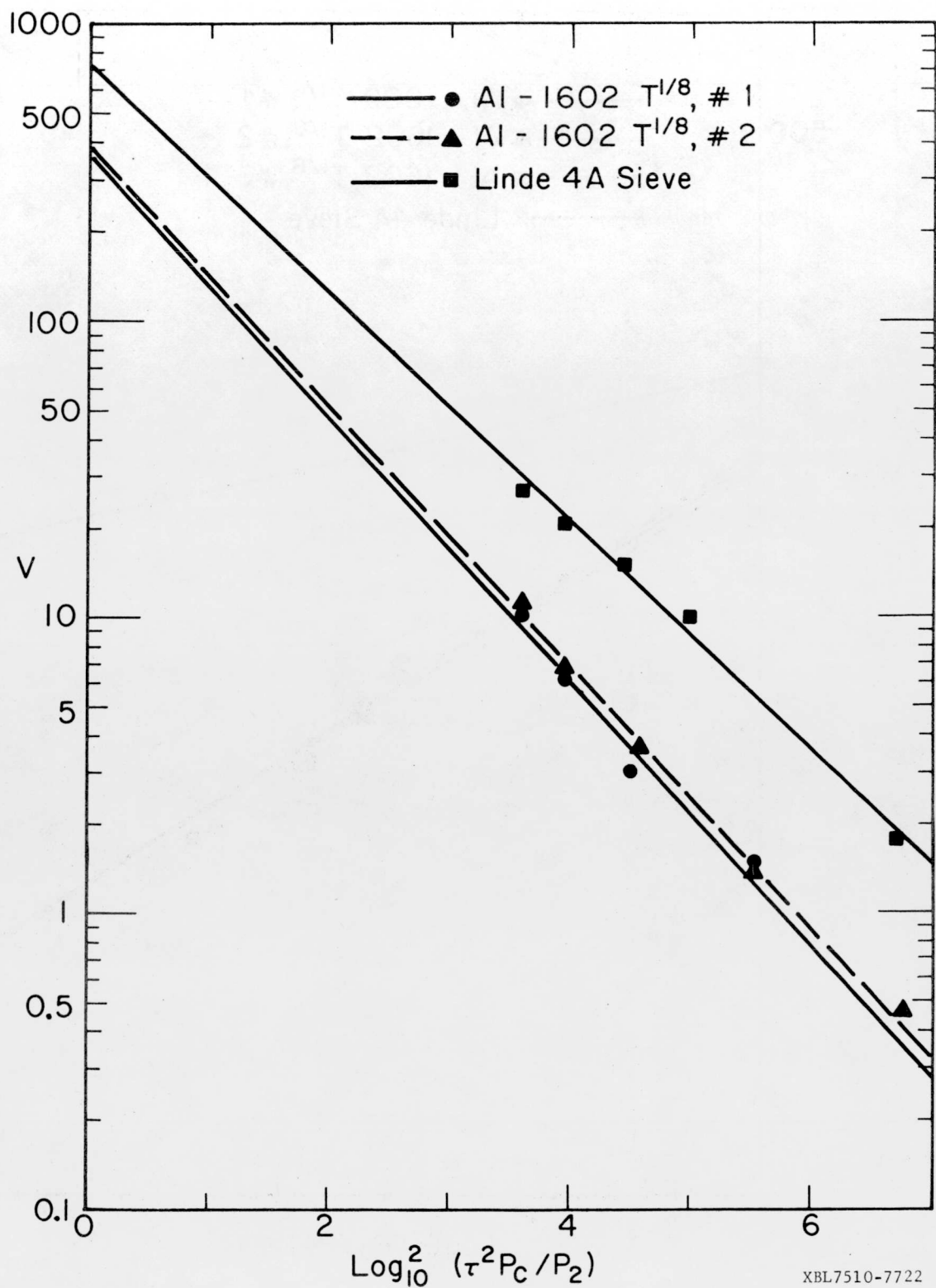


Fig. B-19. D-P Plots for Ar adsorption at 196°K

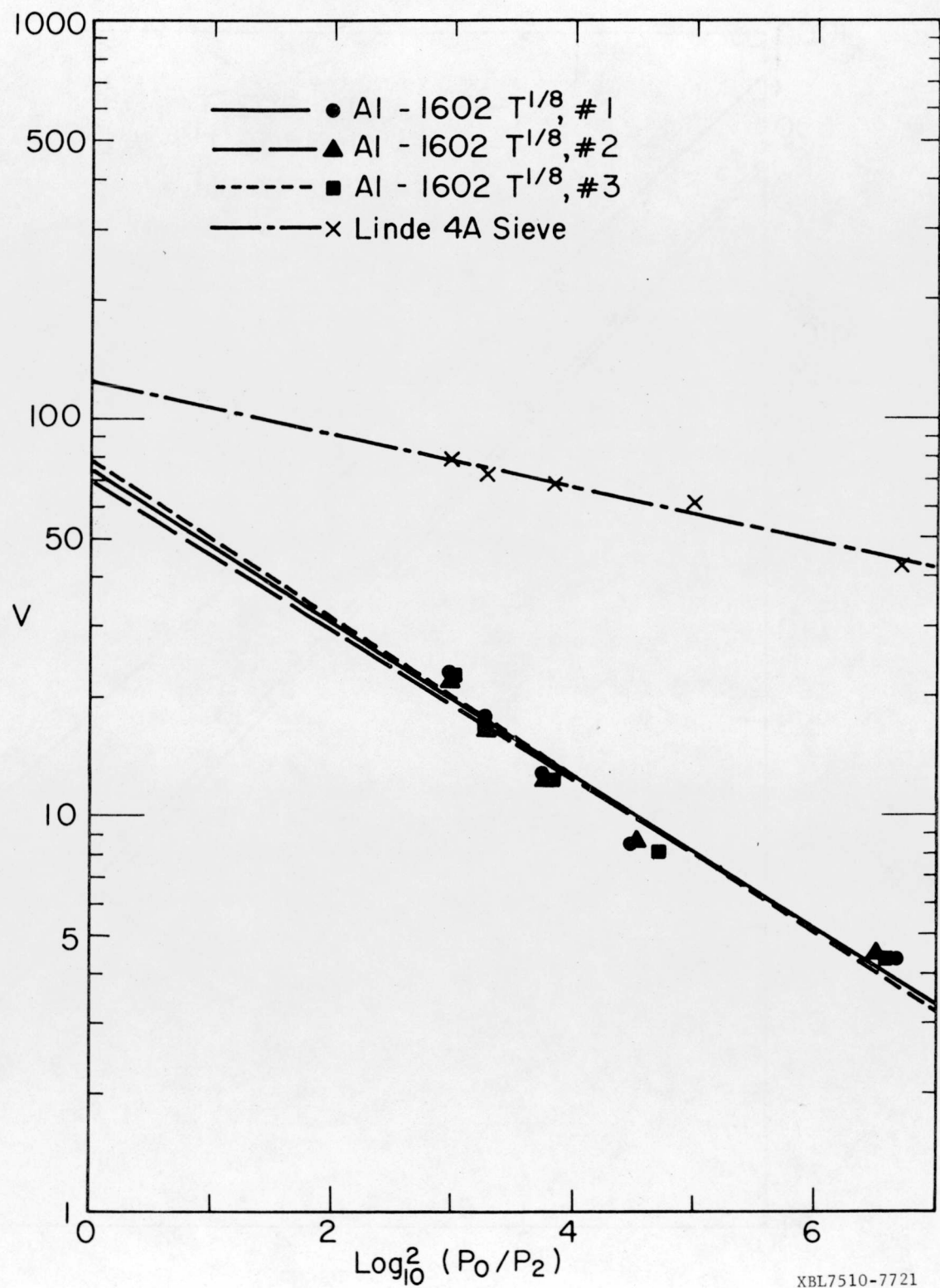
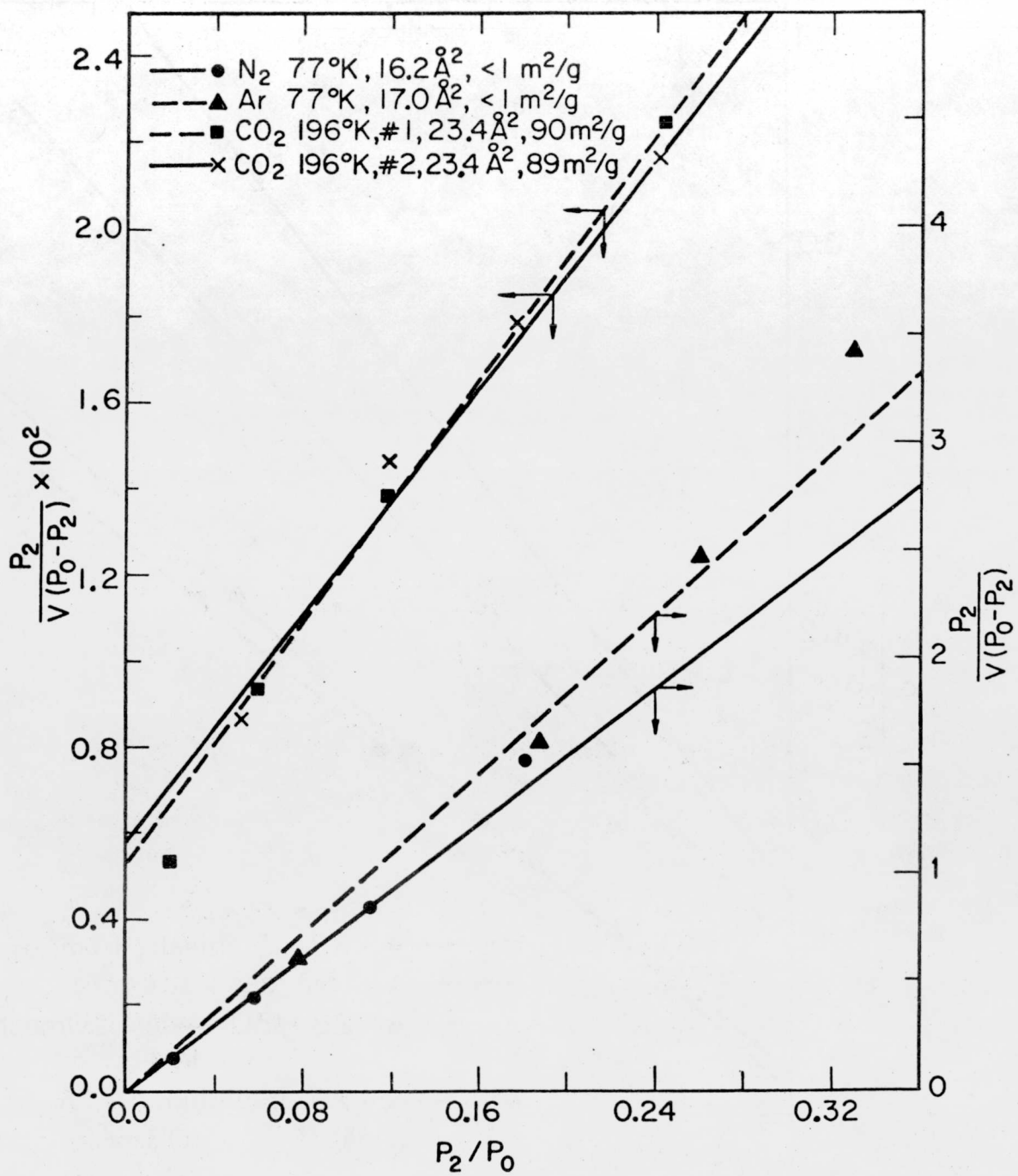


Fig. B-20. D-P Plots for  $\text{CO}_2$  adsorption at  $292^\circ\text{K}$



**Fig. B-21. Adsorption on Wyodak, Roland Seam, Coal: minus-28 mesh**

XBL7510-7720

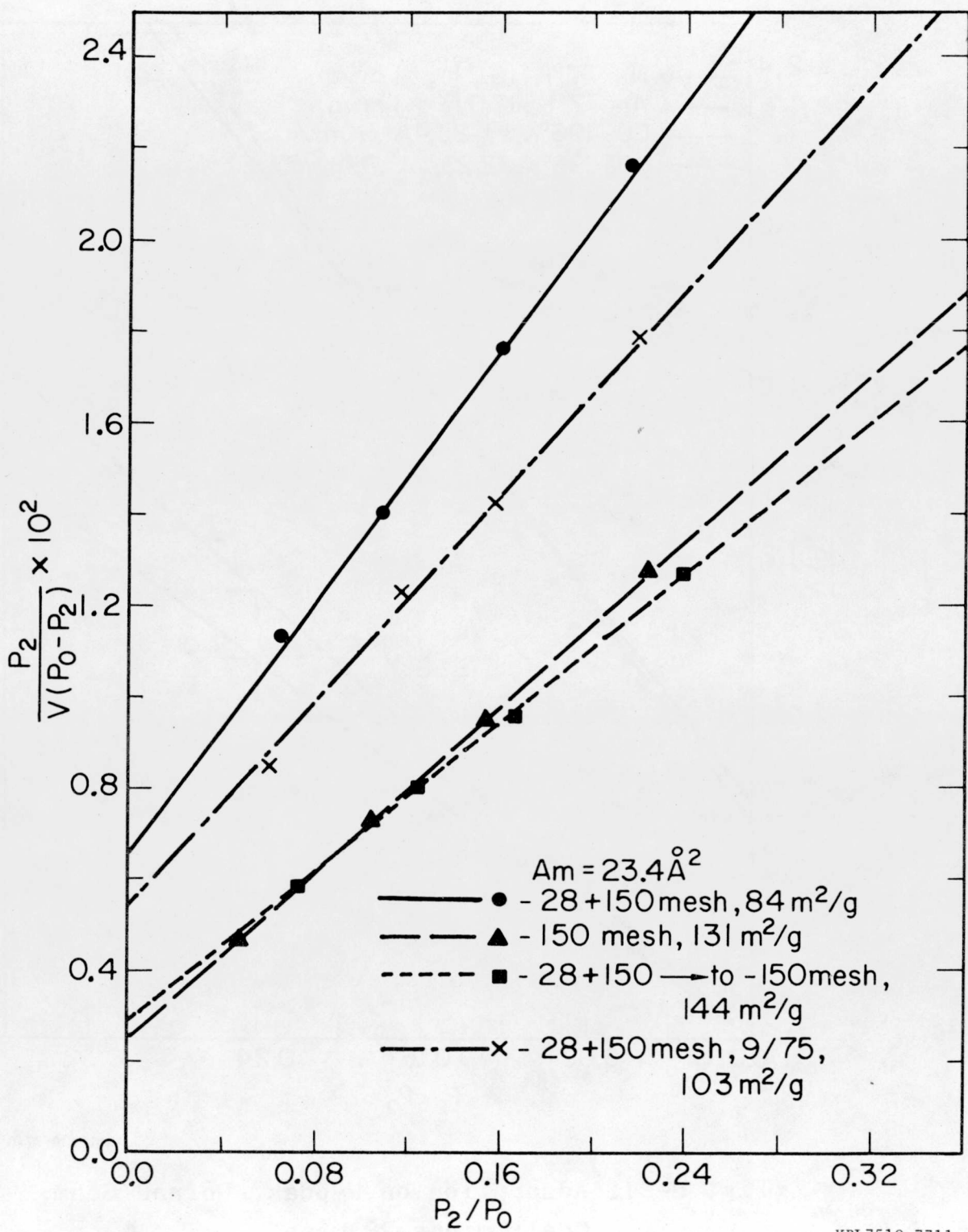
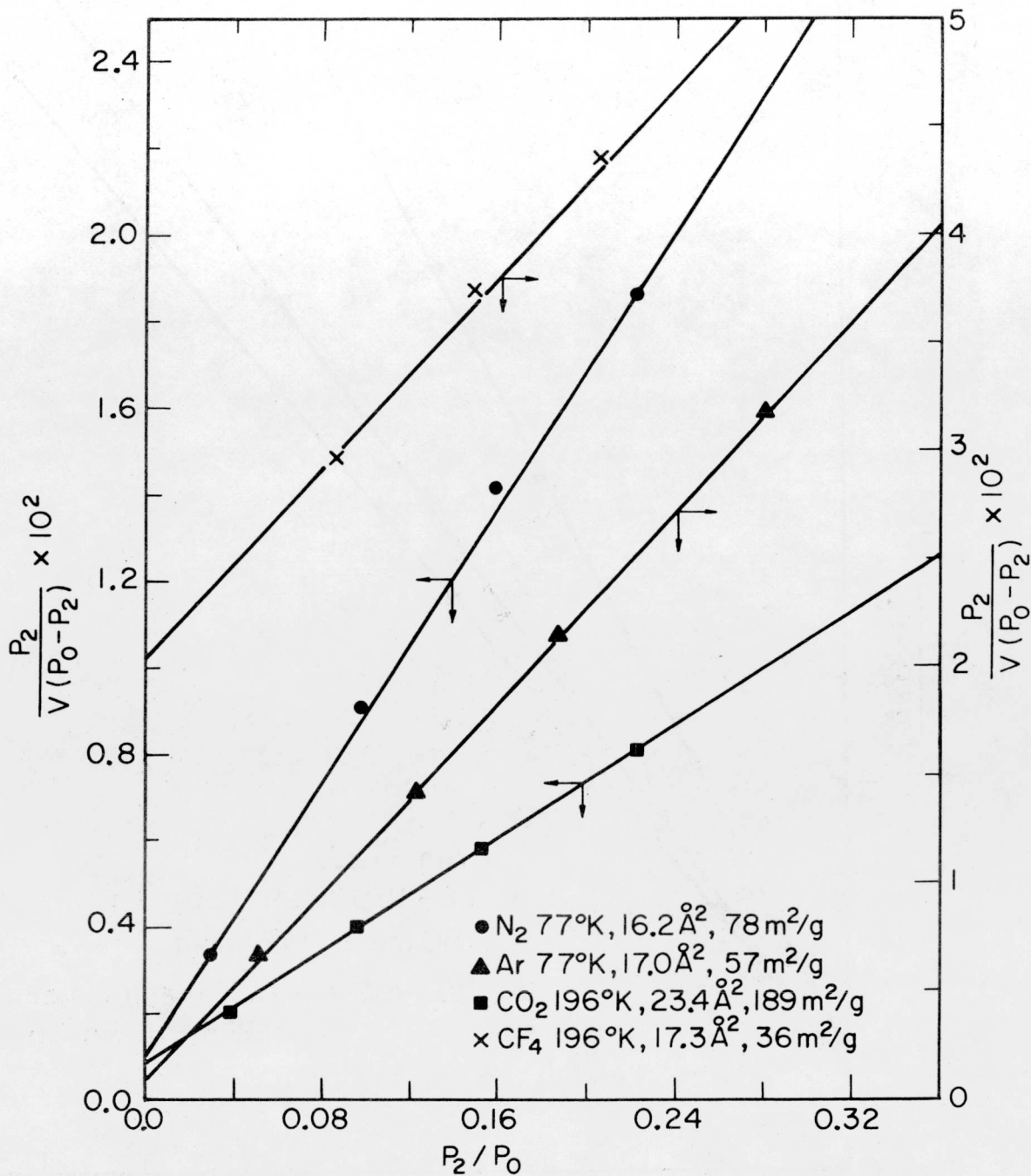


Fig. B-22. Adsorption of  $\text{CO}_2$  at  $196^\circ\text{K}$  on Wyodak, Roland Seam, Coal



XBL7510-7719

Fig. B-23. Adsorption on Illinois No. 6 Coal:  
minus-28 mesh

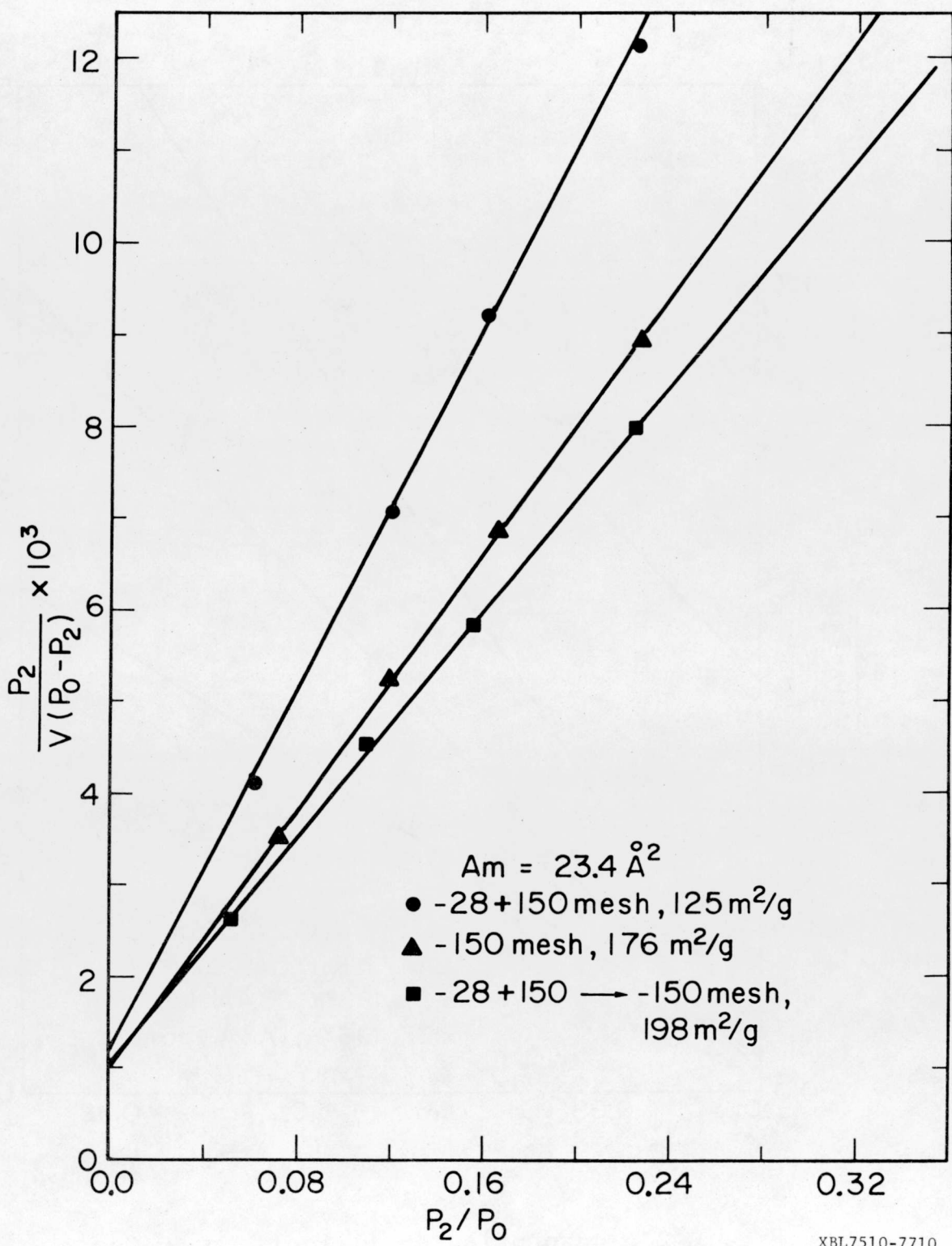


Fig. B-24: Adsorption of  $\text{CO}_2$  at  $196^\circ\text{K}$  on Illinois No. 6 Coal

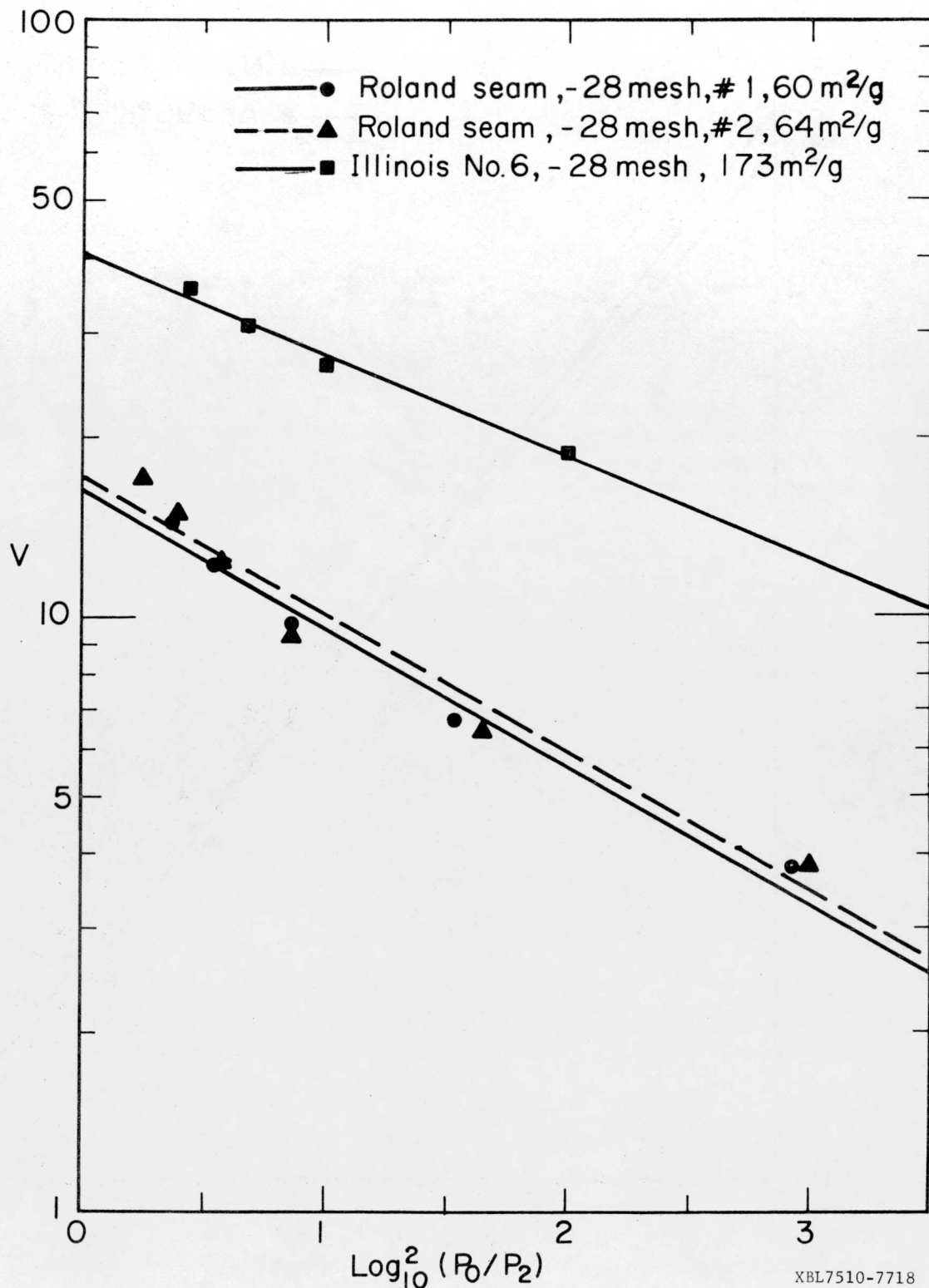


Fig. B-25. D-P Plots for  $\text{CO}_2$  adsorption at  $196^\circ\text{K}$ ,  
 $A_m = 23.4 \text{ \AA}^2$

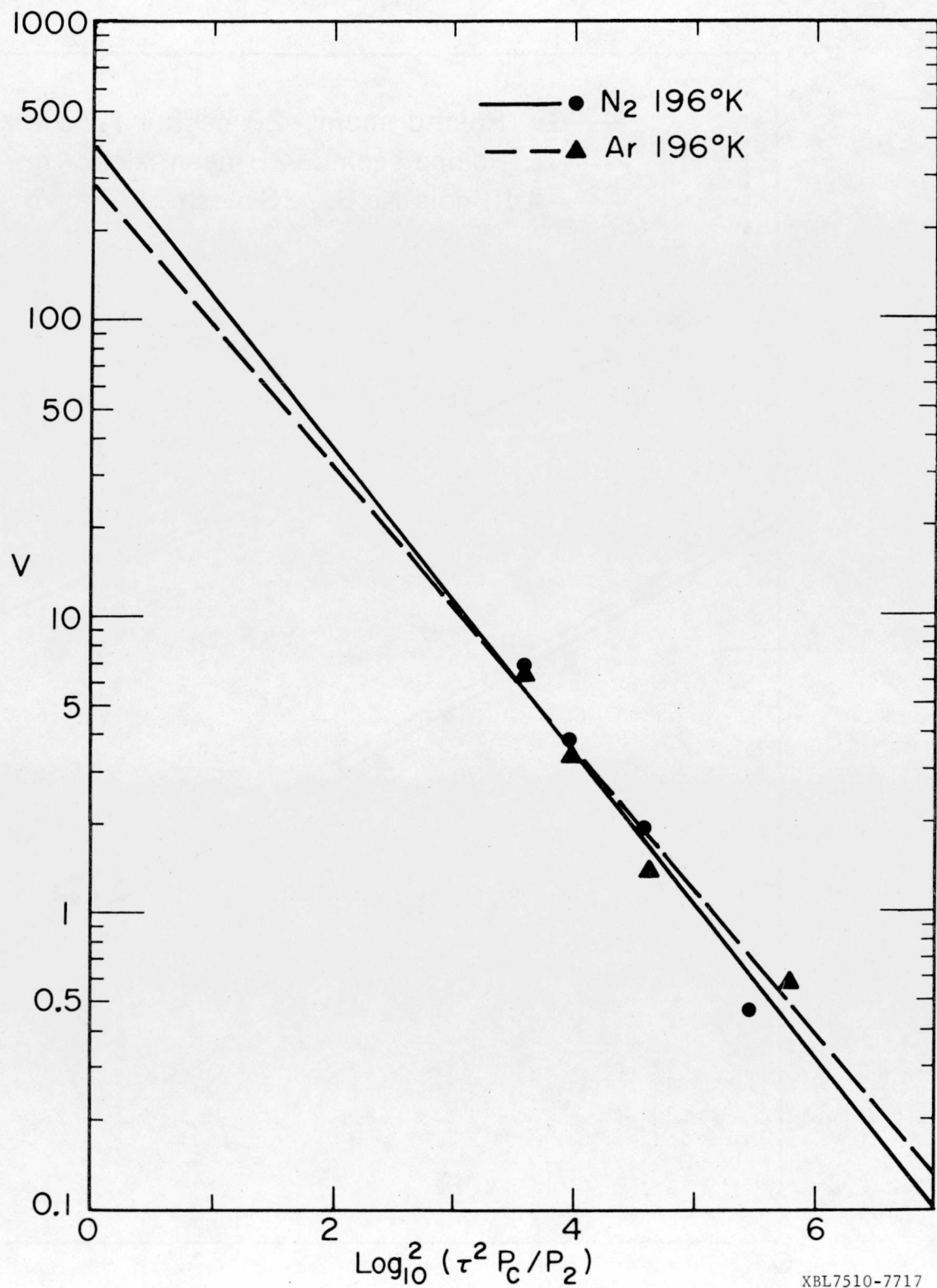
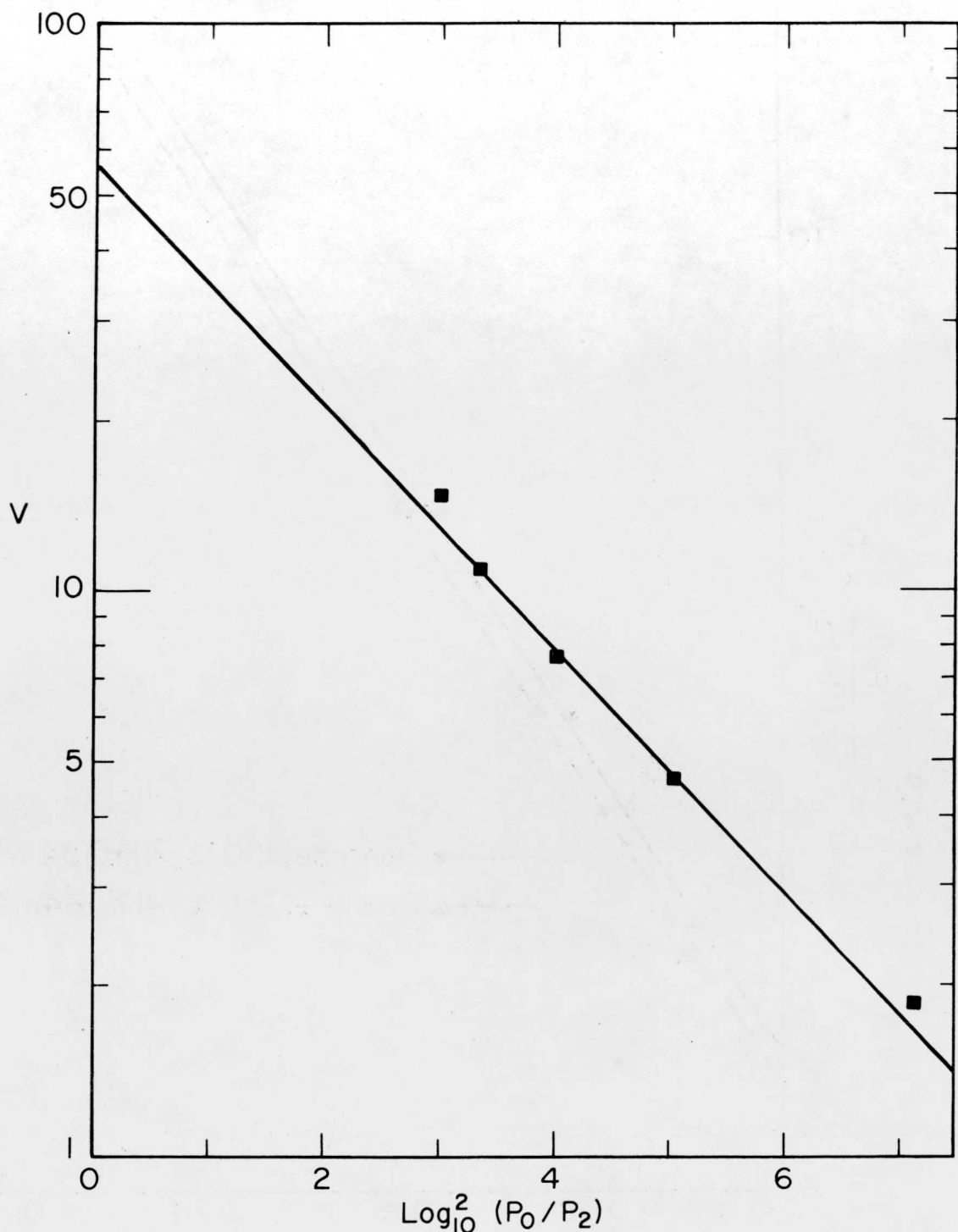


Fig. B-26. D-P Plots for adsorption on Roland Seam  
Coal: minus-28 mesh



XBL7510-7716

Fig. B-27. D-P Plot for  $\text{CO}_2$  adsorption at  $292^\circ\text{K}$  on Roland Seam Coal: minus-28 mesh

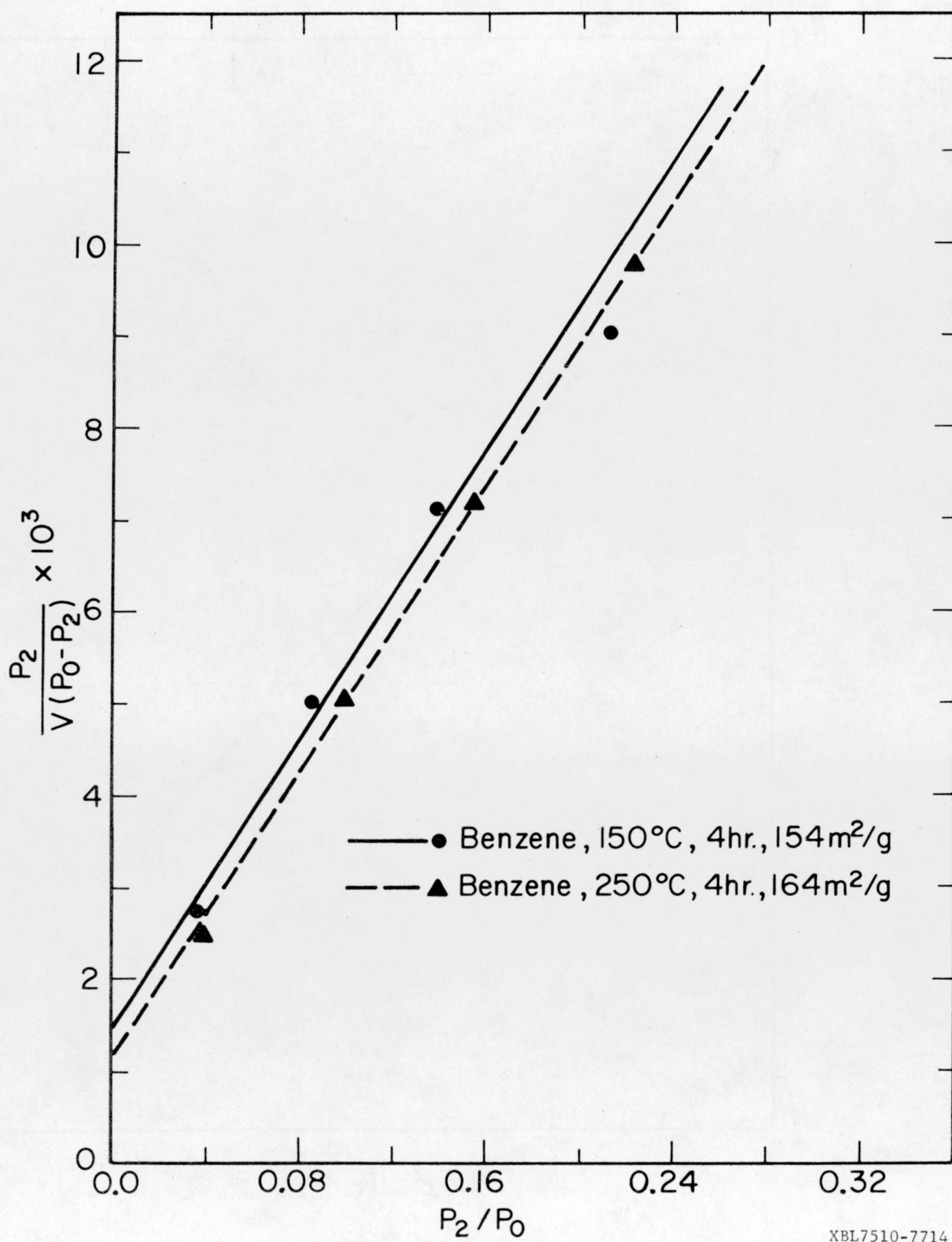


Fig. B-28. Adsorption of  $\text{CO}_2$  at  $196^\circ\text{K}$  on Extracted Roland Seam Coal,  $A_m = 23.4 \text{ \AA}^2$

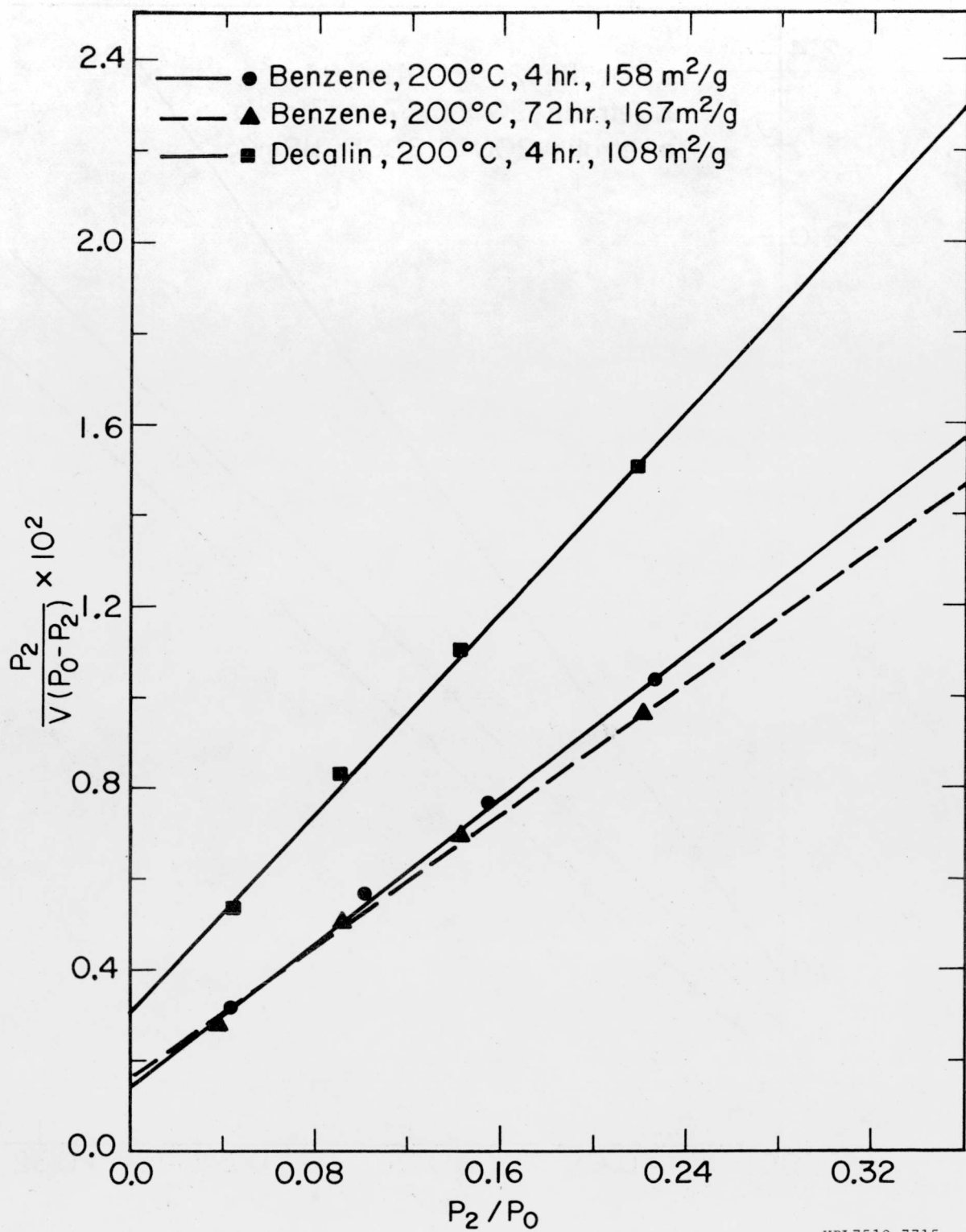
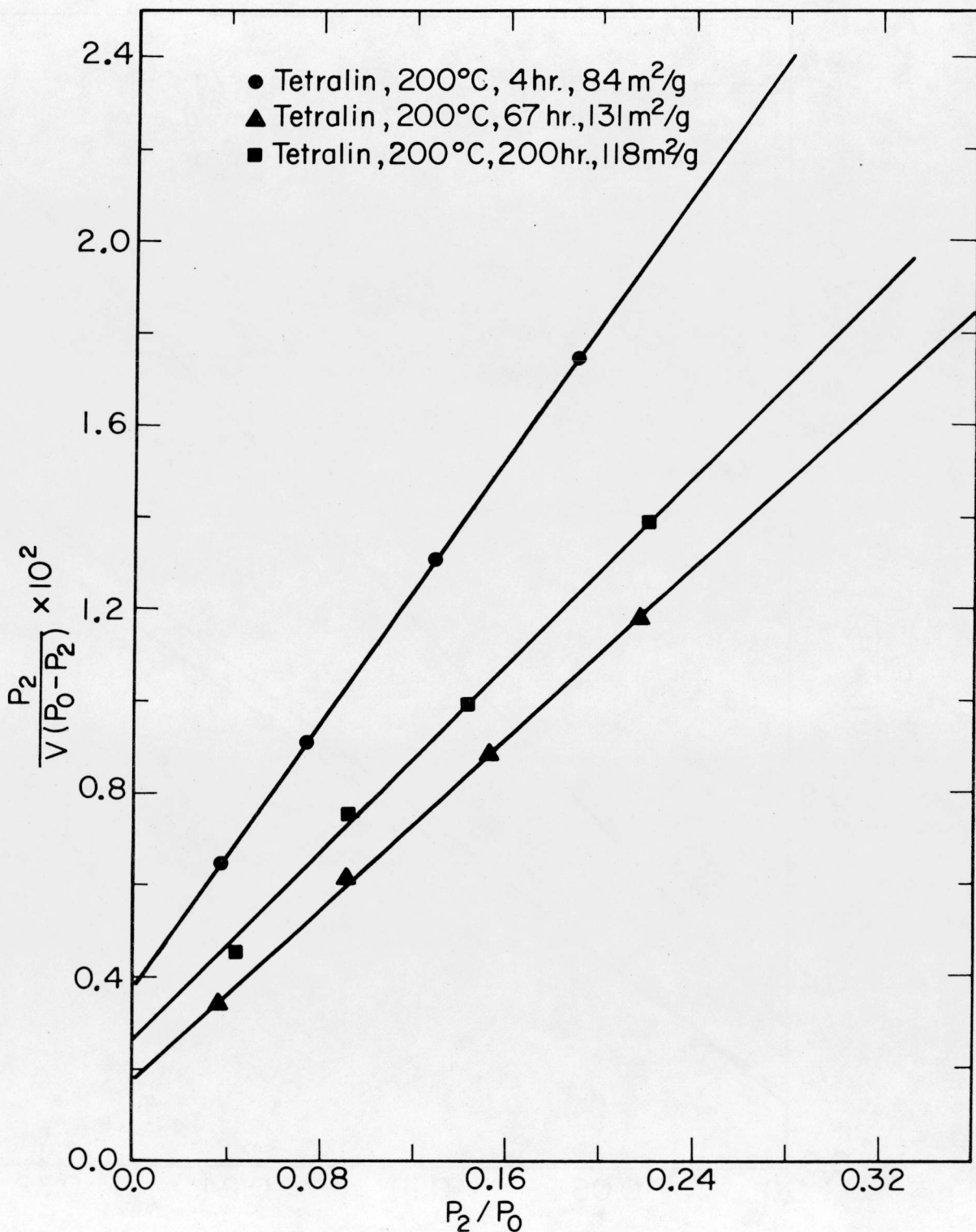


Fig. B-29. Adsorption of  $\text{CO}_2$  at  $196^\circ\text{K}$  on Extracted Roland Seam Coal,  $A_m = 23.4 \text{ \AA}^2$



XBL7510-7713

Fig. B-30. Adsorption of CO<sub>2</sub> at 196°K on Extracted Roland Seam Coal,  $A_m = 23.4 \text{ } \text{\AA}^2$

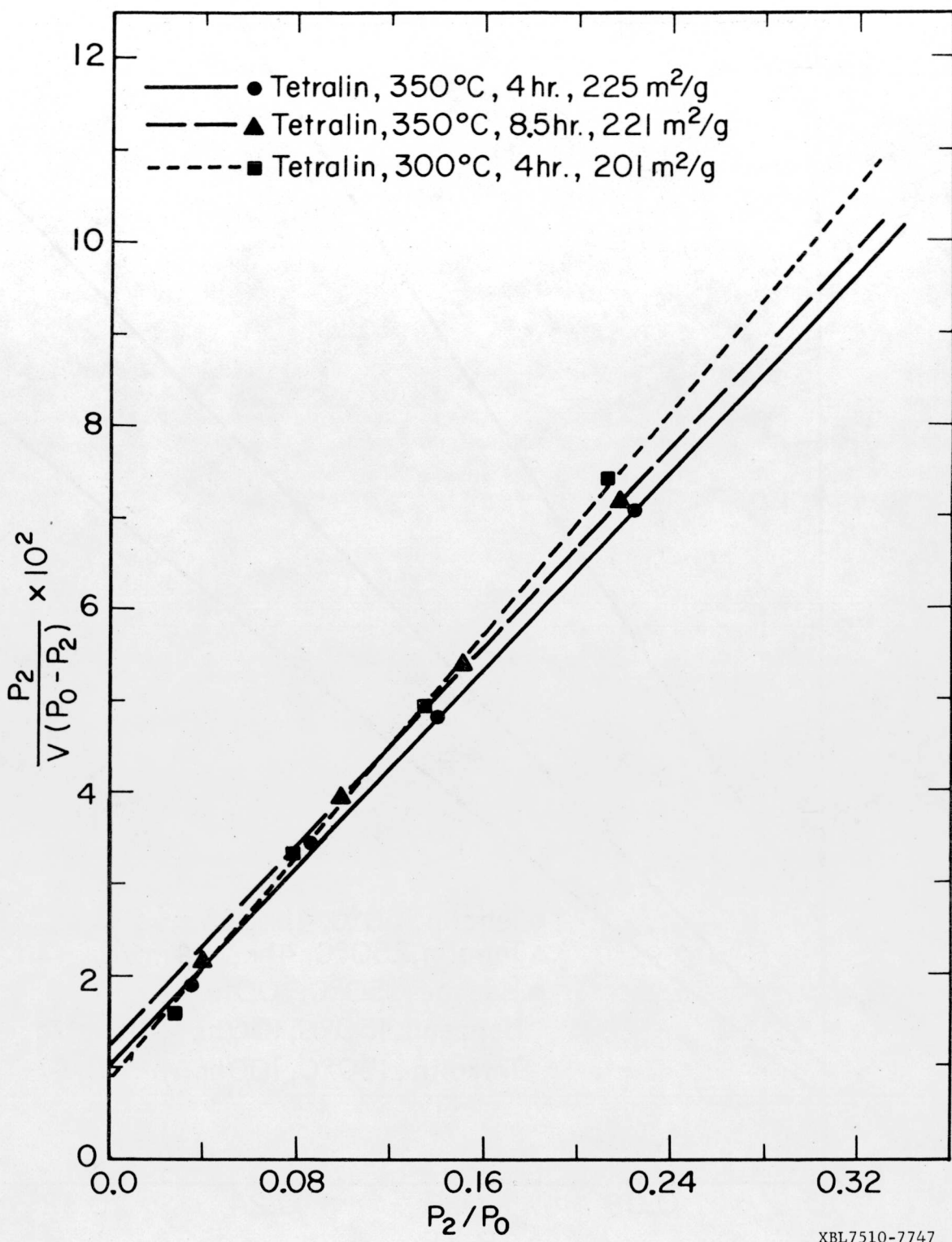


Fig. B-31. Adsorption of  $\text{CO}_2$  at  $196^\circ\text{K}$  on Extracted Roland Seam Coal,  $A_m = 23.4 \text{ \AA}^2$

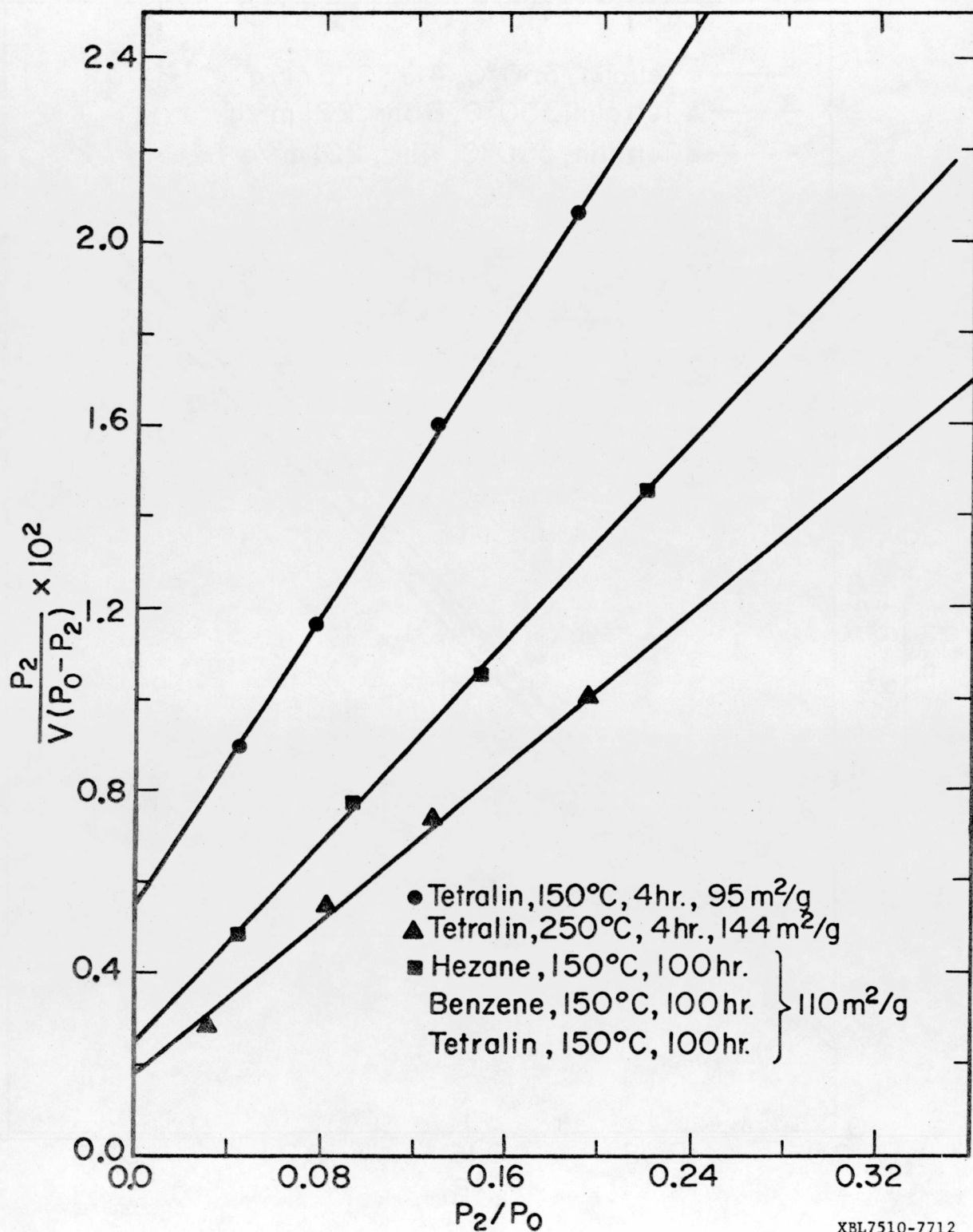


Fig. B-32. Adsorption of  $\text{CO}_2$  at  $196^{\circ}\text{K}$  on Extracted Roland Seam Coal,  $A_m = 23.4 \text{ \AA}^2$

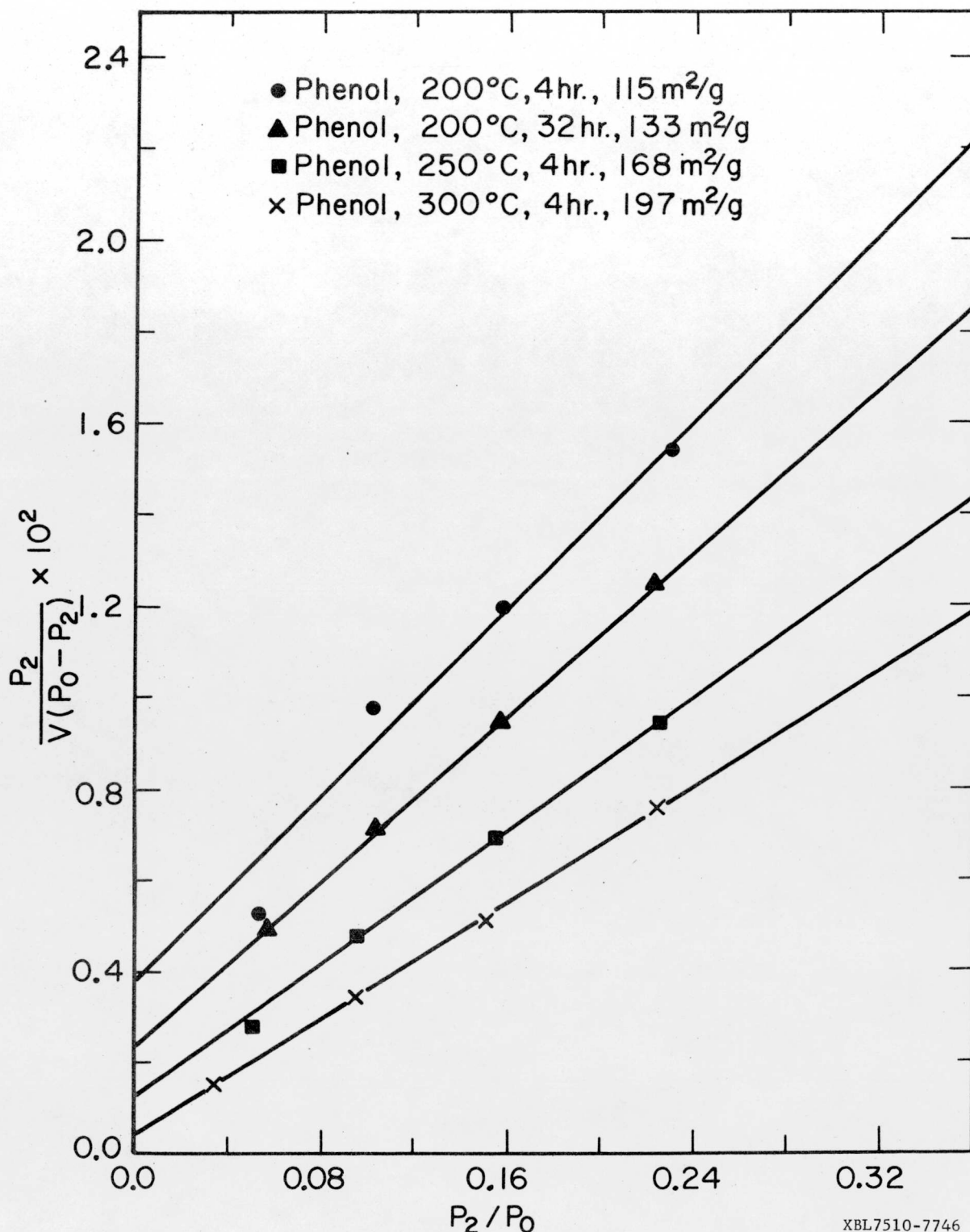


Fig. B-33. Adsorption of  $\text{CO}_2$  at  $196^0\text{K}$  on Extracted Roland Seam Coal,  $A_m = 23.4 \text{ \AA}^2$

#### **LEGAL NOTICE**

*This report was prepared as an account of work sponsored by the United States Government. Neither the United States nor the United States Energy Research and Development Administration, nor any of their employees, nor any of their contractors, subcontractors, or their employees, makes any warranty, express or implied, or assumes any legal liability or responsibility for the accuracy, completeness or usefulness of any information, apparatus, product or process disclosed, or represents that its use would not infringe privately owned rights.*

TECHNICAL INFORMATION DIVISION  
LAWRENCE BERKELEY LABORATORY  
UNIVERSITY OF CALIFORNIA  
BERKELEY, CALIFORNIA 94720